UNIVERSITÀ
DI PAVIA

PhD IN BIOMEDICAL SCIENCES

DEPARTMENT OF BRAIN AND BEHAVIORAL SCIENCES

UNIT OF NEUROPHYSIOLOGY

Role of endogenous TRPV1 in the onset of optical-induced Ca^{2+} signals in endothelial colony forming cells (ECFCs)

PhD Tutor: Professor Francesco Moccia

PhD dissertation of
Sharon Negri

a.a. 2021/2022

Sommario

1 INTRODUCTION

1.1 ENDOTHELIAL COLONY FORMING CELLS IN ANGIOGENESIS

1.1.1 ANGIOGENESIS AND VASCULOGENESIS

The vascular network is a highly specialized, tree-like, tubular system hierarchically organized in arteries, arterioles, veins, venules, and capillaries (Moccia et al 2019, Udan et al 2013). The vasculature is a fundamental tissue that weights ≈ 1 kg and covers a surface area of 4000-6000 m^2, reaching every organ in the human body (Aird 2005). Thereafter, blood vessel formation is an essential process, both during embryonic development and in the adult organism, for the oxygen and nutrient supply and for catabolic waste removal from all the organs (Fischer et al 2006). Moreover, the vascular network contributes to the rapid communication among distant tissues through cytokines and hormones (Udan et al 2013), it is responsible of the temperature stabilization along the body and avoids pH unbalance (Heinke et al 2012). Vascular morphogenesis is accomplished through multiple steps, including endothelial cell proliferation, migration, assembly into tubular structures, branching and anastomose of the existing vessels (Chung & Ferrara 2011). Vasculogenesis and angiogenesis are the two mechanisms involved in the formation and maturation of the vascular network in the embryo and during post-natal life (**Figure 1**) (Chung & Ferrara 2011, Potente et al 2011).

1.1.1.1 Vasculogenesis

Embryonal vasculogenesis represents one of the earliest events during organogenesis, as it already starts during gastrulation (Eichmann et al 2005, Goldie et al 2008). Vasculogenesis consists in the differentiation, expansion, and assembly of endothelial precursors into a functional blood vessel (Naito et al 2020, Udan et al 2013). Vascular development in the embryo is initiated by mesodermal cells, also referred to as hemangioblasts or endothelial progenitor cells (EPCs), which migrate into the yolk sac, to form cellular aggregates known as blood islands. They are small clusters of round mesenchymal cells, which differentiate over time, thereby generating an outer layer of spindle-shaped endothelial precursors, i.e., angioblasts, and inner core of round primitive hematopoietic cells. Hence, angioblasts form sprouts and coalesce with adjacent blood islands to assembly into the early vascular plexus, which in turn generates primitive blood vessels (**Figure 1A**) (Risau & Flamme 1995, Yoder 2018).

1.1.1.2 Angiogenesis

Once the primitive vascular labyrinth has been shaped, blood vessels are finely remodelled, to define tissues structures based on metabolic need, in a hierarchical tree-like network (Moccia et al 2019, Udan et al 2013). The angiogenic process may occur through two mechanisms: sprouting angiogenesis (**Figure 1B**) and intussusceptive angiogenesis (**Figure 1C**). Sprouting angiogenesis is a multistep process induced by a local decrease in oxygen tension. It is characterized by different steps:

vasodilation, increased vascular permeability, endothelial cell proliferation, and migration. In response to a pro-angiogenic stimulus (e.g. vascular endothelial growth factor (VEFG) or platelet derived growth factor (PDGF)) a leading tip cell migrate in the extracellular matrix after the degradation of the basal lamina (Djonov et al 2003). Therefore, endothelial stalk cells start to proliferate and support sprout elongation, form the new capillary lumen, and maintain the connection to the native vessel. Finally, tip cells deriving from different sprouts anastomose to generate functional vessels and to allow the blood to flow (Carmeliet & Jain 2011, Herbert & Stainier 2011). The process continues until the angiogenic stimulus is turn off, and the oxygen supply is rescued (Carmeliet & Jain 2011, Herbert & Stainier 2011), thus naked endothelial cells become quiescent. Depending on the hierarchic branch, different mural cells (e.g. pericytes and vascular smooth muscular cells (VSMCs)) may be recruited to promote maturation and to stabilize new connections (Potente et al 2011). Conversely, intussusceptive angiogenesis is characterized by the splitting of capillaries by the insertion of columns of interstitial tissue, known as pillar, followed by the enlargement of the pillar diameter and the consequent division of the vessel (**Figure 1C**). Sprouting angiogenesis has long been considered the main mechanism involved in vascular remodelling in the adult, however it is now clear that EPCs have a role in *tubulogenesis* also in post-natal life (Banno & Yoder 2018). For instance, EPCs have been found in adult peripheral blood in 1997 by Isner's group. They may be mobilized from perivascular stem cell niches of existing vessels in several situations: i) under non-pathological conditions, EPCs replace senescent endothelial cell; ii) upon an ischemic insult, EPCs stimulate local angiogenesis to rescue the injured tissue through a paracrine mechanism or by engrafting in the vessels (Yoder 2012, Yoder 2018); iii) they are also recruited in the arteriogenic process, which consists in the enlargement and collateralization of existing arterioles into new vessels when the main artery is occluded (Heil et al 2006); iv) finally, EPCs may sustain the initial phases of tumour growth (Moccia & Poletto 2015, Poletto et al 2018).

Physiologically, angiogenesis is a tightly regulated process, controlled by a delicate balance between pro- and anti-angiogenic molecules. When pro-angiogenic cues, such as VEGF, PDGF, stromal derived factor-1α (SDF-1α) and basic fibroblast factor (bFGF), prevail on the anti-angiogenic factors, neovessel formation is promoted. Conversely, an excess of anti-angiogenic molecules (e.g., endostatin, tumstatin, thrombospondin-1 and C-X-C motif chemokine 10 (CXCL10)) blocks the angiogenic process (Carmeliet & Jain 2011, Moccia et al 2019). This fragile balance is altered in several diseases. For instance, a reduction or a malfunctioning of neovessel morphogenesis characterizes hindlimb ischemia, stroke, pre-eclampsia, neurodegeneration, and acute myocardial infarction (AMI) (Potente et al 2011).

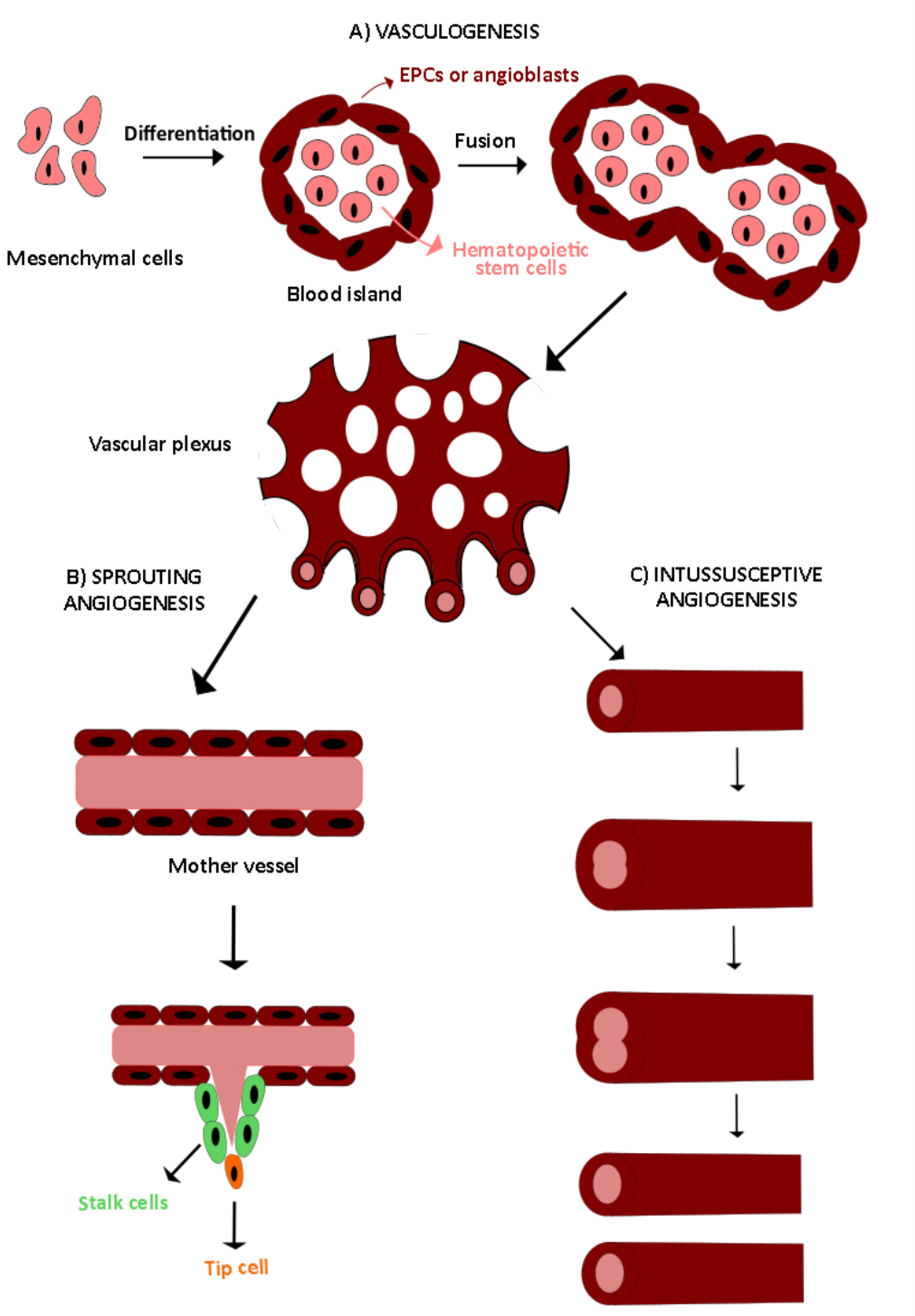

Figure 1 Angiogenesis and Vasculogenesis. **A.** The vasculogenesis, which consists of neovessel formation from EPC aggregation within the blood islands. Thus, several blood islands blend together into the early vascular plexus that in turn originates primitive blood vessels. **B-C.** The angiogenic process generates new vessels from pre-existing vasculature in response to pro-angiogenic cues. It may occur through two different mechanisms: **B.** sprouting angiogenesis and **C.** intussusceptive angiogenesis. See the text for the details. (Negri et al 2019).

Conversely, tumorigenesis and inflammatory disorders are featured by an excessive vessel formation (Carmeliet & Jain 2011, Fischer et al 2006). Therefore, understanding the molecular mechanisms involved in vasculogenesis and angiogenesis is fundamental to design new therapeutic strategies by unravelling novel molecular targets (Moccia et al 2014a, Potente et al 2011). It has long been known

that endothelial Ca^{2+} signals are key players in angiogenesis (Moccia et al 2012a, Moccia et al 2014b). Furthermore, emergent evidence demonstrated that an increase in intracellular Ca^{2+} concentration ($[Ca^{2+}]_i$) also induced EPC proliferation, migration and *tubulogenesis* (Moccia & Guerra 2016). This Thesis work focused on the Ca^{2+}-dependent pathways in the EPC subfamily of endothelial colony forming cells (ECFCs), with a specific interest in the endothelial Ca^{2+} signals mediated by transient receptor potential Vanilloid 1 (TRPV1) and involved in neovessel formation.

1.1.2 ENDOTHELIAL PROGENITOR CELLS (EPCs)

EPCs were firstly identified as a circulating subpopulation of bone-marrow derived mononuclear cells (MNCs) (Asahara et al 1997). They were recognised through flow cytometry, thanks to the presence of specific endothelial markers (e.g., CD133 and CD34). The discovery of EPCs in the adult broke the belief that EPCs had a role only in the embryonic stages. Several pieces of evidence, indeed, showed that EPCs are mobilized during placentation, skeletal muscle growth, ovarian cycle in uterine endometrium, wound healing after traumatic injury and promote postnatal neovessel formation (Chung & Ferrara 2011, Fischer et al 2006). A recent consensus of nomenclature recognised two distinct cell populations in cultured MNCs, based on the time of appearance in culture and on their morphology and marker expression: (i) myeloid angiogenic cells (MACs), also known as circulating angiogenic cells (CACs), pro-angiogenic circulating hematopoietic stem/progenitor cells (pro-CHSPCs or pro-CPCs) or "early" EPCs, and (ii) ECFCs or "late" EPCs (Medina et al 2017) (**Figure 2**).

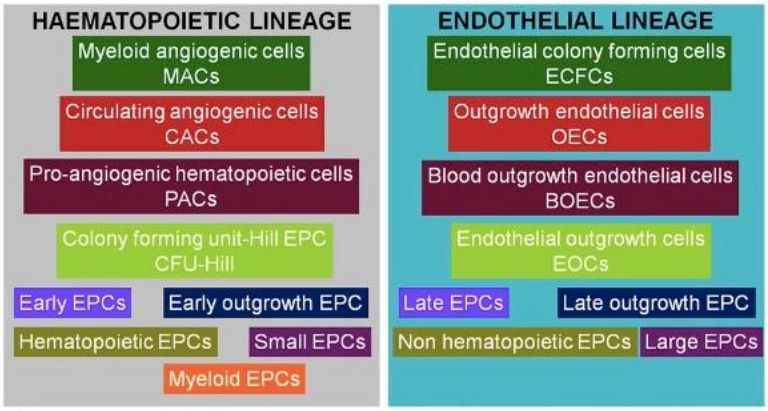

MACs	ECFCs
✓ CD45+ CD14+ CD31+	✓ CD31+ CD105+ CD146+
✓ CD146- CD34-	✓ CD45- CD14-
→ Conditioned media enhances endothelial network formation *in vitro* and *in vivo*.	→ Intrinsic tube forming capacity *in vitro* and *in vivo*.
→ MACs-derived paracrine factors as stimulants of angiogenesis.	→ ECFCs as building blocks for new blood vessel formation or vascular repair

Figure 2 EPC nomenclature: MACs vs ECFCs. EPCs are subdivided in two groups based on the phenotypic lineage: hematopoietic and endothelial. The table describe the immunophenotypic and functional criteria to define MACs and ECFCs (Medina et al 2017).

MACs cannot reach a mature endothelial phenotype and have a low clonogenic potential. They are characterized by endothelial specific markers (e.g., CD45, CD14 and CD31) and macrophage specific markers, such as macrophage scavenger receptor 1 (MSR1), which suggest a potential MAC differentiation into macrophages and their role in endothelial repair (Medina et al 2017). Although MACs do not physically engraft in the neovessels, they promote angiogenesis and neovascularization through paracrine mechanisms (**Figure 3**). Indeed, they release cytokines (e.g., interleukin 8) that activates several angiogenic pathways in endothelial cells, described in paragraph 1.2.1 (Medina et al 2017). Conversely, ECFCs represent the only known EPC subset truly belonging to the endothelial lineage, showing robust *in vitro* clonal potential, and overwhelming *in vivo* neovessel formation (Burger et al 2015). For these reasons, ECFCs are endowed with the highest potential to stimulate therapeutic angiogenesis, by physically engrafting in the injured endothelium and by releasing pro-angiogenic cues to the adjacent cells (Reid et al 2017) (**Figure 3**).

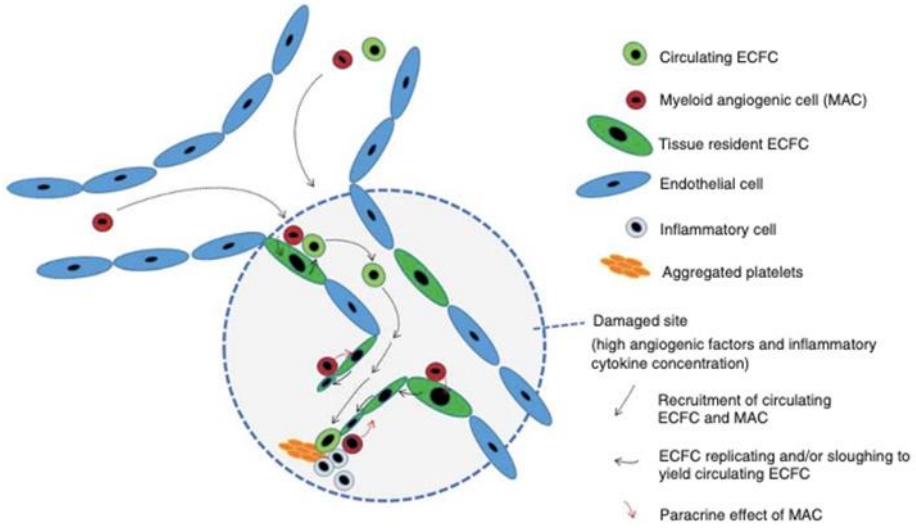

Figure 3 Revascularization process. MACs are recruited on the damage site, where they release several paracrine mediators to attract ECFCs from the circulation or from the perivascular niches. ECFCs migrate, proliferate and physically engraft the injured vessel to rescue the endothelium integrity (Banno & Yoder 2018).

1.1.3 ENDOTHELIAL COLONY FORMING CELLS (ECFCs)

The presence of ECFCs, or late EPCs, in peripheral blood was first identified by Isner's group, which defined them as a MNC subpopulation that were recruited at the ischemic site where they promoted neovascularization and rescued blood perfusion (Asahara et al 1997). However, as reported in the previous paragraph, a recent consensus introduced a more stringent and precise definition (Medina et al 2017). For instance, ECFCs are isolated from adult peripheral blood or umbilical cord blood (UCB) by plating MNCs on type I rat collagen-coated plates, where cobblestone-like colonies appear after 2-3 weeks of culture under endothelial conditions (Ingram et al 2005, Ingram et al 2004). Furthermore, ECFCs are characterized by several typical endothelial markers (e.g. CD34, CD31, VEGF receptor 2 (VEGFR-2), VE-cadherin, and von Willebrand factor) and do not express

mesenchymal stem cells and hematopoietic (e.g. CD14 and CD45) antigens (Yoder et al 2007). Although, describing a specific antigen panel remains an open issue nowadays, ECFCs also present the cytosolic expression of stem cell markers, such as CD133 (Rossi et al 2019).

Initially ECFCs were thought to derive from bone marrow (Lin et al 2000) that is the origin site of MNCs. However, a recent work showed that ECFCs isolated from peripheral blood and venous wall of male patients transplanted with female bone marrow presented a male (XY) genotype (Fujisawa et al 2019). On the other hand, MACs exhibited a female (XX) genotype and lack the endothelial marker CD31, which was consistent with the bone marrow derivation (Fujisawa et al 2019). Moreover, additional recent investigations showed that ECFCs may originate from several perivascular progenitor cell niches located in the aorta, lung tissue, pulmonary artery, saphenous vein and placenta (Faris et al 2020b), or they may derive from white adipose tissue or from human-induced pluripotent stem cells (hiPSCs) (Faris et al 2020b).

1.1.4 ECFCs AND THEIR THERAPEUTIC APPLICATION

It has long been known that ECFC transplantation stimulates revascularization and restores blood perfusion upon an ischemic insult (Paschalaki & Randi 2018). ECFCs promote vascular repair through different mechanisms, which may cooperate to support tissue revascularization: i) physical engraftment within nascent neovessels (Au et al 2008, Melero-Martin et al 2007); ii) paracrine release of pro-angiogenic cues, which induce sprouting angiogenesis from adjoining capillaries, and chemotactic mediators (Smadja et al 2009) that engage mural and/or inflammatory cells (d'Audigier et al 2015); iii) release of microvesicles and/or exosomes that mediate ECFC-dependent vascular repair in multiple pathological conditions (Boscolo et al 2011, Lin et al 2014); and finally, iv) promote the regenerative capacity of MSCs (Kang et al 2017) and adipose stromal cells (Traktuev et al 2009). Moreover, ECFCs may interact with MACs during the neovascularization process. For instance, circulating MACs are the first EPC subtype to be enrolled within the hypoxic tissue, thereby secreting multiple growth factors that engage ECFCs from the peri-vascular progenitor cell niches or from peripheral blood. Next, ECFCs proliferate and engraft within the injured endothelium to promote vascular repair, possibly in combination with the secretion of trophic mediators (Banno & Yoder 2018, Basile & Yoder 2014).

Although, ECFCs represent the most promising tool for cell-based therapy (Banno & Yoder 2018, Medina et al 2017, Moccia et al 2018a, O'Neill et al 2018, Paschalaki & Randi 2018, Tasev et al 2016), they are far from being tested in clinical trials on ischemic patients yet. A recent work summarized the clinical studies that probed EPCs as a therapeutic cellular model against a wide group of disorders (Keighron et al 2018). Only 26 out of 341 clinical trials detected by searching the term “EPC” confirmed the therapeutic outcome of EPCs in severe ischemic diseases, such as coronary artery disease (CAD), peripheral artery disease (PAD), and stroke, while the remaining studies were more observational than experimental (i.e., evaluation of EPC biomarkers in different pathologies). Five

further trials, which were identified on PubMed and on the Web of Science databases, were performed in order to evaluate the impact of EPC-based therapy in PAD, CAD, pulmonary hypertension, and liver cirrhosis (Keighron et al 2018). These investigations showed that EPC therapy was possible and safe; however, it emerged that the EPC populations employed, which derived from either bone marrow or UCB, were widely heterogenous and principally consisted of hematopoietic angiogenic cells, such as MACs (Banno & Yoder 2019, Keighron et al 2018). Intriguingly, no clinical trial has evaluated the therapeutic outcome and practicability of ECFCs as cellular strategy to treat ischemic disorders. Multiple reasons have been proposed to explain why autologous ECFC-based therapy is yet to be tested in ischemic patients. First, circulating ECFC frequency is quite low, ranging from 0.28–15 ECFCs/10^7 (Moccia et al 2017) to 1 ECFCs/10^6-10^8 MNCs (Banno & Yoder 2018). Of course, this is an insufficient amount of ECFCs for a therapeutic output in regenerative medicine (Banno & Yoder 2018, Moccia et al 2014a, Tasev et al 2016). Second, the mobilization of larger number of ECFCs directly in ischemic patients may not induce efficient therapeutic outcomes (Smadja 2019). Although a raise in circulating ECFCs has been noticed upon an ischemic insult, such as AMI (Massa et al 2009), CAD (Guven et al 2006), critical limb ischemia (CLI) (Smadja et al 2012), forearm ischemia (Mauge et al 2014), and pulmonary hypertension (Toshner et al 2014), their angiogenic capacity can be seriously compromised. Third, ECFCs' angiogenic activity is usually affected in the presence of cardiovascular risk factors that favour the onset of ischemic events; this is an additional issue that discourages the employment of circulating ECFCs for autologous cell-based therapy (Banno & Yoder 2018, Smadja 2019, Tasev et al 2016). Furthermore, CAD (Su et al 2017), aging (Shelley et al 2012), diabetes (Jarajapu et al 2014), abdominal aortic aneurysm (Sung et al 2013), venous thromboembolic disease (Hernandez-Lopez et al 2017), congenital diaphragmatic hernia (Fujinaga et al 2016) and systemic lupus erythematosus (Komici et al 2020) are characterized by a significantly lower frequency and/or angiogenic capacity of circulating ECFCs. Fourth, ECFCs' vasoreparative potential could be also reduced by the tough microenvironment of ischemic tissues. For instance, ECFC proliferation and tube formation are impaired upon inflammatory conditions (Mena et al 2018), by oxidative stress (Gremmels et al 2017) and hypoxia (Tasev et al 2018), and in the presence of damage-associated molecular patterns (DAMP), such as extracellular histones (Mena et al 2016) and monosodium urate (Mena et al 2019). Fifth, the therapeutic use of UCB-derived ECFCs, which show a greater proliferative activity (up to 100 population doublings), higher angiogenic potential and enhanced telomerase activity than circulating ECFCs (Ingram et al 2004), is currently not employed (Banno & Yoder 2019). For instance, the heterologous administration of UCB-derived ECFCs may lead to an immunological response, both *in vitro* and *in vivo*, because of the expression of the of class I and class II major histocompatibility complex (MHC) molecules, which are, respectively, identified and bound by $CD8^+$ and $CD4^+$ T cells (Merola et al 2019, Suarez et al 2007). In addition, processing and freezing a sufficient amount of UCB-derived ECFCs for each human at birth, in order to be used during adulthood, is still too expensive (Banno & Yoder 2019). For all these reasons, alternative strategies

are needed to ameliorate ECFC therapeutic outcome. Notably, the investigation of the molecular mechanisms responsible of the ECFCs' angiogenic activity is fundamental to promote the development of novel and alternative strategies to ameliorate their therapeutic outcome.

1.2 CALCIUM SIGNALLING IN ECFCs AND ANGIOGENESIS

1.2.1 Ca^{2+} SIGNALS IN ANGIOGENESIS

The increase in $[Ca^{2+}]_i$ is known to be a crucial element in pro-angiogenic mechanisms and lies at the centre of an intricate signalling network that controls and regulates endothelial cells and ECFC fate (Moccia et al 2019, Negri et al 2019, Simons et al 2016). In this view, chemokines and growth factors promote the angiogenic pathway by inducing intracellular Ca^{2+} signals, which stimulate endothelial cell proliferation, adhesion, migration and *tubulogenesis* (Moccia et al 2014b, Patton et al 2003). Moreover, vasoactive and inflammatory cues (e.g. ATP, thrombin and acetylcholine) and pleiotropic hormones (e.g erythropoietin) participate to pro-angiogenic process by evoking an increase in endothelial $[Ca^{2+}]_i$ (Moccia et al 2019). Finally, mechanical injury of the vascular intima and laminar shear stress typical of arteriogenesis may induce endothelial Ca^{2+} waves that are thought to promote cell proliferation and migration (Moccia et al 2019). Of note, different patterns of endothelial Ca^{2+} signals have been described, which depend on the exogenous stimulus, the vascular bed, the species, and the molecular elements engaged (Moccia et al 2012a, Noren et al 2016).

Extracellular stimuli operate by inducing extracellular Ca^{2+} entry and by mobilizing endogenous Ca^{2+} release from the intracellular stores (e.g. endoplasmic reticulum (ER) and lysosomes), which will be described in the following paragraphs (Moccia et al 2019). Likewise, the restoration of resting $[Ca^{2+}]_i$ is driven by a sophisticated Ca^{2+} toolkit composed by pumps and transporters. Notably, the key players are the Sarco-endoplasmic reticulum Ca^{2+}-ATPase (SERCA), which sequesters cytosolic Ca^{2+} into the ER, Plasma Membrane Ca^{2+}-ATPase (PMCA) and Na^+/Ca^{2+} exchanger (NCX), which extrude Ca^{2+} across the plasma membrane. In addition, mitochondria have emerged as important Ca^{2+} buffers that redirect entering Ca^{2+} to the ER via the mitochondrial NCX (Malli et al 2003, Malli et al 2005).

Pro-angiogenic cues target specific tyrosine kinases receptors (TKRs) and $G_{q/11}$-protein coupled receptors ($G_{q/11}$PCR), which in turn cause an increase in $[Ca^{2+}]_i$ by recruiting, respectively, phospholipase C (PLC) γ1-2 and PLCβ1-4. Thereafter, PLCγ and PLCβ isoenzymes hydrolyse the membrane phosphatidylinositol 4,5-bisphosphate (PIP_2) into the two intracellular second messengers inositol 1,4,5-trisphosphate ($InsP_3$) and diacylglycerol (DAG) (Berridge et al 2003). DAG causes an increase in $[Ca^{2+}]_i$ by activating TRP Canonical 3 (TRPC3) and TRPC6 on the endothelial plasma membrane, conversely $InsP_3$ diffuses in the cytoplasm and gate the non-selective cation channels, $InsP_3$ receptors ($InsP_3$Rs) and release Ca^{2+} from the ER. The reduction of $[Ca^{2+}]_{ER}$ leads to the activation of store-operated Ca^{2+} entry (SOCE), the main mechanism of Ca^{2+} influx in non-excitable cells, which will be described in paragraph 1.2.1.2 (**Figure 4**) (Moccia & Guerra 2016, Moccia et al 2014a, Moccia et al 2019).

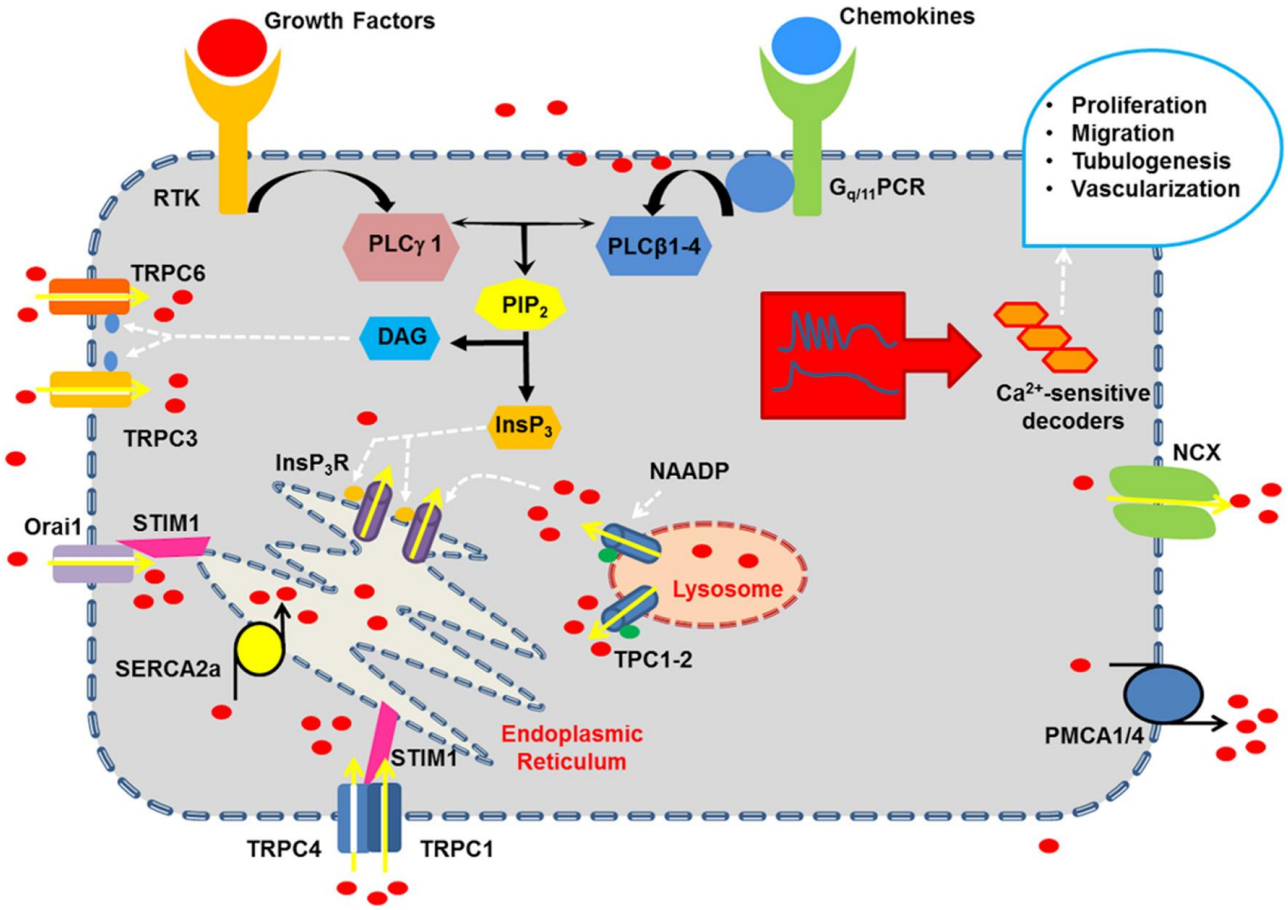

Figure 4 The endothelial Ca^{2+} toolkit. Pro-angiogenic cues, such as VEGF and SDF-1α, target, respectively, tyrosine kinases receptors (TKRs) and $G_{q/11}$-protein coupled receptors ($G_{q/11}$PCR) and activate different phospholipase C (PLC) isoforms and the downstream pathways. See the text for the description (Moccia et al 2019).

1.2.1.1 Endogenous Ca^{2+} release induced by pro-angiogenic factors: $InsP_3Rs$ and two pore channels (TPC)

$InsP_3$ elicits endogenous Ca^{2+} mobilization by gating the $InsP_3Rs$ localized on the membrane of the ER, the largest endogenous Ca^{2+} store in endothelial cells (Moccia et al 2012a, Sun et al 2017). The subsequent opening of the channel causes the release of Ca^{2+} from the ER, along the electrochemical gradient, to the cytosol, where the $[Ca^{2+}]_i$ quickly increases from 100 nM up to 1 μM (Moccia et al 2012a, Sun et al 2017). For this reason, InP_3Rs regulate several cell functions such as proliferation, migration and gene expression (Berridge 2009). Vascular endothelial cells (Hertle & Yeckel 2007, Mountian et al 1999, Sun et al 2017) and ECFCs (Faris et al 2020b) express all the three isoforms of $InsP_3Rs$ ($InsP_3R1$-3), however the expression pattern changes depending on the vascular bed and the species. $InsP_3R$ are primed by $InsP_3$ thereby becoming sensitive to ambient Ca^{2+} concentration (≈50-200 nM), conversely higher $[Ca^{2+}]_i$ inhibits the channel opening (Prole & Taylor 2019). The three isoforms present different affinity for $InsP_3$ ($InsP_3R2$ > $InsP_3R1$ > $InsP_3R3$) and different sensitivity to Ca^{2+}-dependent inhibition (Foskett et al 2007). Therefore, $InsP_3R1$ and $InsP_3R2$ are more prone to induce long-lasting Ca^{2+} oscillations, while $InsP_3R3$ mediate more likely a monophasic Ca^{2+} signal (Foskett et al 2007, Sun et al 2017). $InsP_3Rs$-dependent endogenous Ca^{2+} release may be amplified

by the engagement of the adjacent ryanodine receptors (RyRs) through the Ca^{2+}-induced Ca^{2+} release (CICR) process (Moccia et al 2012b). RyRs exist in three isoforms (RyR1-3) in mammalian cells and modulate several cell functions, such as muscle contraction, insulin release from pancreatic β-cells, and release of vasoactive mediators from endothelial cells (Santulli et al 2018). However, only RyR3 has been found in a limited percentage (5-25%) of vascular endothelial cells (Kohler et al 2001), and they are absent in ECFCs (Sanchez-Hernandez et al 2010, Zuccolo et al 2016).

It is important to recall that emerging evidence pointed out that also the endolysosomal (EL) system is an important Ca^{2+} reservoir within endothelial cells, and it interacts with the ER to generate pro-angiogenic outcomes (Favia et al 2014, Moccia et al 2018a) (**Figure 4**). The EL Ca^{2+} store is targeted by the second messenger nicotinic acid adenine dinucleotide phosphate (NAADP), which gates the novel members of the voltage-gated Ca^{2+} channels, TPC1 and TPC2 (Patel 2015). Notably, TPC and NAADP regulate several cell functions, such as membrane trafficking nutrient sensing, autophagy, and proliferation (Faris et al 2019, Patel 2015). NAADP is thought to be produced by the multifunctional CD38 enzyme, and it is generated in endothelial cells following the autacoid stimulation (e.g histamine) (Esposito et al 2011). EL Ca^{2+} release is the base of the so called "trigger hypothesis" proposed by Antony Galione (Galione 2015), according to which TPC-dependent Ca^{2+} efflux from EL system is amplified into a regenerative Ca^{2+} wave by the recruiting of the juxtaposed (< 30 nm) $InsP_3Rs$ (Galione 2015). Nevertheless, the crosstalk between EL system and the ER is bidirectional, as a matter of a fact $InsP_3Rs$ may refill acidic vesicles with ER-derived Ca^{2+} (Ronco et al 2015, Yang et al 2018).

1.2.1.2 Extracellular Ca^{2+} influx induced by pro-angiogenic factors: SOCE

SOCE is the principal Ca^{2+} entry pathway in non-excitable cells, such as endothelial cells and ECFCs (Moccia et al 2015b, Prakriya & Lewis 2015), and it refills the ER Ca^{2+} reservoir, regulate gene expression, cell cycle, nitric oxide (NO) release and cyclic AMP production (Parekh 2007, Prakriya & Lewis 2015). SOCE is a key player in the endothelial Ca^{2+} influx induced by pro-angiogenic cues (Groschner et al 2017), and it is activated by the $InsP_3R$-dependent ER Ca^{2+} depletion. In this view, the single pass ER membrane protein STIM1 detects the reduction in ER Ca^{2+} levels in response to pro-angiogenic stimuli and undergoes an intricate conformational reorganization that results in a translocation of STIM1 oligomers in the external ER *cisternae*. Herein, STIM1 oligomers gather into specific clusters, known as *puncta*. The *puncta* are tightly close (≈20 nm) to the plasma membrane, where they may interact with Orai1 proteins, the pore-forming subunit of SOCE (Abdullaev et al 2008, Li et al 2011). Orai1 channels are highly Ca^{2+} permeable hexamers that mediate the Ca^{2+}-release activated Ca^{2+} current (I_{CRAC}) (Prakriya & Lewis 2015). I_{CRAC} is characterized by an extremely low unitary Ca^{2+} conductance (10-25 fS), very positive reversal potential ($E_{rev} \approx +60$ mV), high selectivity for Ca^{2+} compared to the monovalent cations ($P_{Ca}/P_{Na} > 1000$) and inwardly-rectifying current-to-voltage (I-V) relationship (Prakriya & Lewis 2015). STIM1 and Orai1 mediate SOCE in different endothelial cells, such as human umbilical vein endothelial cells (HUVECs) (Antigny et al 2011,

Brandman et al 2007, Daskoulidou et al 2015, Di Giuro et al 2017, Zhou et al 2014), human aortic endothelial cells (HAECs) (Daskoulidou et al 2015), human pulmonary artery endothelial cells (HPAECs) (Abdullaev et al 2008) and in HUVEC-derived cell line, EAhy926 (Antigny et al 2011, Di Giuro et al 2017). Vascular endothelial cells also express the other STIM isoform (STIM2) and Orai isoforms (Orai2 and Orai3) (Daskoulidou et al 2015, Zuccolo et al 2019). STIM2 is a weaker activator of Orai1, and it is featured by a higher affinity for ER Ca^{2+} (≈ 500 μM), for this reason STIM2 is activated by a lower depletion of ER store, thereby activating Orai1 and SOCE in HUVECs (Brandman et al 2007). On the other hand, Orai2 and Orai3 serve as dominant negative of Orai1-dependent Ca^{2+} entry (Eckstein et al 2019, Vaeth et al 2017). Furthermore, SOCE in endothelial cells may involve the TRPC1 and TRPC4 channels (Cioffi et al 2012). For instance, one subunit of TRPC1 interact with two TRPC4 to form a supramolecular ternary complex in vascular endothelial cells (Cioffi et al 2010, Cioffi et al 2012). Both could interact with STIM1 that confers the sensitivity to ER Ca^{2+} to the complex (Cioffi et al 2010). In addition, Orai1 may associate with TRPC4 and potentially with TRPC1 upon ER Ca^{2+} depletion, thereby reinforcing the Ca^{2+}-selectivity of the channel pore (Cioffi et al 2012).

1.2.1.3 The Ca^{2+}-dependent decoders in angiogenesis

Several Ca^{2+}-activated decoders transform the increase in endothelial $[Ca^{2+}]_i$ into a pro-angiogenic output. The most important are: extracellular signal-regulated kinase (ERK1/2) (Andrikopoulos et al 2017, Favia et al 2014, Inoue & Xiong 2009), phosphoinositide 3-kinases (PI_3K)–protein kinase B (Akt) (Favia et al 2014, Lee et al 2010), Ca^{2+}/CaM-dependent protein kinase II (CaMKII) (Ashraf et al 2019, Chen et al 2018), endothelial NO synthase (eNOS) (Brouet et al 2001, Faehling et al 2002, Favia et al 2014), calpain, myosin light-chain kinase **(**MLCK) (Negri et al 2019) and the transcription factors cAMP responsive element binding protein (CREB), nuclear factor of activated T cells (NFAT) and nuclear factor kappa enhancer binding protein (NF-κB) (Kim et al 2001, Kurusamy et al 2017, Lodola et al 2019a, Rozen et al 2018). For instance, low doses of VEGF induces intracellular Ca^{2+} oscillations that induce the nuclear translocation of NFAT and promote endothelial cell proliferation; conversely higher VEGF doses lead to a biphasic increase of the $[Ca^{2+}]_i$ that stimulate migration through the Ca^{2+}-dependent effector MLCK (Noren et al 2016). In accord, VEGF can mediate repetitive Ca^{2+} oscillations in either tip or stalk cells sprouting from the dorsal aorta in zebrafish (Yokota et al 2015). Moreover, VEGF-dependent endothelial Ca^{2+} oscillations were fundamental for the formation of endothelial filopodia and for the induction of NOTCH signalling that is a key player in the coordination of vascular morphogenesis in zebrafish (Savage et al 2019).

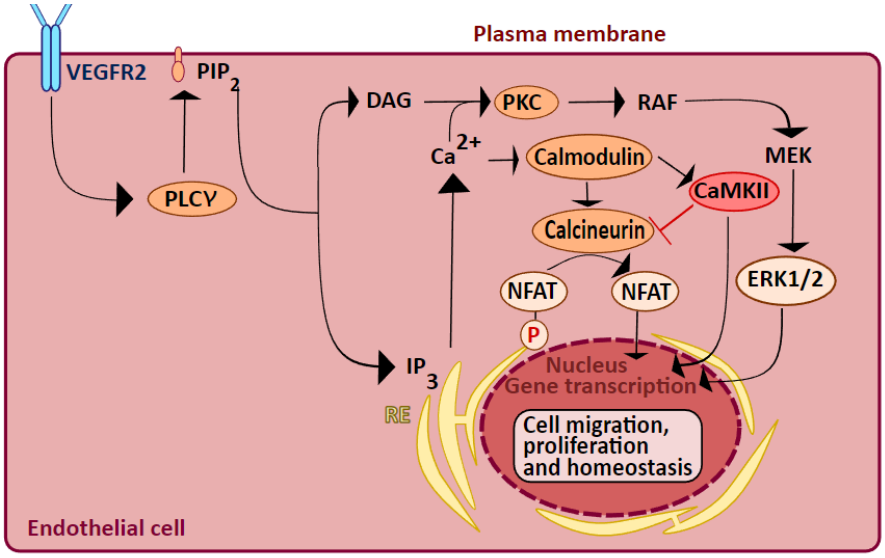

Figure 5 Role of endothelial Ca^{2+} signalling pathways in vasculogenesis and angiogenesis. VEGF targets VEGFR2 thereby leading to the activation of PLCγ and the following $InsP_3$-dependent Ca^{2+} release from the ER. The resulting increase in $[Ca^{2+}]_i$ activates the Ca^{2+}-dependent decoders, such as calmodulin, which in turn activates calcineurin and CaMKII. Calcineurin dephosphorylates NFAT, thereby causing its translocation into the nucleus, where it induces the transcription of genes responsible for cell proliferation and migration. On the other hand, CaMKII inhibits calcineurin activity, but promotes angiogenesis by phosphorylating several targets (i.e., Akt and Src, not shown). In addition, the increase in $[Ca^{2+}]_i$ stimulates cytosolic protein kinase C (PKC) relocation toward the plasma membrane, where it is activated by DAG and stimulates ERK1/2 phosphorylation cascade. Modified from (Negri et al 2020).

1.2.2 Ca^{2+} SIGNALLING IN ECFCs

ECFCs maintain the resting Ca^{2+} levels through most of the same mechanisms described above, which are SERCA and PMCA, while they do not seem to expression the endothelial NCX isoforms (Poletto et al 2016). Likewise, the increase in $[Ca^{2+}]_i$ induced by exogenous stimulation is mediated both by extracellular Ca^{2+} entry and endogenous Ca^{2+} mobilization. Intracellular Ca^{2+} release is operated mainly by $InsP_3R1$-3 (Dragoni et al 2011) on the ER and by TPC1 (Zuccolo et al 2016) on EL vesicles. Notably, the main PLC isoform involved in $InsP_3$ production in ECFCs is PLCβ2, which is activated following $G_{q/11}$PCR stimulation (Maeng et al 2009). Conversely, it is not clear if both PLCγ1 and PLCγ2 isoforms are expressed in these cells and mediate the Ca^{2+} response upon TKR stimulation by pro-angiogenic growth factors (Berridge et al 2003).. The main mechanism involved in extracellular Ca^{2+} entry induced by chemical stimulation is SOCE (Sanchez-Hernandez et al 2010) that is mediated by STIM1, Orai1 and TRPC1 (Lodola et al 2012, Sanchez-Hernandez et al 2010). As mentioned above, ECFC Ca^{2+} signals are fundamental to drive their angiogenic activity. For instance, upon an ischemic insult, multiple chemokines, such as SDF-1α, are released in circulation where they recruit circulating ECFCs or promote ECFC mobilization and stimulate ECFC physical engraftment within nascent neovessels (Maeng et al 2009, Tu et al 2016). SDF-1α, in turn, elicits a biphasic increase in $[Ca^{2+}]_i$ in circulating ECFCs that is triggered by the G_iPCR, CXCR4, initiated by $InsP_3$-dependent ER Ca^{2+} mobilization and sustained by SOCE (Dragoni et al 2014, Zuccolo et al 2018). The interaction between $InsP_3Rs$ and SOCE engages the PI_3K/Akt and ERK1/2 signalling pathways, which in turn

mediate ECFC migration *in vitro* and neovessel formation *in vivo* (Zuccolo et al 2018). Likewise, VEGF is massively released by ischemic tissues to induce circulating ECFC integration in the damaged vessels (Joo et al 2015, Su et al 2017). It has been demonstrated that VEGF induced repetitive oscillations in $[Ca^{2+}]_i$ by binding VEGFR2 in circulating (Dragoni et al 2011) and UCB-derived ECFCs (Dragoni et al 2013). Specifically, VEGF-dependent Ca^{2+} oscillations in circulating ECFCs are mediated by the rhythmical ER Ca^{2+} efflux through $InsP_3Rs$ followed by SERCA-driven Ca^{2+} uptake into the ER lumen. In addition, SOCE is important to maintain the spiking response by restoring the ER Ca^{2+} levels during prolonged stimulation (Dragoni et al 2011). Of note, UCB-derived ECFCs show higher and more frequent oscillations (Moccia et al 2015a), which is indicative of their higher sensitivity to VEGF (Ingram et al 2004). In accord, UCB-derived ECFCs express TRPC3 that mediates an influx of Ca^{2+} influx that triggers the complex interplay between endogenous Ca^{2+} release and SOCE (Dragoni et al 2013). For this reason, TRPC3 overexpression has been proposed as an alternative strategy to rejuvenate the reparative capacity of aging ECFCs, typical of cardiovascular patients (Moccia et al 2018b). VEGF stimulates proliferation and *in vitro* neovessel formation through the Ca^{2+}-dependent nuclear translocation of NF-κB (Dragoni et al 2011). The putative responsible for the activation of NF-κB is CaMKII, which is known to be sensitive to Ca^{2+} oscillations (Aromolaran et al 2007) and to stimulate ECFC proliferation (Wu et al 2017). Finally, a recent investigation revealed that TPC1 triggers VEGF-induced proangiogenic Ca^{2+} oscillations in circulating ECFCs by promoting EL Ca^{2+} release (Moccia et al 2021). According to the trigger hypothesis, lysosomal Ca^{2+} efflux could be amplified by juxtaposed $InsP_3Rs$ on ER cisternae (Zuccolo et al 2015). However, we cannot exclude that InP_3R-mediated Ca^{2+} release is necessary to refill EL Ca^{2+} store (Faris et al 2018, Yang et al 2018), and that NAADP interacts with $InsP_3$ to start the rhythmic Ca^{2+} oscillations in circulating ECFCs.

1.2.3 TARGETING THE INTRACELLULAR Ca^{2+} TOOLKIT TO IMPROVE THE THERAPEUTIC OUTCOME OF ECFCs

The ECFC shortage in peripheric blood represents the main limitation for their therapeutic use; however, multiple strategies have been proposed to prime ECFCs *ex vivo*, thereby increasing their angiogenic activity (Moccia et al 2019, Smadja 2019). For instance, *ex vivo* expansion could be increased by replacing foetal bovine serum (FBS) with human platelet lysate in the culture medium (Siegel et al 2018, Tasev et al 2015). Furthermore, ECFC proliferation is increased with pro-angiogenic cues, such as fucoidan (Lee et al 2015, Sarlon et al 2012), SDF-1α (Zemani et al 2008), with the erythroid growth factor (EPO) (Bennis et al 2012, Hache et al 2016), with nicotine (Yu et al 2011) and with an acidic growth medium (Mena et al 2014). Intriguingly, ECFC expansion before infusion may be promoted by an increase in $[Ca^{2+}]_i$ (Dragoni et al 2015b, Lodola et al 2017a, Moccia & Guerra 2016). For instance, SDF-1α, which can prime ECFCs to boost dependent neovascularization and rescue blood flow in a mouse model of hindlimb ischemia (Zemani et al 2008), has been shown to induce a biphasic elevation in $[Ca^{2+}]_i$ that is shaped by $InsP_3$-induced ER Ca^{2+} mobilization and SOCE

(Zuccolo et al 2018). Similarly, the liposomal delivery of NAADP stimulated ECFC proliferation in a Ca^{2+}-dependent manner (Moccia et al 2018a), which is consistent with its triggering role in VEGF-induced intracellular Ca^{2+} oscillations. Similarly, arachidonic acid promotes ECFC expansion via TRP Vanilloid 4 (TRPV4)-mediated Ca^{2+} signals and eNOS activation (Dragoni et al 2015a, Zuccolo et al 2016). In addition, a promising strategy to improve ECFCs' angiogenic potential is to genetically equip them with the pro-angiogenic signalling pathways endowed to UCB-derived ECFCs, which are featured by a remarkably higher proliferative rate and clonogenic potential (Moccia et al 2018a). For instance, the plasmid vector-mediated overexpression of NADPH-oxidase (NOX) 4, which induces pro-angiogenic ROS signalling, was found to enhanced ECFC-dependent angiogenesis (O'Neill et al 2019). Notably, NOX4 is the most abundant NOX isoform in endothelial cells, and it is implicated in the proliferation and migration regulatory processes in ECFCs derived from saphenous vein and mammary artery (Hakami et al 2017). In this context, O'Neill and coworkers demonstrated that the transplantation of the modified ECFCs ameliorated neovessel formation and blood flow in a mouse model of hindlimb ischemia (O'Neill et al 2019). In addition, it has been proposed that circulating ECFCs could be engineered with TRPC3 before the transplantation into ischemic tissues (Moccia et al 2018a). TRPC3 is activated by the PLC product, DAG, and sustains Ca^{2+} influx induced by extracellular stimuli in vascular endothelial cells (Andrikopoulos et al 2017, Yeon et al 2014). A recent study showed that VEGF-dependent intracellular Ca^{2+} oscillations are increased in UCB-ECFCs due to the activation of TRPC3. The authors demonstrated that TRPC3-mediated Ca^{2+} entry favoured the interplay between $InsP_3Rs$ and SOCE that patterns the oscillatory response (Dragoni et al 2013). The oscillatory pattern, in turn, underpins the higher proliferative response to VEGF observed in UCB-ECFCs as compared to circulating ECFCs (Dragoni et al 2013, Ingram et al 2004). TRPC3 could increase ECFC proliferation through two different mechanisms. First, the increased frequency of VEGF-dependent intracellular Ca^{2+} oscillations may amplify the engagement of Ca^{2+}-dependent proangiogenic decoders (e.g., NF-κB and ERK/MAPK pathway) (Moccia et al 2018a). Second, TRPC3 could physically associate with several Ca^{2+}-sensitive decoders that are selectively recruited by local TRPC3-mediated Ca^{2+} signals (e.g., CaMKII, eNOS and PI_3K/Akt pathway) (Moccia et al 2018a). SOCE represent an alternative target due to its activity in the maintenance of VEGF- and SDF-1α-dependent intracellular Ca^{2+} signals in ECFCs (Dragoni et al 2011, Zuccolo et al 2018). Although technically challenging, the molecular components of SOCE machinery, i.e., STIM1, Orai1, and TRPC1, could be overexpressed in ECFCs to enhance their regenerative potential (Moccia et al 2012c). Likewise, the genetic manipulation of TPC1 levels could enhance ECFC-dependent neovascularization (Moccia et al 2018a), as suggested by the recruitment of NAADP signalling by many pro-angiogenic cues [e.g. arachidonic acid (Zuccolo et al 2016) and VEGF (Moccia et al 2021). In agreement with this hypothesis, delivery of exogenous NAADP via a liposomal preparation stimulated ECFC proliferation in a Ca^{2+}-dependent manner (Di Nezza et al 2017). Taken together,

these investigations further demonstrated the crucial role of Ca^{2+} signals in ECFCs' angiogenic activity and their potential role in the treatment of cardiovascular disorders (CVDs).

1.3 TRP CHANNELS AND Ca^{2+} SIGNALS

1.3.1 TRP CHANNELS: DISCOVERY

TRP channels were discovered in 1969 in a blind mutant strain of *Drosophila melanogaster*, which was able to fly normally in the presence of low light conditions but not under bright lights. Interestingly, the mutants did not show any difference with the wild-type flies in the external morphology and histological properties of retinal structure. However, they presented an altered electroretinogram (Cosens & Manning 1969). Subsequent investigation showed, indeed, that short light stimuli elicited a similar electric response in wild-type and mutant individuals. Conversely, the mutants' retinal cells response to prolonged light stimulation was featured by a transient decay in the receptor potential (*transient receptor potential, trp*), opposite to the wild-type more sustained receptor potential response (Minke 1977, Minke et al 1975). Nevertheless, the isolation (Montell et al 1985) and cloning of the entire *trp* cDNA (Montell & Rubin 1989) occurred several years later and it enriched the knowledge of the *trp* gene product function. As a matter of fact, Montell and co-workers noticed, through hydropathy plots, that the *trp* gene product consisted in a membrane protein featured by intracellular amino- and carboxy- termini and six to eight transmembrane domains, evocative of the earlier characterized voltage-dependent proteins. For these reasons, the authors proposed that the *trp* gene could encode for an ion channel (Montell & Rubin 1989). The hypothesis was confirmed through electrophysiological investigation of *trp* and the related gene *trp-like (trpl)* in the Sf9 insect cells, where *trp* encoded a Ca^{2+}-permeable non-selective cation channel (Vaca et al 1994). Subsequently, additional studies demonstrated that light-sensitive membrane conductance in flies' photoreceptors is driven by *trp*- and its homolog *trpl*-mediated Na^{+} and Ca^{2+} currents. In particular, *trpl* was thought to be responsible of the residual light-induced current in *trp* mutants (Hardie 1992). Three years later, the Bennett's group demonstrated the expression of homologues Drosophila *trp* gene in vertebrate (e.g. mouse brain and Xenopus oocytes) (Petersen et al 1995), and two independent groups identified the first TRP channel in humans, where it was named as TRP Canonical 1 (TRPC1) (Wes et al 1995, Zhu et al 1995). The human TRPC1 discovery starts a 10 year long scientific race to clone and characterize all the TRP channels. Nowadays, all the mammalian 28 TRP channels have been identified and are still studied in physiological and pathophysiological conditions by being a suitable therapeutic target for several diseases, including CVDs.

1.3.2 TRP CHANNEL TAXONOMY AND CHANNEL STRUCTURE

Mammalian TRP channels superfamily is composed by 28 non-selective cation channels, which are divided into six subfamilies based on sequence homology: TRP Canonical (TRPC1-7), TRP Vanilloid (TRPV1-6), TRP Melastatin (TRPM1-8), TRP Ankyrin 1 (TRPA1), TRP Mucolipin (TRPML1-3), and TRP Polycystin (TRPP) (Earley & Brayden 2015, Gees et al 2010, Smani et al 2018, Thakore & Earley 2019) (**Figure 6**). Nevertheless, TRPC2 is only a pseudo-gene in humans (Gees et al 2010).

Furthermore, the TRPP subfamily is an exception, it consists in eight members but only TRPP2, TRPP3 and TRPP5 display the molecular structure and function of an ion channel (Gees et al 2010).

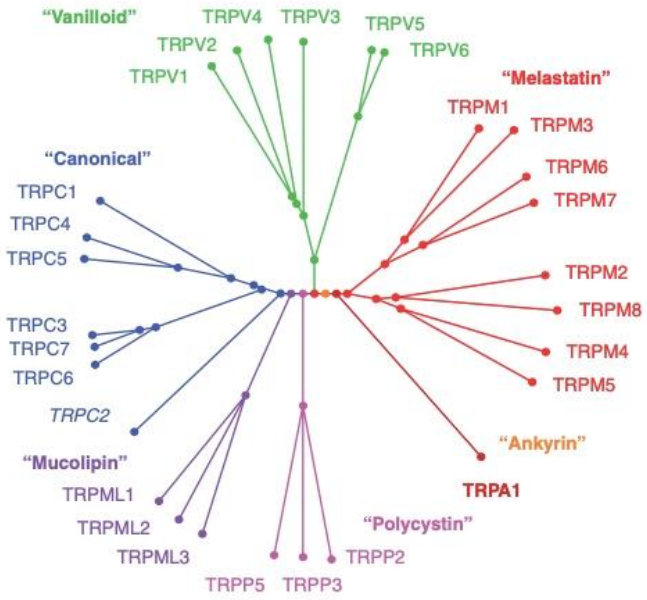

Figure 6 Phylogenetic tree of mammalian TRP channels. (Gees et al 2010).

The TRP subunits consist in 553-2022 amino acids polypeptides (~ 64-230 kDa) organised in six transmembrane (TM1-6) α-helices, with cytosolic amino- and carboxy-termini and a re-entrant loop between TM5 and TM6. Furthermore, immediately distal to TM6, a ~25-residue conserved TRP domain has been identified in TRPC, TRPM and TRPV subfamilies. The TRP domain is characterized by two highly conserved six-amino acids elements, known as TRP-box1 and TRP-box2, which delimit a more variable central region (Rohacs 2014). Three variations of the Glu-Trp-Lys-Phe-Ala-Arg (EWKFAR) motif constitute TRP-box1 that provides the binding site for phosphatidylinositol phosphates (e.g., PIP_2) (Birnbaumer 2009) or is engaged in subunit assembly (Venkatachalam & Montell 2007). TRP-box 2 is more variable between different TRPC and TRPM subunits; however, it consists in a proline-rich sequence (Venkatachalam & Montell 2007). As mentioned in the previous paragraph, the overall structure is quite similar to that of voltage-gated K^+ channels, although TRP channels miss the voltage-sensor in TM4 (Gaudet 2008). Nevertheless, the amino- and carboxy-terminal tails bordering the TM domain may highly differ in length between different TRP subfamilies and may perform diverse functions, such as engaging and providing regulatory domains for cytosolic kinases and other cellular/cytoskeletal proteins (Gaudet 2008, Gees et al 2010). For instance, multiple ankyrin repeats (ARDs) feature the amino-terminal of the TRPC, TRPV and TRPA subunits. TRPA1 presents the higher number of repeats (i.e., ~15-19), which are involved in channel regulation by chemical and mechanical stimuli (Earley & Brayden 2015). Moreover, the TRPC carboxy-terminal is endowed with the calmodulin (CaM)-$InsP_3R$-binding (CIRB) sites and Ca^{2+}-binding EF hands domains. Intriguingly, the TRPM6 and TRPM7 carboxy-termini present a serine-

threonine kinase activity, while an ADP-ribose-binding NUDIX phosphohydrolase domain has been found in the TRPM2 carboxy-terminal (Earley & Brayden 2015).

The functional TRP channel is composed of four subunits, which may assemble in homomeric and heteromeric complexes around a central pore lined by TM5, TM6 and the connecting loop (Gaudet 2008). Although all TRP subunits preferentially aggregate into homomeric structures (Lepage & Boulay 2007), with the possible exception of TRPC1 (Storch et al 2012), they may form also heteromeric channels that have been widely described in naïve cells, including vascular endothelial cells (Cheng et al 2010). Heteromerization has been widely studied in the TRPC subfamily. Indeed, TRPC1 may assemble with TRPC3, TRPC4 or TRPC5 (Smani et al 2018). In addition, TRPC3, TRPC6 and TRPC7 may form a functional heteromeric element both in heterologous expression systems (Hofmann et al 2002) and in naïve cells (Goel et al 2002). Nevertheless, also TRPV and TRPM heteromeric structures have been described. For instance, every two members of TRPV1-4 may assemble in heteromeric channels (Cheng et al 2010, O'Leary et al 2019). Likewise, TRPV5 and TRPV6 may assemble into heteromeric complexes in the kidney and gastrointestinal tract, but they are yet to be reported in vascular endothelium (Cheng et al 2010, Thakore & Earley 2019). Likewise, TRPM6 and TRPM7 may easily assemble thanks to their close similarity (Voets et al 2004). Finally, TRP channels from different subfamilies may interact to form hetero-tetramers, such as TRPC1/TRPV6 (Schindl et al 2012), TRPV4/TRPC6 (Goldenberg et al 2015), TRPV4/TRPC1 (Ma et al 2011), TRPC1/TRPP2 (Berrout et al 2012), TRPP2/TRPV4 (Stewart et al 2010) and TRPML3/TRPV5 (Guo et al 2013).

1.3.3 TRP CHANNELS IN ENDOTHELIAL CELLS

TRP channels constitute the most versatile signal transduction pathway in vascular endothelium because of their capacity to integrate a wide array of chemical and physical stimuli (Negri et al 2019, Smani et al 2018, Thakore & Earley 2019). In accord, the majority of TRP channels have been found in mammalian vascular endothelial cells, including TRPC1/3-7; TRPV1-2/4; TRPP1-2, TRPA1 and TRPM1-4/6-8. However, they are distributed differently through the vascular tree and between different species (Wong & Yao 2011). For instance, TRPC1 is expressed in mouse, but not rat, aortic endothelial cells, TRPC3 is present in human, but not in bovine, pulmonary artery endothelial cells. In addition TRPC1-6 have been found in mouse brain microvascular endothelial cells, but not in human cells (Negri et al 2019). Notably, the same endothelial cell types express different TRP isoforms by igniting the debate on the molecular remodelling of cells in culture and by confirming a different TRP expression *in vivo* compared to *in vitro* studies (Earley & Brayden 2015, Moccia et al 2012b, Smani et al 2018). Therefore, *in vivo* investigations are necessary to confirm the endothelial TRP channels expression and role in different vascular compartments. As mentioned earlier, the homomeric expression is complicated by the presence of several heteromeric complexes, which expand the array of gating and biophysical properties of TRP channels. Of note, TRPV4/TRPC1 can

assemble into functional channels into vascular endothelial cells from different vascular districts (Negri et al 2019), including HUVECs (Ma et al 2010), rabbit mesenteric artery endothelial cells (Greenberg et al 2017), and mouse aortic endothelial cells (MAECs) (Ma et al 2011), whereas TRPV4 has been shown to interact with TRPC1 and TRPP2, to form a flow-sensitive mechanosensor in naïve vascular endothelial cells (Du et al 2014).

1.3.4 TRANSIENT RECEPTOR VANILLOID 1 (TRPV1)

The TRPV1 channel, also named vanilloid receptor 1 (VR1), is the most studied and characterized TRPV member (Caterina et al 1997). It shares the molecular structure with the other TRP channels, described in paragraph 1.3.2. TRPV channels are featured by the conserved TRP domain, however they lack the TRP-box2. Surprisingly, TRPV1 presents a TRP-domain with a similar configuration and function as the one in TRPC channels (Smani et al 2018). Furthermore, the TRPV1 amino-terminal tail is enriched with several ARDs that are responsible for the interaction with cytoskeleton, with other TRP subunits for tetramerization and for the detection of membrane mechanical deformation (Gaudet 2008). TRPV subunits can assemble into homo- and heterotetramers, although it is not clear which combinations are present in the vascular system (Earley & Brayden 2015). It has long been known that TRPV1 and TRPV4 subunits form a heteromeric channel that is exclusively located on the plasma membrane (Cheng et al 2007). In accord, TRPV4 was found to associate with TRPV1 into a functional heteromeric channel complex in mouse primary retinal microvascular endothelial cells (RMECs) (O'Leary et al 2019). Nevertheless, TRPV1 hardly interacts with TRPV4 in ECFCs, since the Ca^{2+} response to a specific TRPV4 agonist (GSK1016790A) was not inhibited by capsazepine (Dragoni et al 2015a).

1.3.4.1 TRPV1 structure

TRPV1 has been the first TRP channel to be solved at cryo-EM resolution (Cao et al 2013, Liao et al 2013). This analysis confirmed that each TRPV1 subunit consists of six TM domains arranged around a central ion conduction pathway constituted by TM5 and TM6 and the re-entrant pore loop between them (**Figure 7**). The highly conserved TRP domain forms an interfacial helix that is positioned at the carboxy-terminus of TM6 and interacts with the pre-TM1 helix and the cytosolic linker between TM4 and TM5, thereby enabling channel ligands to allosterically modulate pore conformation. The outer mouth of TRPV1 tetramers is remarkably wide, although it is followed by a dual-gate channel pore presenting two restriction points at G643 (4.6 Å, the selectivity filter) and at I679 (5.3 Å, the hydrophobic lower gate) that are closed in the non-conducting state. However, TRPV1 activation requires major structural rearrangements in the ion conduction pore, including the re-entrant loop, the selectivity filter, and the lower gate. Capsaicin, which is a potent activator of the channel, binds to a cytosolic pocket in proximity of the inner mouth and gates TRPV1 by pulling TM6 from adjacent subunits apart and dilating the lower gate, while the constriction at the selective filter is not relieved. Conversely, the spider toxin binds to an extracellular site near to the re-entrant pore and gates TRPV1

by tilting the pore helix away from the central axis of the ion conduction pathway, thereby widening the selectivity filter from 4.6 Å to 7.6 Å. At the same time, the channel pore is further expanded by disruption of the hydrogen bonds bridging the loops between TM5 and TM6 (Cao et al 2013, Liao et al 2013).

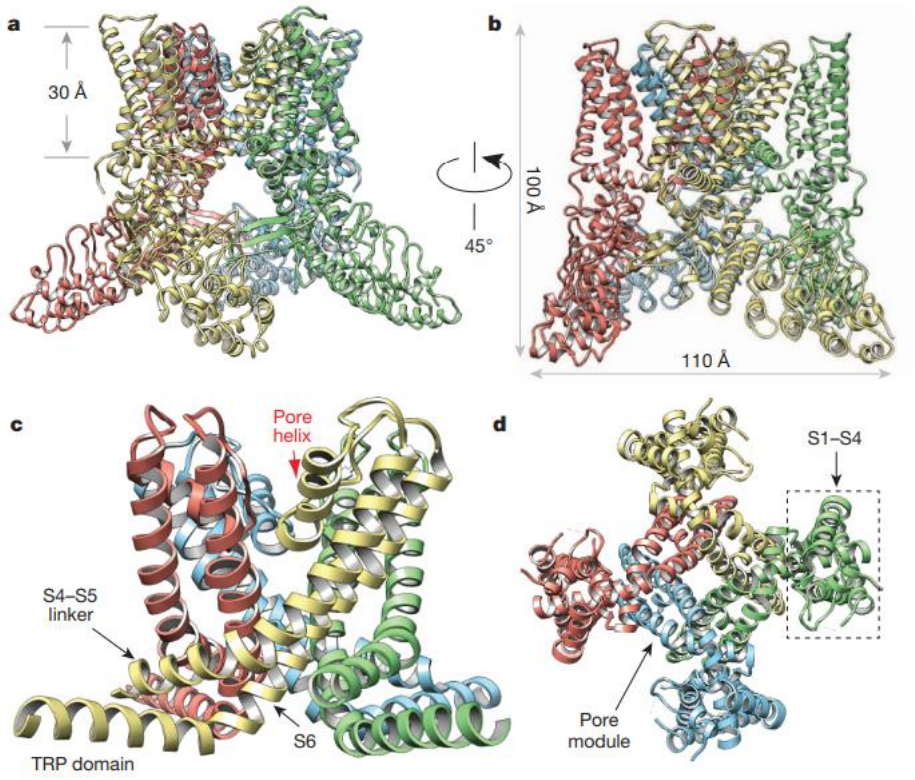

Figure 7 TRPV1 structure. TRPV1 subunit consists of six TM domains arranged around a central ion conduction pathway contributed by TM5 and TM6 and the re-entrant pore loop between them (Liao et al 2013).

1.3.4.2 TRPV1 biophysical properties and gating mechanisms

TRPV1 is a non-selective cation channel that presents an outwardly rectifying current to voltage (I-V) relationship with a negative slope conductance region at membrane potentials more negative than -70 mV (Rosenbaum & Simon 2007). TRPV1 is featured by similar permeabilities to Na^+ and K^+, but it is considerably more permeable to Ca^{2+} and Mg^{2+} ($P_{Ca}/P_{Na} = 9.6$; $P_{Mg}/P_{Na} = 5$) and displays a surprisingly high permeability to large cations (Munns et al 2015, Rosenbaum & Simon 2007). Being mainly located on the plasma membrane, TRPV1 activation results in extracellular Ca^{2+} entry down the electrochemical gradient at physiological membrane potentials (Rosenbaum & Simon 2007). TRPV1 is a polymodal cation channel activated by several mechanical and chemical stimuli, such as extracellular protons, products of plants origin (e.g., capsaicin and gingerol), noxious heat (>42 °C), spider-derived vanillotoxins, and hydrogen sulphide (H_2S) (Caterina et al 1997, Geron et al 2017, Kuzhikandathil et al 2001, Negri et al 2019, Patacchini et al 2005, Siemens et al 2006, Tominaga et al 1998). TRPV1 may also be gated by some endogenous agonists, including fatty acids conjugated with amines (e.g., N-arachidonylethanolamine (AEA, anandamide), N-arachidonoyldopamine (NADA), N-oleoylethanolamine (OLEA), N-arachidonolylserine, and various N-acyltaurines and N-

acylsalsolinols), ATP, adenosine, polyamines (e.g., as spermines and spermidines), prostaglandins, leukotriene B4 and pH < 5.9 (Ahern et al 2006, Appendino et al 2008, Huang et al 2002, McNamara et al 2005, Vriens et al 2009, Xu et al 2005). Interestingly, an elegant investigation by the Nilius' group showed that TRPV1 is also sensitive to membrane depolarization and that heat and capsaicin can function as gating modifiers through voltage-to-current relationship shifts (Voets et al 2004). Indeed, at room temperature (22–23 °C), the voltage-dependent activation of TRPV1 requires a strong positive shift in the membrane potential (up to around +150 mV). Conversely, at higher temperatures, i.e., 40–45 °C, TRPV1 activation may already occur at -50 mV. This means that heat and capsaicin induce the channel to open at more physiological voltages (Voets et al 2004). It has been demonstrated that also extracellular protons act in a similar manner, thereby promoting TRPV1 activation at resting temperature, which provides an additional explanation of TRPV1 involvement in inflammatory conditions (Aneiros et al 2011). Finally, TRPV1 undergoes desensitization, mainly through a Ca^{2+}-dependent mechanism. Extracellular Ca^{2+} influx, mediated by TRPV1 itself, activates an inhibitory feedback signal by recruiting multiple signalling pathways. First, incoming Ca^{2+} could engage the Ca^{2+}-dependent phosphatase, calcineurin, to counteract protein kinase C (PKC)- and protein kinase A (PKA)-dependent phosphorylation. Second, Ca^{2+} could promote desensitization by binding to calmodulin (Vennekens et al 2008).

1.3.5 TRPV1 IN THE ENDOTHELIUM

TRPV1 has been discovered in neuronal cells, and in particular in rat dorsal root ganglia (DRG) (Caterina et al 1997), and rapidly found also in trigeminal (TG) and nodose (NG) ganglia (Tominaga et al 1998). Multiple investigations until our days have proved TRPV1 expression also in non-neuronal cell, e.g., smooth muscular cells, keratinocytes, urothelium, liver, glial cells, mast cells, and macrophages (Caterina & Julius 2001, Vennekens et al 2008). Regarding the vasculature, TRPV1 is widely expressed in the plasma membrane of the intimal layer of peripheral blood vessels, and in UCB-derived (Hofmann et al 2014) and circulating ECFCs. TRPV1 expression has also been found in the ER in several cell types, including rat nociceptive neurons (Karai et al 2004), and breast (Lozano et al 2018) and prostate (Pecze et al 2016a) cancer cell lines. Endogenous localization of TRPV1 has been recently described in bovine retinal microvascular endothelial cells (RMECs) (O'Leary et al 2019). and in HUVECs, in which it has been detected in mitochondria (Otto et al 2020) It is, however, still unclear whether and how intracellular TRPV1 contributes to endothelial Ca^{2+} signalling.

1.3.6 TRPV1 ACTIVATION PROMOTES ANGIOGENESIS

TRPV1 has been showed to be involved in the angiogenic process by several evidence (Earley & Brayden 2015, Negri et al 2019, Smani et al 2018, Thakore & Earley 2019). However, two powerful TRPV1 agonists, capsaicin and piperine, were initially found to reduce angiogenesis both *in vitro* and *in vivo* (Doucette et al 2013, Min et al 2004). Min and co-workers found that capsaicin was able to inhibit VEGF-dependent DNA synthesis, proliferation, migration and *tubulogenesis* in HUVECs. In

addition, capsaicin was showed to negatively influence VEGF-induced vascularization in Matrigel plugs *in vivo* (Min et al 2004). This study, however, did not assess TRPV1 contribution in the anti-angiogenic effect of capsaicin. Furthermore, it could be supposed that chronic TRPV1 activation could induce an aberrant raise in $[Ca^{2+}]_i$, thereby inducing Ca^{2+}-dependent cell death (Moccia 2018). This hypothesis is supported by the notion that capsaicin-induced prolonged Ca^{2+} entry promotes apoptosis in prostate cancer cells (Pecze et al 2016b), breast cancer cells (Wu et al 2014), and cervical tumour cells (Ramirez-Barrantes et al 2018). On the other hand, a subsequent investigation revealed that intraperitoneal administration of evodiamine, a TRPV1 agonist, stimulated angiogenesis in Matrigel plugs *in vivo* (Ching et al 2011). TRPV1-dependent extracellular Ca^{2+} entry activated PI_3K/Akt/CaMKII pathway, which in turn led to: i) TRPV1 phosphorylation, ii) eNOS and TRPV1 physical interplay; iii) eNOS phosphorylation and, finally, iv) NO release (Ching et al 2011) (**Figure 8**). In accord, evodiamine was not able to stimulate angiogenesis when Matrigel plugs were implanted in eNOS- or TRPV1-knock out mice (Ching et al 2011). Intriguingly, it has long been known that NO promotes endothelial cell proliferation, migration, and *tubulogenesis* (Mancardi et al 2011). Furthermore, TRPV1 stimulates AMP-activated protein kinase (AMPK) phosphorylation, which supported the formation of a TRPV1-eNOS complex, thereby increasing NO release and angiogenesis both in Matrigel plugs and in an hindlimb ischemia mouse model (Ching et al 2012). In addition, TRPV1 mediates simvastatin-, erythropoietin-, epigallocatechin- 3-gallate- and 14,15-EET-induced angiogenesis. The 3-hydroxy-3-methylglutaryl-CoA reductase inhibitor simvastatin, which is used in hypercholesterolaemia and CVD therapy, promoted *in vivo* angiogenesis by inducing NO release through the formation of the TRPV1-Akt-CaMKII-AMPK-eNOS complex described above (**Figure 8**) (Su et al 2014b). The same signalling pathway is engaged to promote *tubulogenesis in vitro* and neovessel formation *in vivo* by erythropoietin (Yu et al 2017) and epigallocatechin-3-gallate, the major catechin present in the green tea (Guo et al 2015). Lastly, pharmacological (with capsazepine) and genetic (with a selective siRNA) inhibition of TRPV1 interfered with 14,15-EET-dependent Ca^{2+} influx, NO release, *in vitro* tube formation and *in vivo* angiogenesis in human mammary epithelial cells (HMECs) (Su et al 2014a). A recent work showed that TRPV1 may assemble with TRPV4 into a heteromeric complex in RMECs (O'Leary et al 2019). The TRPV1/TRPV4 channel did not induce VEGF-dependent extracellular Ca^{2+} entry and sprouting angiogenesis, but it was *per se* able to mediate Ca^{2+} influx and drive RMEC proliferation, motility and capillary-like tube formation (O'Leary et al 2019). Although, these studies outlined extracellular Ca^{2+} entry as the main mechanism whereby TRPV1 induces angiogenesis, an alternative pathway has been discovered in EA.hy926 cells (Hofmann et al 2014). Hofmann and collaborators demonstrated that TRPV1 promoted the uptake of the endogenous cannabinoid, anandamide, with a Ca^{2+}- independent mechanism. The intracellular transport of anandamide, in turn, induced EA.hy926 cell proliferation and tube formation (Hofmann

et al 2014), which confirms the emerging notion that TRP channels also stimulate angiogenesis independently on their capacity to permeate extracellular Ca^{2+} (Abdullaev et al 2008).

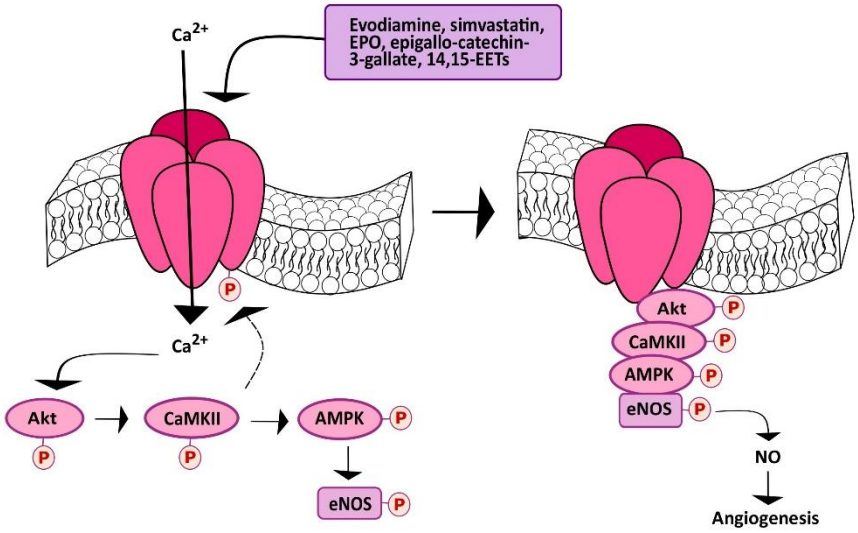

Figure 8 Proposed molecular mechanism of TRPV1-induced angiogenesis. Multiple extracellular agonists induce TRPV1-mediated Ca^{2+} influx, which in turn stimulates PI_3K/Akt/CaMKII signalling and the consequent TRPV1 and eNOS phosphorylation. Moreover, TRPV1 may work as a scaffold for the formation of a supramolecular complex made of Akt, AMPK, CaMKII and eNOS (Negri et al 2020).

TRPV channels may additionally confer temperature sensitivity to endothelial cells. For instance, Mergler and collaborators demonstrated that TRPV1 could detect heat increases to over 40 °C in human corneal endothelial cells (Mergler et al 2011). The temperature sensibility of TRPV channels in endothelial cells has been related to variation in NO release, which in turn regulates vascular tone and endothelial permeability (Mergler et al 2010, Watanabe et al 2002). Whole-body hyperthermia (41.5–42.5 °C for 15 min, from a resting temperature of 37 °C) may operate as an angiogenic stimulus in rat cardiac myocardium. Similarly, far-infrared dry sauna (39 °C for 15 min followed by 34 °C for 20 min once daily for four weeks), also known as Waon therapy, stimulated an enhancement in myocardial capillary density and ameliorated cardiac hypertrophy in hypertensive rats (Ihori et al 2016). The same approach was found to promote myocardial revascularization and attenuate maladaptive cardiac remodelling in a murine model of AMI (Sobajima et al 2011). Finally, near-infrared red optical stimulation promoted capillary growth in human subjects' skin and locally increased the temperature from 37 to 42 °C (Kim et al 2006). Of note, the increase in the whole-body and local temperature caused by these procedures was not enough to activate TRPV1. The use of TRPV1 knock out mice or the effect of Waon therapy in the presence of TRPV1 blockers are, however, needed to confirm TRPV1 involvement in the angiogenic switch observed in response to temperature increases. These studies strongly suggest that the pharmacological stimulation of TRPV1 represents a promising pathway to induce angiogenesis in the presence of cardiovascular risk factors or upon an ischemic insult.

1.3.7 TRPV1 CONTROLS THE ANGIOGENIC ACTIVITY IN ECFCs

Growing evidence showed the crucial role of Ca^{2+} signalling in circulating and UCB-derived ECFCs (Moccia 2020, Moccia & Guerra 2016), as mentioned in Paragraph 1.2.2. In addition, the control of ECFC fate is emerging as an urgent need for regenerative medicine (Griffin et al 2015). In this view, manipulating the signalling cascades that drive ECFC proliferation, migration, differentiation, and neovessels formation could ameliorate their therapeutic outcome *in vivo* (O'Neill et al 2018, Tasev et al 2016). As mentioned in Paragraph 1.2.3, Ca^{2+} signalling could also be targeted to increase the regenerative potential of autologous ECFCs (Moccia et al 2018a, Moccia et al 2018b). It has recently been demonstrated that TRPV1 is expressed and mediates extracellular Ca^{2+} entry in ECFCs (Hofmann et al 2014, Lodola et al 2019a). Notably, TRPV1 regulates ECFCs' angiogenic activity both in a Ca^{2+}-dependent and independent manner (Hofmann et al 2014, Lodola et al 2019a). An early work from Hofmann and collaborators demonstrated that TRPV1 mediates anandamide entry into a HUVEC-derived cell line (i.e., EA.h926) and in UCB-ECFCs, thereby eliciting proliferation and tube formation in a Ca^{2+}-independent manner (Hofmann et al 2014). In accord, anandamide uptake was significantly reduced by pharmacological (with SB366791) or genetic (through a siTRPV1) manipulation of TRPV1, while it was increased upon TRPV1 overexpression. Moreover, capsaicin inhibited anandamide uptake, by suggesting a form of competition for the same binding site and is an additional corroboration of TRPV1 engagement. Of note, anandamide entry was not altered by removal of extracellular Ca^{2+}, which seems to exclude a role of intracellular Ca^{2+} signalling in the downstream effects of TRPV1 (Hofmann et al 2014). Nevertheless, anandamide triggered proliferation and *tubulogenesis* in UCB-ECFCs, but this pro-angiogenic effect was abrogated by interfering with TRPV1 activity (with capsazepine) or expression (via a specific siTRPV1). It is important to point out that TRP channels, such as TRPC1 and TRPC4, have already been shown to support angiogenesis in a flux-independent manner (Negri et al 2019). Nevertheless, the evidence that TRPV1 mediates pro-angiogenic Ca^{2+} signals in vascular endothelial cells strongly suggests that it could do so also in ECFCs.

1.4 ORGANIC SEMICONDUCTORS

1.4.1 ORGANIC SEMICONDUCTORS AND CONJUGATED POLYMERS

Organic semiconductors are emerging as promising tools in biotechnology because of many attractive properties, such as mechanical flexibility, low-cost production, light weight, low temperature processing, abundant availability, and for these reasons they have been proposed to substitute their inorganic counterparts (Di Maria et al 2018, Li et al 2019). Organic semiconductors are made up by mainly carbon-carbon strong bonds and hydrogen atoms and sometimes by heteroatoms (e.g nitrogen, sulfur and oxygen), which confer them a high biocompatibility and mechanical conformability. Although they have long been thought to be electrically inert, in the '50s Pope and collaborators described the electrical conductivity in organic molecules thereby initiating the research field of Electroluminescence (Pope et al 1963). Subsequent studies by Shirakawa, Heeger and MacDiarmid demonstrated how to enormously increase the conductivity of polyacetylene, up to a level near to that typical of a metal (Shirakawa 2001). This discovery occurred in the 70' and led the three scientists to be awarded with the Nobel Prize in Chemistry in 2000. Multiple investigations revealed, indeed, that organic semiconductors absorb visible and near UV light and are characterized by reasonable electric properties due to their wide π-electron delocalization (Lanzani et al 2015). In this context, light has recently emerged as a useful tool for the stimulation of cells and living systems. Optical stimulation presents some interesting advantages compared to conventional methodologies (i.e., mechanical, chemical, electrical or magnetic cues) since it permits to stimulate single cells, or even defined sub-cellular elements, with unprecedented spatial and temporal precision and through a contactless mechanism (Antognazza et al 2019, Di Maria et al 2018). Several strategies have, indeed, been devised to achieve this objective. Optogenetics is more likely the first example that allowed to target specific cell types by inducing the expression of light-sensitive microbial channels with genetic engineering (Di Maria et al 2018). It was firstly employed in neuroscience and lately extended to the cardiac field, thanks to its ability to control cell electrical properties in a very selective and specific manner (Entcheva & Kay 2021). Nevertheless, optogenetics presents some limits, such as safety problems linked to the use of viral transfection. In this view, recent evidence revealed an alternative strategy featured by an unprecedented spatio-temporal resolution, which employs organic semiconductors (Di Maria et al 2018, Li et al 2019). Among others, thiophene-based materials represent the most studied and characterized family of organic semiconductors, and in particular the conducting polymer regio-regular poly(3-hexylthiophene-2,5-diyl), abbreviated in rr-P3HT (excitation/emission wavelengths, 520/660 nm), has been successfully used for multiple cellular applications, either in the thin film shape or as nanoparticles (Antognazza et al 2015, Martino et al 2016). Originally, organic semiconductors were employed mainly as thin films. This represents the easiest way to study the abiotic/biotic coupling since it allows to seed the cells directly on the selected material. This method is fundamental for the general understanding of the transduction mechanisms (Di Maria et al 2018). Multiple dimensional

modifications to materials have been developed (e.g nanotubes, nanoparticles, nanopores) and have allowed to enhance materials' sensitivity and efficiency in the generation of biological relevant signals (Kim et al 2022). In particular, the development of nanoparticles (i.e., three dimensions material in the scale of nanometres) is towering over the use of thin films since they are less invasive and highly specific for a precise stimulation. Nanoparticles, due to their dimensions, may operate by binding cells receptors, by behaving themselves as receptors, or they may be internalized in living cells thereby exploiting an endogenous function (Bossio et al 2018, Di Maria et al 2018). Finally, nanoparticles may be functionalized on the surface to selectively target a specific cell type (Di Maria et al 2018, Zucchetti et al 2017). For these reasons, nanoparticles are being studied as next-generation materials shapes.

1.4.2 PHOTOTRANSDUCTION MECHANISMS

Organic semiconductors, as components of a photovoltaic interfaces, act as light absorbers or transducers. They are typically characterized by a high optical absorbance and, when covered by an electrolyte solution, they convert absorbed light into: (i) heat via photo-termal reaction; (ii) electricity via capacitive and Faradaic processes; and (iii) chemical species (e.g., ROS) via photocatalytic reactions (Medagoda & Ghezzi 2021). Ideally, only one phototransduction mechanism is involved in the cell stimulation; however, the three processes may coexist and depend on the illumination protocol and on the material parameters (Medagoda & Ghezzi 2021). Regarding the electrical effects, light absorption generates charges that are directly transferred to the electrolyte solution (Faradaic process) (Ejneby et al 2020) or they are accumulated at the polymer surface exposed to the liquid phase (electrolytic double-layer, or capacitive, effect) (Martino et al 2013, Rand et al 2018). Although Faradaic processes seems to be useless for biological applications, growing evidence highlights the involvement of the capacitive process, which is provided by the coupling between electronic charges accumulated on the material and the ionic charges in the recording bath, in the activation of excitable cells (e.g. neurons) (Ferlauto et al 2018, Lanzani et al 2015, Rand et al 2018). Upon photon absorption, positive charges leave the polymer that becomes negatively charged. The negative charges promote a rearrangement of the ions in the interface between the polymer and the cells, thereby stealing positive charges from the cell plasmalemma and causing the cell membrane depolarization (Lodola et al 2017b, Martino et al 2013). The photo-thermal effect usually occurs when excitons, produced by photo simulation, recombine, and release their energy as thermal radiation (Martino et al 2015). Thermal reactions may occur upon long or short, but intense light exposures; however, they are usually undesired and the increase in temperature is often too low to activate specifically temperature-dependent receptors, such as TRPV1 (Lodola et al 2017b). Finally, photochemical reactions, mainly reduction/oxidation processes, are the most interesting light-induced photo transduction mechanism in the context of this Thesis. They mainly consist in the reduction of electron-acceptors in solution and the simultaneous oxidation of electron-donors (Derek et al 2020). Oxygen reduction to superoxide (O_2^-) or hydrogen peroxide (H_2O_2) has been shown to be relevant during optical excitation of organic

semiconductors (Bellani et al 2015). The above mentioned products are considered reactive oxygen species (ROS) and they have several consequences on the living cells, ranging from the toxicity a high concentration to the regulatory effect on ion channels or the role of signalling molecule at low concentrations (Derek et al 2020). Intriguingly, multiple TRP channels, included TRPV1, are sensitive to ROS concentration (Negri et al 2020). Parallel to oxygen reduction, the photochemical reactions induce a variation in the extracellular pH that may interfere with the activity of several plasmalemmal receptors (Lodola et al 2017b, Negri et al 2020). Recent work showed that illumination of rr-P3HT thin films immersed in water solutions causes the progressive acidification of the solution in the proximity to the polymer thin film, due to aggregation of photo-generated electrons, which are continuously balanced by the formation of an acidic layer of polarized water molecules (Mosconi et al 2016). Intriguingly, a series of experiments at different pH conditions revealed that acidic solutions decreased optimal-mediated TRPV1 activation (Lodola et al 2017b). Probably this is due to the pre-activation of the channel, before the enlightenment, caused by an higher proton concentration (Lodola et al 2017b). Taking together, this information shed light on the fundamental importance of photocatalytic reactions in the context of non-excitable cells, such as ECFCs.

1.4.3 TRPV1 TRANDUCES THE OPTICAL EXCITATION OF ORGANIC SEMICONDUCTORS IN A BIOLOGICALLY RELEVANT SIGNAL

As mentioned above, rr-P3HT has been developed in a planar thin film form and as nanoparticles. rr-P3HT-enlightment has been employed to modulate the resting membrane potential (Vm) in HEK-293 cells (Martino et al 2016) and astrocytes (Benfenati et al 2014) and to stimulate/inhibit the onset of action potentials in primary mouse hippocampal neurons (Feyen et al 2016, Ghezzi et al 2011). Notably, rr-P3HT-based hybrid interfaces have been successfully used in animal models of retinal degeneration. For instance, a fully organic multi-layered SILK-PEDOT:PSS-P3HT prosthesis re-established light-sensitivity and visual acuity in Royal College of Surgeons rats (Antognazza et al 2016, Maya-Vetencourt et al 2017) and was then translated in a large scale animal, such as domestic pig (Maya-Vetencourt et al 2020). Interestingly, the rr-P3HT interface has been exploited to optically stimulate cardiomyocytes derived from hiPSCs (Lodola et al 2019b), which provides the evidence for the possible use of organic semiconductors for CVD treatment. Organic semiconductors, upon optical excitation in electrolyte solution, can transduce light in electricity via photocapacitative and Faradaic process, in ROS via photochemical/photocatalytic reactions, and heat via photothermal conversion (Antognazza et al 2019, Di Maria et al 2018, Li et al 2019). In this view, the polymodal TRPV1 channel is a promising molecular switch to convert optical stimulation in a biologically relevant signal since it is activated by a local increase in temperature (> 42°C) and by ROS produced at the interface between rr-P3HT thin films and cell membrane (DelloStritto et al 2016a, Moccia et al 2020, Negri et al 2020). In addition, recent evidence showed that optical stimulation of rr-P3HT thin films induced HEK-293 cells depolarization via TRPV1 activation (Lodola et al 2017b). Similarly, rr-P3HT nanoparticles

excitation resulted also in a significant increase in $[Ca^{2+}]_i$ in the same cell type (Bossio et al 2018). These data suggested that photostimulation of rr-P3HT, either as thin film or nanoparticles, might stimulate a pro-angiogenic outcome of ECFCs, since TRPV1 is expressed and triggers angiogenic pathways in this cell model (Negri et al 2020). In accord, a recent investigation from our group revealed that optical stimulation of ECFCs plated on rr-P3HT thin films stimulates ECFC proliferation and neovessel formation upon TRPV1 activation and membrane depolarization (Lodola et al 2019a). The subsequent Ca^{2+} influx in turn led to the downstream activation of Ca^{2+}-dependent transcription factor, NF-κB, thereby inducing the expression of multiple pro-angiogenic genes that converted the initial optical stimulation into an angiogenic response (**Figure 9D**). Notably, NF-κB is the Ca^{2+}-dependent decoder that translates the intracellular Ca^{2+} oscillations induced by VEGF into a pro-angiogenic outcome (Dragoni et al 2011). Pharmacological manipulation confirmed that the polymer photostimulation induced ECFC depolarization via TRPV1, rather than TRPV4, activation (Lodola et al 2019a). The authors shone light also on the phototransduction mechanism. They demonstrated that direct photothermal transduction, i.e., the local increase in temperature, does not seem to be the predominant process involved in *tubulogenesis* (Lodola et al 2019a). Conversely, optical stimulation of rr-P3HT thin films induced a robust increase in ROS levels and, as mentioned earlier, ROS may

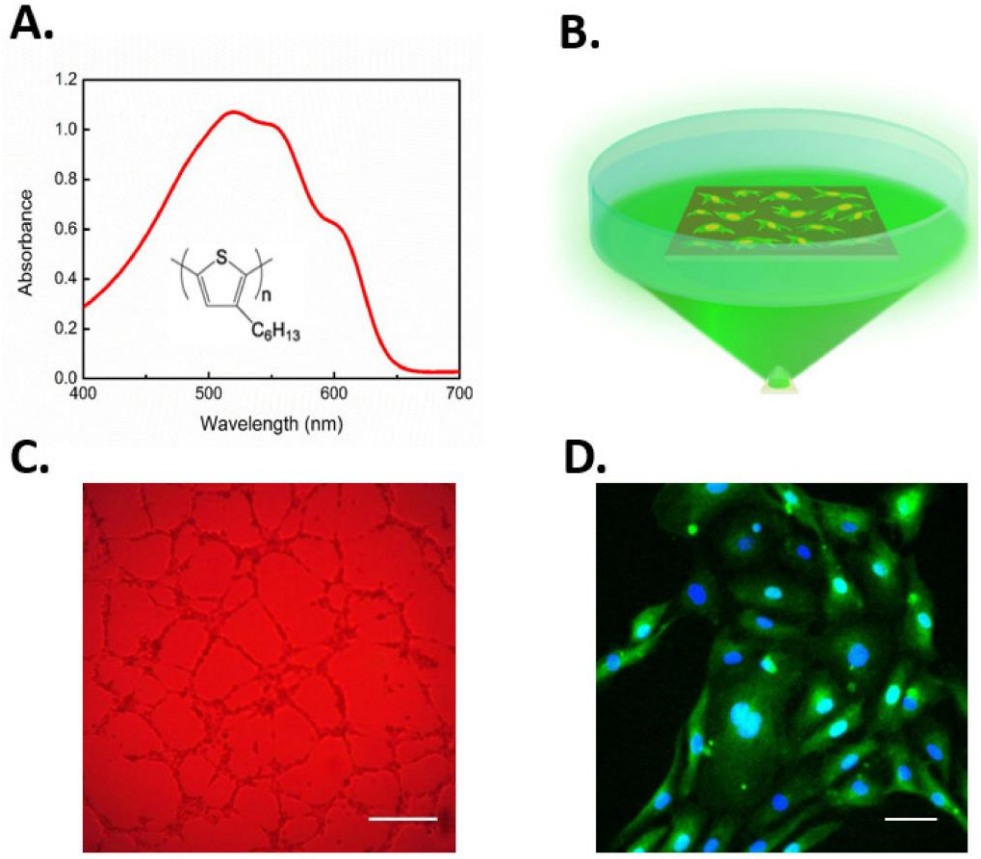

Figure 9 **A.** Chemical structure and optical absorption spectra of P3HT thin films. **B.** Experimental setup of the photostimulation of ECFCs plated on P3HT thin films. **C.** Representative image of in vitro *tubulogenesis* of ECFCs plated on P3HT thin films and stimulated by light. **D.** Immunofluorescence staining, showing light-induced NF-κB nuclear translocation. Cell nuclei are detected by DAPI (blue) while cytoplasmic p65 NF-κB subunit with a secondary chicken anti-rabbit Alexa (488)-conjugated antibody (green). Figures adapted from (Lodola et al 2017b, Lodola et al 2019a).

activate TRPV1. It has, therefore, been suggested that optical stimulation of rr-P3HT thin films induces the production of singlets and charge states, which in turn reduce oxygen dissolved in the medium to form superoxide. Superoxide spontaneously dismutates to H_2O_2, which can permeate the plasma membrane and thereby activate TRPV1 (Lodola et al 2017b, Lodola et al 2019a) The phototransduction mechanisms responsible for TRPV1 activation, however, remain still unclear. Likewise, it is yet to confirm that the optical excitation of TRPV1 triggers an increase in $[Ca^{2+}]_i$ in ECFCs.

1.5 REACTIVE OXYGEN SPECIES AND Ca^{2+} SIGNALLING IN ECFCs

1.5.1 ROS PRODUCTION AND ELIMINATION IN ENDOTHELIAL CELLS

ROS is the general term used to describe multiple reactive molecules obtained from the incomplete reduction of oxygen, such as hydroxyl anion (OH^-), O_2^-, and H_2O_2 (**Figure 10**). Several endogenous and extracellular cues are responsible of the continuous production and transformation of ROS under physiological and pathological conditions, thereby regulating multiple biological processes, such as cellular growth, immune response, embryogenesis, spermatozoa capacitation, and transcription factor activation (Costa et al 2021, Zhang & Shah 2014). Notably, ROS regulate vascular functions (e.g., vasodilatation, vasoconstriction, apoptosis, migration, proliferation, angiogenesis) (Costa et al 2021, Panieri & Santoro 2015). For this reason, there is a tightly regulated balance between ROS generation and ROS degradation (Panieri & Santoro 2015). When ROS production overcomes the cellular antioxidant defences (i.e., the toxic threshold), the cells show DNA damage, protein and lipid modifications, energetic deficit, and cell death due to the oxidative stress condition (Panieri & Santoro 2015, Zhang & Shah 2014). Conversely, a finely controlled production of ROS may reversibly activate or inhibit multiple molecular targets (e.g., ion channels, transmembrane proteins, and transcriptional factors) under both physiological and pathological conditions, by triggering the so-called redox signalling (Burgoyne et al 2012). Furthermore, different ROS species are characterized by different reactivity and specificity for their target(s). The most reactive ROS is OH^-, which has the shortest lifetime. Likewise, O_2^- is rapidly neutralized in H_2O_2 either spontaneously or by superoxide dismutase (SOD); however, it is characterized by a lower selectivity toward molecular targets (Costa et al 2021). On the other hand, H_2O_2 shows all the features to be a second messenger, with a longer half-time life and the consequent ability to activate targets that are far from the production site (Veal & Day 2011). ROS mainly modify the cysteine thiols located in the active site or in the regulatory domain of the protein target; they induce the S-glutathionylation of protein thiolate anions, or oxidate the iron–sulphur cluster-containing centres (Panieri & Santoro 2015). Endothelial ROS production may occur through multiple mechanisms (**Figure 10**), including enzymatic systems, such as uncoupled eNOS, NOXs, xanthine oxidoreductase, and the mitochondrial respiratory chain. In addition, ROS may originate from the arachidonic acid metabolism via lipoxygenase (LOX), cyclooxygenases (COX) or cytochrome P450 (CYP) (**Figure 10**) (Breton-Romero & Lamas 2014). All these processes operate by reducing the molecular oxygen (O_2) into O_2^- through the translocation of one electron. As mentioned above, O_2^- is highly unstable and is rapidly converted in H_2O_2 (Breton-Romero & Lamas 2014, Cai 2005a). Herein, we summarize the main mechanisms responsible for ROS production in endothelial cells.

1.5.1.1 NADPH Oxidase-Mediated ROS Production in Endothelial Cells

A growing number of evidence shows that NOX is a crucial player in ROS production in vascular cells, including endothelial cells (Cai 2005b, Drummond & Sobey 2014, Schroder et al 2012) and ECFCs (O'Neill et al 2019). There are 7 different transmembrane NOX isoforms (NOX1-5 and DUOX1-2), which are all characterized by 6 transmembrane segments and cytosolic amino- and carboxy-terminal tails. Furthermore, NOXs originate ROS as a primary product through a finely regulated process. For instance, they comprise a catalytic core and multiple regulatory subunits (i.e., p22phox, p67phox, p40phox, p47phox, p67phox, and Rac1). NOXs reduce the O_2 by translocating electrons from NADPH through biological membranes in order to produce firstly O_2^-, which can subsequently be dismutated into H_2O_2 (**Figure 10**) (Breton-Romero & Lamas 2014, Panieri & Santoro 2015). These enzymes are expressed both on the plasma membrane or in intracellular organelles (e.g. endosomes, nucleus, ER) thereby determining where ROS generation occurs (Panieri & Santoro 2015). The predominant NOX isoform expressed in endothelial cells (Cai 2005b, Drummond & Sobey 2014, Schroder et al 2012) and ECFCs (O'Neill et al 2019) is NOX4, which is constitutively activated at a low level, by being only regulated by its expression (Breton-Romero & Lamas 2014, Zhang & Shah 2014). For this reason, it maintains the basal ROS production typical of the physiological metabolic activity of the vasculature (Schroder et al 2012). On the other hand, NOX4 is overexpressed upon ischemia/hypoxia conditions, starvation and transforming growth factor-β (TGF-β) stimulation (Zhang & Shah 2014). Interestingly, the main NOX4 product is H_2O_2, which is characterized by a higher stability and higher biological activity compared to O_2^-; however, its ability to permeate the membranes is lower (Gough & Cotter 2011). Thereafter, NOX2, the second NOX isoform for abundance in vascular endothelium, is activated downstream of $G_{q/11}$PCRs or TKRs on the plasma membrane and by metabolic regulators, such as glucose and insulin (Zhang & Shah 2014), whereas NOX5 is recruited by an increase in $[Ca^{2+}]_i$ (Sakurada et al 2019). In addition, mechanical stimulation, evoked by blood flow, may elicit NOX-dependent ROS production in endothelial cells (Brandes et al 2014). Of note, NOX-derived ROS could induce an additional ROS release from several intracellular source, including mitochondria, xanthine oxidoreductase, and eNOS, and thereby amplifying the oxidative stress imposed to vascular endothelial cells (Zhang & Shah 2014, Zinkevich & Gutterman 2011). Finally, in the presence of iron (Fe^{2+}), H_2O_2 is turned into OH^- by the Fenton reaction thereby inducing the lipid peroxidation (Cai 2005a, Sullivan et al 2015). In this context, it is important to recall that endogenous products of lipid peroxidation, such as 4-hydroxy-2-nonenal (4-HNE), may activate or inhibit some endothelial TRP channels (e.g. TRPA1) (DelloStritto et al 2016b, Dreher & Junod 1995, Pires & Earley 2017).

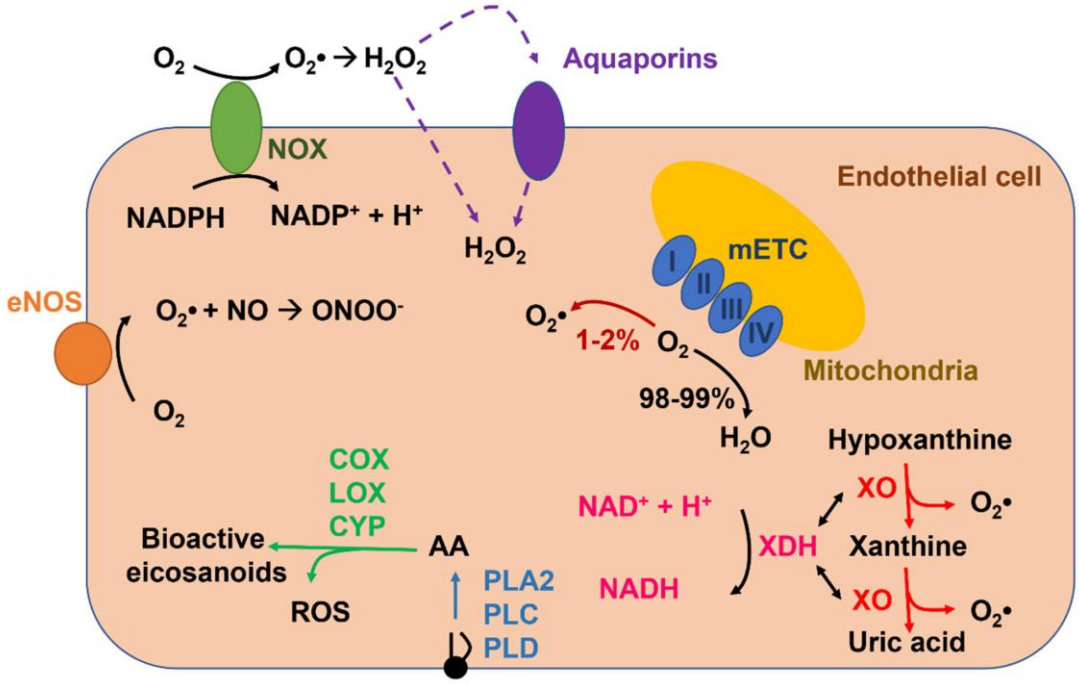

Figure 10 Principal mechanisms of ROS production in endothelial cells. The NOX transfers an electron from NADPH to O_2, thereby generating O_2^- in the extracellular matrix. O_2^- is rapidly converted into H_2O_2, which may permeate into the cytosol through aquaporins or simply across the plasma membrane. O_2^- is incessantly produced in the mitochondria by different complexes of the electron transport chain machinery (mETC) localized on the inner mitochondrial membrane. For instance, 1-2% of the O_2 is converted into O_2^- and not into H_2O. A minor percentage of the O_2^- generated diffuses in the cytoplasm through the outer mitochondrial membrane protein VDAC, the rest is converted into H_2O_2 that diffuses in the cytosol. O_2^- may be also produced as a secondary product of the hypoxanthine reduction to uric acid, and by the metabolization of arachidonic acid in bioactive eicosanoids (Negri et al 2021).

1.5.1.2 Xanthine oxidoreductase

Xanthine oxidoreductase (XOR) consists in a multiple-level regulated enzyme that is characterized by two interconvertible isoforms: xanthine dehydrogenase (XDH) and xanthine oxidase (XO) (Kelley et al 2010). XOR is a 300 KDa molybdic-flavoenzyme that mediate the reduction of hypoxanthine and xanthine into uric acid thereby producing the secondary products H_2O_2 and O_2^- during purine catabolism (**Figure 10**) (Furuhashi 2020). The balance between XO and XDH is indispensable to establish the amount of ROS produced. For instance, XDH reduces NAD^+ to NADH; conversely, XO mediates the conversion of O_2 into O_2^- and H_2O_2 (Incalza et al 2018). Although under physiological conditions XDH is the main isoform expressed in perfused tissues, it is turned into XO under several pathological conditions (e.g ischemia, inflammation, and hypoxia) through multiple processes, such as proteolysis and thiol oxidation (Incalza et al 2018, Panieri & Santoro 2015). XO, indeed, is the principal fount of ROS during the ischemia-reperfusion injury (Incalza et al 2018). Herein, XDH is released in circulation by damaged epithelial cells (e.g., those of mammary gland, intestine, and liver) and it is subsequently converted into XO. XO in turn binds to vascular endothelial cells glycosaminoglycans by inducing severe endothelial damages during liver and intestine disorders (Incalza et al 2018). Moreover, NOX may increase XDH conversion to XO by enhancing the oxidative stress (Landmesser et al 2007). Finally, XOR directly donates electrons to O_2, thereby leading to the production of H_2O_2 (Cai 2005a, Sullivan et al 2015).

1.5.1.3 Uncoupled eNOS

NO is a crucial player in the regulation of several endothelial-dependent functions, such as the regulation of vascular tone and the angiogenesis (Khaddaj Mallat et al 2017, Mancardi et al 2011). Three different isoforms of NOS exist in mammals: eNOS or NOS3, neuronal NOS (nNOS or NOS1), which are constitutively activated, and inducible NOS (iNOS or NOS2) that is activated in response to proangiogenic stimuli or upon inflammatory conditions. All the isoforms are homodimers featured by a flavin- and heme-centres, which require multiple cofactors (i.e., COQ10, L-arginine and tetrahydrobiopterin or BH4) to maintain the monomeric structure indispensable to produce NO. NOSs act as oxidoreductases by inducing flavin-dependent electron transfer from the carboxy-terminal bound of NADPH to the iron-centre and BH4 that are localized on the amino terminus, thus allowing the oxidation of L-arginine to L-citrulline and the consequent generation of NO (coupled NOS) (Panieri & Santoro 2015). This two-step reaction could be divided into: (i) NOS hydroxylates L-arginine to N^{ω}-hydroxy-L-arginine; then (ii) it oxidates N^{ω}-hydroxy-L-arginine to L-citrulline and NO (Forstermann & Munzel 2006). On the other hand, eNOS may be uncoupled from NO release, mainly in shortage of substrates and/or cofactors, such as BH4, thereby restricting NO bioavailability, and leading to the reduction of O_2 to O_2^- (uncoupled eNOS) (**Figure 10**) (Breton-Romero & Lamas 2014, Panieri & Santoro 2015). The balance between O_2^- and NO production is a fundamental determinant of endothelial cell fate. For instance, an excess of O_2^- induces the formation of peroxynitrite radical ($ONOO^-$) by reacting with NO. $ONOO^-$, in turn, further worsens NO production and causes endothelial dysfunction (Daneva et al 2021, Hare 2004). Uncoupled eNOS-derived O_2^- has been related to several CVDs featured by endothelial dysfunction, such as diabetes, hypertension, and atherosclerosis (Elrod et al 2006, Li & Forstermann 2013, Li et al 2015). Intriguingly, eNOS uncoupling is favoured by NOX-dependent ROS production, which reduces BH4 bioavailability, thereby enhancing the oxidative stress imposed on endothelial cells (Incalza et al 2018).

1.5.1.4 Mitochondria

The principal endogenous origin of ROS is represented by the mitochondrial electron transport chain machinery (mETC) that is localized in the inner mitochondrial membrane (Panieri & Santoro 2015). The mETC consists of 5 complexes: NADH-quinone oxidoreductase (Complex I), succinate dehydrogenase (Complex II), coenzyme Q-cytochrome C oxidoreductase (Complex III), cytochrome C oxidase (Complex IV), and ATP synthase (Complex V) (Fukai & Ushio-Fukai 2020). The Krebs cycle produces $FADH_2$ or NADH that, in turn, are used as electron donors in four complexes (I-IV) in the mETC, each catalysing the reduction of O_2 to H_2O through a single-electron transfer reaction (Panieri & Santoro 2015). Nevertheless, 1%-2% of the O_2 consumed is transformed into O_2^- and not into H_2O (Breton-Romero & Lamas 2014). In this context, mitochondrial ROS are not only a secondary product of the mETC, but they adopt a functional role in signalling pathways within the mitochondria or between other organelles (Gorlach et al 2015, Panieri & Santoro 2015). Furthermore, ROS production may occur: i) in the intermembrane space through the action of protein p66shc, which

causes the oxidation of cytochrome c and the partial reduction of O_2 into O_2^- (Incalza et al 2018); ii) in the mitochondrial matrix, by metabolic enzymes (α-ketoglutarate dehydrogenase and aconitase); or iii) in the external mitochondrial membrane due to the action of monoamine oxidase (MAOA and MAOB) (Finkel 2012). Notably, a little fraction of O_2^- may permeate into the cytosol via the voltage-dependent anion channel (VDAC) in the external mitochondrial membrane. However, the major fraction is converted by mitochondrial SOD (Mn-SOD or SOD2) into H_2O_2, which may diffuse in the cytosol (Fukai & Ushio-Fukai 2020, Lambert & Brand 2009). Finally, when the H_2O_2 levels start to be a source of toxicity, it is converted into H_2O by catalase, glutathione peroxidase and peroxiredoxins (Fukai & Ushio-Fukai 2020, Gorlach et al 2015).

1.5.1.5 Arachidonic Acid Metabolizing enzymes

The polyunsaturated fatty acid, arachidonic acid, is a crucial element in the regulation of NO production and in the angiogenic process within the endothelial cells (Berra-Romani et al 2019, Moccia 2018). PLA2, PLC and PLD cleave arachidonic acid from glycerophospholipids, both on the plasma membrane and on the nuclear membrane (**Figure 10**) (Wang et al 2021) and it is subsequently metabolized into multiple bioactive eicosanoids, e.g., prostanoids, thromboxane, leukotrienes, and epoxyeicosatrienoic acids (EETs). Intriguingly, ROS may be generated as by-products during arachidonic acid metabolization, performed by three different families of enzymes, respectively: COXs, LOXs, and CYP ω-hydroxylases and epoxygenases (Kim et al 2008, Wang et al 2021). Moreover, LOXs- and COXs-derived arachidonic acid metabolites may, in turn, activate several NOX isoforms, including NOX1 and NOX4, to induce ROS signalling in response to chemical cues (Kim et al 2008, Wang et al 2021).

1.5.1.6 ROS elimination

Endothelial cells have developed sophisticated antioxidant defence mechanisms in order to avoid endogenous ROS accumulation and endothelial dysfunction (e.g., glutathione (GSH), SOD, catalase, peroxiredoxins (Prx), and thioredoxin (Trx)) (Incalza et al 2018, Panieri & Santoro 2015). GSH is particularly important in the cellular redox state balance. For instance, the ratio of the reduced GSH to oxidized disulphide GSH (GSH/GSSG) is considered as a trustworthy indicator of oxidative stress. In this view, S-glutathionylation provides the maintenance of a correct redox signalling and the defence of oxidative cell damage, by interfering with the irreversible alteration of protein thiol groups induced by H_2O_2. The conversion between GSH and GSSG is driven by GSH peroxidase (GPx), which oxidizes GSH to GSSG, and by the NADPH-dependent GSH reductase, which reduces GSSG to GSH (Hidalgo & Donoso 2008). On the other hand, endothelial SOD operates mainly by neutralizing O_2^- into H_2O_2. In mammalian cells, SOD exists in three isoforms: cytoplasmic SOD (SOD-1 or Cu/Zn-SOD), mitochondrial SOD (SOD-2 or Mn-SOD), and extracellular SOD (SOD-3 or EC SOD). H_2O_2 is subsequently converted into water and oxidized glutathione by GPx or into water and O_2 by catalase. Finally, the Trx system is composed of a family of 12 kDa oxidoreductases that maintain reduced the

thiol groups of Prx, thereby providing the maintenance of Prx-dependent reduction of H_2O_2 to water. Of note, most of these antioxidant enzymatic systems rely on NADPH as the ultimate donor of reductive power (Incalza et al 2018, Madreiter-Sokolowski et al 2020).

1.5.2 ROS-DEPENDENT Ca^{2+} SIGNALS IN ENDOTHELIAL CELLS

1.5.2.1 ROS-induced endogenous Ca^{2+} release

ROS have been shown to be involved both in extracellular Ca^{2+} influx and in the endogenous Ca^{2+} mobilization. It has long been known that extracellular stimuli usually evoke Ca^{2+} signals in endothelial cells mainly by causing the mobilization of intracellular Ca^{2+}, which is sustained over the time by store- or second messengers-operated Ca^{2+} influx through TRP channels (Faris et al 2020b, Moccia et al 2019, Negri et al 2019). As mentioned in the paragraph 1.2.1, the ER represents the most important endogenous Ca^{2+} store, and $InsP_3Rs$ are the main pathway involved in ER Ca^{2+} release engaged downstream of $G_q/_{11}PCRs$ or TKRs localized on the plasma membrane (Moccia et al 2012b, Moccia et al 2019). Notably, $InsP_3Rs$ need a nearby permissive Ca^{2+} concentration (50-200 nM) to be activated by $InsP_3$ (Woll & Van Petegem 2022). Moreover, InP_3R1 channel is closely regulated by cellular redox state (Joseph 2010); for instance, ROS may oxidate crucial endogenous thiol groups by making $InsP_3Rs$ sensitive to low concentration of $InsP_3$ or basal $[Ca^{2+}]_i$ (Bansaghi et al 2014, Joseph et al 2018). In addition, $InsP_3Rs$ activity may also be regulated by mitochondria, which establish close interactions with ER cisternae (known as mitochondria-associated ER membranes or MAMs) (Groschner et al 2012) and significantly reduce $InsP_3$-induced Ca^{2+} release in endothelial cells through a H_2O_2-dependent mechanism (Zhang et al 2019).

Several strategies have been developed in order to investigate the effect of oxidative stress on Ca^{2+} signalling, for example the O_2^- generating system (hypo)xanthine (H)X/XO (Wesson & Elliott 1995), the H_2O_2-generating system, glucose/glucose oxidase (G/GO) (Volk et al 1997), the administration of exogenous H_2O_2 (Doan et al 1994), diamide (Lock et al 2012), thimerosal (Gericke et al 1993), or tert-butyl hydroperoxide (t-BOOH) (Henschke & Elliott 1995). Notably, in the last decade, these strategies allowed multiple groups to demonstrate that ROS are able to induce an increase in endothelial $[Ca^{2+}]_i$. For instance, high doses of (H)X/XO correlated with a raise in $[Ca^{2+}]_i$, which was reduced by scavenging O_2^- with SOD and by preventing the Fenton reaction (Dreher & Junod 1995). Following investigations showed that low intracellular O_2^- concentration could stimulate $InsP_3Rs$ to release Ca^{2+} from the ER (Graier et al 1998). In addition, recently Bansaghi and collaborators discovered that exogenous O_2^- might oxidize several thiols groups of $InsP_3R1$ and $InsP_3R2$ channels thereby inducing ER Ca^{2+} release (Bansaghi et al 2014).

On the other hand, the idea that H_2O_2 could operate as a Ca^{2+} releasing second messenger in vascular endothelial cells was originally proposed by Dreher and Junod, who found that catalase had an inhibitory effect on the Ca^{2+} response to (H)X/XO (Dreher & Junod 1995, Volk et al 1997).

The first real spatiotemporal characterization of H_2O_2-induced endothelial Ca^{2+} signals was provided by Ziegelstein's group (Hu et al 1998). First, the authors investigated how exogenous administration of H_2O_2 induced a dose-response increase in $[Ca^{2+}]_i$ in HAECs. Upon stimulation with >100 μM concentration of H_2O_2, the authors recorded an oscillatory Ca^{2+} response, which was independent of extracellular Ca^{2+} entry but the oscillations disappeared upon depletion of the $InsP_3$-sensitive ER Ca^{2+} pool (Hu et al 1998). At higher doses (>1 mM), H_2O_2 induced intracellular Ca^{2+} oscillations featured by an increased frequency, which immediately fused in a prolonged plateau phase (Hu et al 1998). Subsequently, two independent works confirmed that H_2O_2 elicited a robust reduction in $[Ca^{2+}]_{ER}$ upon $InsP_3R$ stimulation in HUVECs (Zheng & Shen 2005) and calf pulmonary artery endothelial cells (CPAECs) (Wesson & Elliott 1995). Furthermore, H_2O_2 might induce $InsP_3$-mediated Ca^{2+} mobilization from the ER by directly engaging PLCγ1 (Hong et al 2006, Yuan et al 2009) and/or by stimulating $InsP_3Rs$ (Bansaghi et al 2014, Joseph 2010). Exogenous administration of intermediate to high concentrations (500 μM-5 mM) of H_2O_2 stimulated $InsP_3$ production in mouse aortic and mesenteric artery endothelial cells (Sun et al 2011). Alternatively, variation in the thiol redox state could precondition $InsP_3R1$ to be activated by both, the low environment $InsP_3$ concentration (Bansaghi et al 2014, Joseph et al 2018) or by basal $[Ca^{2+}]_i$ (Lock et al 2012). Only $InsP_3R1$ has been characterized for the reactivity of cysteine residues. $InsP_3R1$ primary sequence presents 60 thiol groups, ~70% of which are subject to oxidant-induced post-translational changes (Joseph et al 2006). In particular, two specific cytosolic (Cys-292 and Cys-1415) and two intraluminal (Cys-2496 and Cys-2533) cysteine residues of $InsP_3R1$ are normally oxidized in intact cells, while H_2O_2 may oxidize three supplementary cysteines (Cys-206, Cys-214, and Cys-1397) that are located at the amino terminal domain (Joseph et al 2018). Furthermore, several mechanisms may add further levels of complexity to H_2O_2-dependent regulation of endothelial InP_3Rs. These include: i) the different pattern of $InsP_3R$ expression ($InsP_3R1$ *vs.* $InsP_3R2$ and $InsP_3R3$); ii) the inhomogeneities in local $[Ca^{2+}]_{ER}$; iii) the variability of endothelial Ca^{2+} toolkit in different vascular beds (Sun et al 2011); iv) the accessibility of the reactive thiols (Joseph 2010); v) the redox compartmentalization (Go & Jones 2008); and vi) the interplay of $InsP_3Rs$ with regulatory proteins, e.g., homer-1, which serve as additional sensors of oxidant stress (Guo et al 2016).

Intracellular ROS may also be produced downstream the recruitment of $G_{q/11}PCRs$ on the plasma membrane and thereby contributing to the onset of endothelial Ca^{2+} signals. An early investigation by Ziegelstein's group demonstrated that the activation of endothelial NOX by exogenous NADPH promoted the production of H_2O_2 and O_2^-, which increased $InsP_3R$ sensitivity to ambient $InsP_3$ concentration and induced ER Ca^{2+} release (Hu et al 2000). The same group afterwards showed that NOX maintained the intracellular Ca^{2+} oscillations elicited in HAECs by histamine (Hu et al 2002). A recent work verified that NOX was involved in histamine-induced increase in $[Ca^{2+}]_i$ and von Willebrand factor secretion also in HUVECs (Avdonin et al 2019). An elegant investigation revealed that muscarinic M2 receptors may stimulate cytosolic PLA2 (cPLA2) in endothelial cells of rat

mesenteric arteries, thereby promoting H_2O_2 production upon CYP450 2C9 isoform-dependent metabolism of AA (Chidgey et al 2016). The hydroxyl radical, OH^-, produced from H_2O_2 through the Fenton reaction, sensitizes $InsP_3Rs$ to mediate intracellular Ca^{2+} release and Ca^{2+}-dependent vasodilation via NO release and EDH (Chidgey et al 2016). Furthermore, acetylcholine was found to recruit CYP450 2C11 and CYP450 2C23 isoforms to induce H_2O_2 generation and stimulate EDH in rat renal arteries (Munoz et al 2017). Interestingly, several autacoids may stimulate endothelial ROS release via an increase in $[Ca^{2+}]_i$ that results in the activation of the Ca^{2+}/CaM-sensitive NOX5 isoform. For example, bradykinin-induced ROS generation in PAECs requires $InsP_3R$-mediated ER Ca^{2+} release, while SOCE is inefficient at engaging NOX5 (Sakurada et al 2019). Likewise, angiotensin II and endothelin 1 stimulate O_2^- production in HMECs through a Ca^{2+}-dependent mechanism, but the molecular signalling pathway has not been clarified yet (Montezano et al 2010).

1.5.2.2 ROS regulate SOCE in vascular endothelial cells

STIM and Orai proteins present different number of reactive cysteines that influence redox sensitivity to SOCE. STIM1 presents two highly conserved thiol groups (Cys49 and Cys56) in the intraluminal amino-terminus, which are adjacent to the Ca^{2+}-binding site and are responsible for STIM1 modulation by ROS. H_2O_2-induced S-glutathionylation of Cys49 and Cys56 reduces STIM1 affinity for Ca^{2+}, thereby simulating the effect of ER Ca^{2+} depletion and inducing STIM1 activation and translocation close to the plasma membrane (Hawkins et al 2010). On the contrary, the intraluminal protein, Erp57, could induce the formation of a disulphide bond between Cys49 and Cys59 that avoids STIM1 activation and recruitment into submembrane *puncta* subsequent the reduction in $[Ca^{2+}]_{ER}$ (Prins et al 2011). The redox-induced S-glutathionylation of Cys49 and Cys56 may in turn release STIM1 from Erp57-dependent blockage and result in SOCE activation. STIM2 protein presents a greater number of cysteine residues as compared to STIM1 (15 *vs.* 4), and the majority of these (11 *vs.* 1) is localised in the cytosolic carboxy-terminus (Bhardwaj et al 2016, Niemeyer 2017), which underpins STIM oligomerization and gating of Orai proteins (Lewis 2020). It has been recently demonstrated that H_2O_2-dependent sulfonylation of the cytoplasmic Cys313 hampers STIM2 oligomerization and, therefore, hinders Orai1 activation (Gibhardt et al 2020). On the plasma membrane, Orai1 and Orai2 share three extremely conserved cysteine residues: Cys126 in the second TM segment, Cys143 in the cytosolic loop between the second and third TM segments, and Cys195 at the extracellular extremity of the third TM segment. Orai3 contains two additional cysteine residues in the long extracellular loop between the third and fourth TM domains but lacks Cys195 (Bhardwaj et al 2016, Niemeyer 2017). Bogeski et al. revealed that Cys195 consists in the major reactive cysteine of Orai1 and is responsible for H_2O_2-induced inhibition of I_{CRAC} and SOCE in HEK293 cells transfected with STIM1 and Orai1, Jurkat T cells, and CD4+ T cells (Bogeski et al 2010, Niemeyer 2017). Cys195 oxidation influences Orai1 subunits interaction and hampers efficient Orai1 gating by STIM1, thereby maintaining the CRAC channel in a closed conformation (Alansary et al 2016). Conversely, Orai3, which lacks the extracellular Cys195, is redox-insensitive (Bogeski et al 2010). Intriguingly, the presence of Orai3 in

the heteromeric complex, which mediates SOCE, renders Orai1 less susceptible to oxidative stress, as showed in effector TH cells (Bogeski et al 2010) and prostate cancer cells (Holzmann et al 2015).

Intriguingly, ROS signalling could indirectly modulate the I_{CRAC} by targeting $InsP_3Rs$. For instance, Grupe and co-workers demonstrated that H_2O_2 triggers $InsP_3$-mediated ER Ca^{2+} efflux thereby activating SOCE in RBL-2H3 cells, HEK293 cells and Jurkat T cells (Grupe et al 2010). An alternative mechanism of indirect SOCE activation by ROS signalling could impinge on the S-glutathionylation of SERCA2B Cys674. Indeed, an increase in the rate of SERCA2B activity would lead to ER Ca^{2+} overload, which, in turn, stimulates $InsP_3Rs$ and initiates the functional crosstalk between STIM and Orai proteins (Berridge 2007). Surprisingly, SERCA2B inhibition by excessive production of oxidants could induce SOCE activation as ER Ca^{2+} efflux through leakage channels is no longer balanced by SERCA2B-mediated sequestration into ER lumen and may promote ER Ca^{2+} depletion (Yoon et al 2017).

Early investigations report that acute generation of intracellular ROS stimulates Ca^{2+} influx in endothelial cells from several vascular beds, including HUVECs (Volk et al 1997), CPAECs (Wesson & Elliott 1995), MAECs (Sun et al 2011) and PAECs (Az-ma et al 1999, Graier et al 1998). On one hand, these studies recognised $InsP_3Rs$ as the main ER Ca^{2+}-releasing elements activated by ROS (Lock et al 2012, Sun et al 2011, Wesson & Elliott 1995, Zheng & Shen 2005). On the other hand, there was not any straightforward conclusion on the molecular nature of the ROS-induced Ca^{2+} entry pathway in the plasma membrane. It is important to underline that these investigations were carried out before the discovery of TRP channels and that SOCE was considered the most important Ca^{2+} entry pathway in vascular endothelial cells (Lounsbury et al 2000).

It is worth of mentioning that prolonged exposure to oxidative stress has an inhibitory effect on SOCE in endothelial cells (Groschner et al 2017). Indeed, an early work showed that 1 hour of pre-treatment of CPAECs with t-BOOH, which causes a reduction in the endogenous antioxidant system, significantly reduced SOCE, while it did not affect the $InsP_3$-sensitive ER Ca^{2+} pool (Elliott & Doan 1993). This evidence was then confirmed by the Blatter's group (Florea et al 2017) and suggests that either the store-operated channel on the plasma membrane or the $[Ca^{2+}]_{ER}$-sensing mechanism are affected by this pharmacological manipulation. More recently it has been demonstrated that treatment of the bovine brain cerebrovascular endothelial cells with H_2O_2 (30 μM) for 24 h significantly inhibited SOCE, probably through the oxidation of the extracellular Cys195 of Orai1 (Yamamura et al 2016). Interestingly, longer (> 24 h) exposure to intracellular ROS could cause a significant increase of endothelial STIM1 and Orai1 proteins expression. Tamareille and collaborators showed that culturing HUVECs for 96 h in the presence of high glucose determined a huge increase in the amplitude of both I_{CRAC} and SOCE that was partially dependent on intracellular H_2O_2 production (Tamareille et al 2006). Also in this case, the authors proposed that prolonged oxidant stress induce the upregulation of STIM1 and Orai1 in HUVECs (Abdullaev et al 2008, Galeano-Otero et al 2021, Zhou et al 2014), through the activation of the Ca^{2+}-dependent phosphatase, calcineurin (Tamareille et al 2006). In agreement with

this observation, Daskoulidou and co-workers showed that chronic treatment (72 h) with high glucose promoted the nuclear translocation of NFATc3 through the activation of calcineurin, thereby increasing the protein expression of Orai1-3 and STIM1-2 in several types of human endothelial cells (Daskoulidou et al 2015).

1.5.3 ROS TRIGGER ENDOTHELIAL Ca^{2+} SIGNALS THROUGH THE ACTIVATION OF TRP CHANNELS

1.5.3.1 TRPV1

As already reported in paragraph 1.3.5.2, TRPV1 may be gated by ROS (**Figure 11**) (Chuang & Lin 2009, Pantke et al 2021), however there is not clear evidence that this channel protein functions as a sensor of endothelial redox signalling (Pires & Earley 2017). The molecular mechanism responsible for ROS sensitivity differs among different species. For instance, TRPV1 in the chicken is activated gradually by the oxidation of multiple Cys residues in the amino- and carboxy-terminal tails (Chuang & Lin 2009). Conversely, rat TRPV1 is engaged by H_2O_2 via the oxidation of extracellular Cys261 (Susankova et al 2006). Conversely, the human TRPV1 presents two sensitive Cys residues, Cys258 and Cys754 that are located, respectively, in the amino and carboxy-termini and provide the stability of the heterotetramers through the formation of disulphide bond (Ogawa et al 2016). However, only one Cys258 is employed in the disulphide bridge, the other Cys of the dimer can be oxidized by H_2O_2 thereby leading to a conformational change and activation of TRPV1 (Ogawa et al 2016). In addition, DelloStritto and collaborators recently showed that TRPV1 may sense the redox state in coronary artery endothelial cells and bovine aortic endothelial cells, where it mediates non-selective cation currents. Therefore, TRPV1 activation induced vasodilation of mouse coronary artery (DelloStritto et al 2016a). Moreover, H_2O_2 was able to boost the bioelectrical signals caused by capsaicin. Notably, prolonged (1 h) treatment with H_2O_2 prevented capsaicin-dependent cation currents in bovine aortic endothelial cells and coronary artery vasodilation in mouse (DelloStritto et al 2016a). These data allow to speculate that endothelial TRPV1-dependend pathways may be severely compromised by the prolonged exposure to oxidative stress.

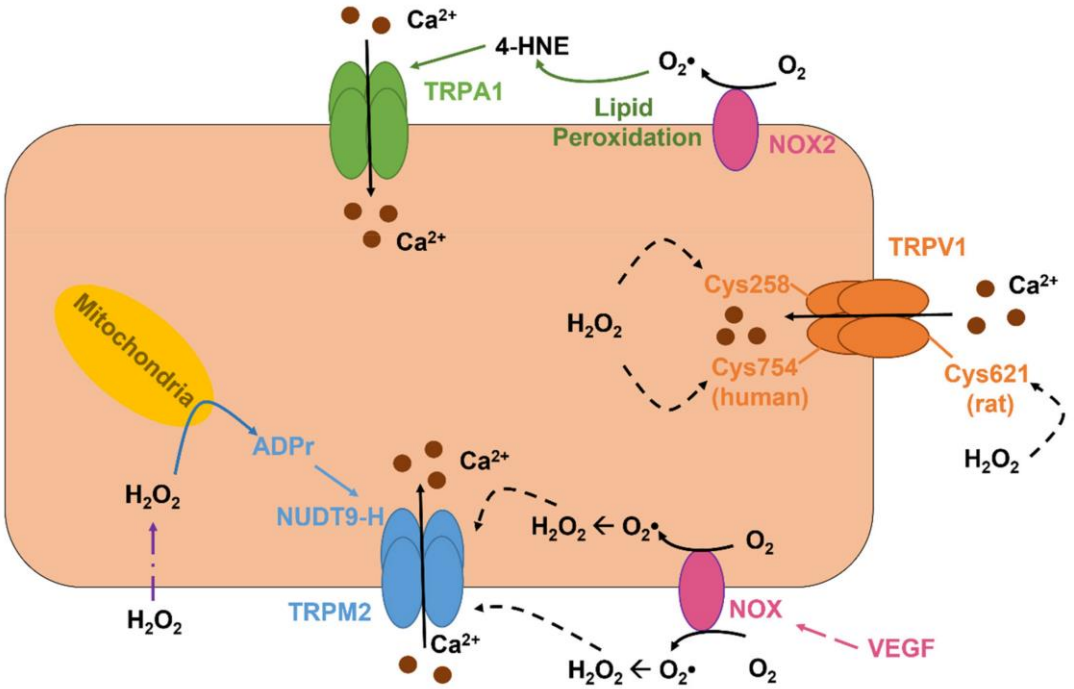

Figure 11 ROS induce endothelial TRPV1, TRPA1 and TRPM2 activation. H_2O_2 directly activates TRPV1 by modifying the cytosolic Cys258 and Cys274 and the extracellular Cys621 in human and rat endothelial cells, please read the detail in the text. Conversely, H_2O_2 indirectly activates TRPM2 by stimulating the mitochondrial production of ADPr. In addition, VEGF-dependent NOX2 activation leads to TRPM2 stimulation after intracellular ROS production. Finally, NOX2-dependent O_2^- production causes lipid membrane peroxidation and 4-HNE formation, which in turn binds to TRPA1 and stimulates the Ca^{2+} entry (Negri et al 2021).

1.5.3.2 TRPA1

TRPA1 is an additional example of a versatile endothelial cation channel mostly permeable to Ca^{2+} that may be activated by several stimuli, including dietary agonists (e.g. allicin, cinnamaldehyde and allyl isothiocyanate) electrophilic compounds and proalgesic agents (Marsakova et al 2017). TRPA1 is widely distributed along the cerebral vascular network, conversely it is not detectable in any other vascular bed (Alvarado et al 2021). Interestingly, TRPA1 is concentrated in the heterocellular myoendothelial gap junctions (MEGJs), where it colocalizes with NOX2 and intermediate- and small-conductance Ca^{2+}-dependent K^+ channels (IK_{Ca} and SK_{Ca} respectively). Herein, TRPA1-mediated Ca^{2+} influx, indeed, activates IK_{Ca} and SK_{Ca} thereby mediating the hyperpolarization of plasma membrane through the so-called endothelium-derived hyperpolarization (EDH) mechanism (Sullivan et al 2015). For instance, the Early's group showed that NOX2-derived O_2^- induced lipid membrane peroxidation thereby leading to the production of 4-HNE via the Fenton reaction. 4-HNE, in turn, evoked TRPA1-mediated Ca^{2+} signals and the consequent dilatation of cerebral arteries by inducing EDH (Sullivan et al 2015). Furthermore, the same group demonstrated that TRPA1 is also expressed in brain capillary endothelial cells and may sustain the functional hyperaemia during prolonged sensory stimulation (Thakore et al 2021). TRPA1 may mediate the haemodynamic response by sensing both neuronal (Pfeiffer et al 2021) and astrocytes (Tapella et al 2020) activity. For instance, TRPA1-mediated Ca^{2+} signals trigger a vasorelaxing signal that is propagated from the capillary network to the upstream pre arteriole bed through the Ca^{2+}-dependent release of ATP via pannexin 1 (Panx1). Herein, ATP gates

P2X receptors to increase the $[Ca^{2+}]_i$ thereby initiating the Ca^{2+} wave that is propagated to the adjacent cells (Thakore et al 2021). Once the signal reaches the post arteriole transitional segment the local Ca^{2+} signal is transformed into the electric EDH signal, which induce the dilation of intraparenchymal arterioles and the local increase in CBF (Alvarado et al 2021). Of note, TRPA1 has been demonstrated to have a neuroprotective role during brain stroke (Alvarado et al 2021). Pires and collaborators, indeed, showed that hypoxia (pO_2 of ~10-15 mmHg) promotes mitochondrial ROS generation followed by 4-HNE production and TRPA1-mediated vasodilation of cerebral pial arteries and intraparenchymal arterioles (Pires & Earley 2018), and limits the ischemic damage to the brain.

1.5.4 MANIPULATION OF ROS-DEPENDENT Ca^{2+} SIGNALS AS AN ALTERNATIVE STRATEGY TO PROMOTE THERAPEUTIC ANGIOGENESIS AND RESTORE BLOOD FLOW PERFUSION

VEGF may influence the local and precisely regulated intracellular generation of ROS in order to stimulate angiogenesis and restore local blood flow in ischemic tissues (Fukai & Ushio-Fukai 2020, Panieri & Santoro 2015). Similarly, an increase in $[Ca^{2+}]_i$ promotes endothelial cell proliferation, migration, and tube formation (Moccia et al 2018b, Moccia et al 2019). For instance, VEGF-dependent proangiogenic Ca^{2+} signals in HAECs are sustained by S-glutathionylation of SERCA2B Cys674 following NOX4-mediated H_2O_2 production (Evangelista et al 2012). Likewise, VEGF-induced extracellular Ca^{2+} entry in human lung vascular endothelial cells requires the ROS-dependent stimulation of TRP Melastatin 2 (TRPM2), and this mechanism contributes to VEGF-mediated postischemic angiogenesis in a mouse model of hindlimb ischemia (Mittal et al 2015). It is important to also recall that the redox-dependent activation of endothelial TRPA1, upon hypoxic condition, may induce cerebral artery relaxation thereby attenuating the ischemic damage derived from brain stoke (Pires & Earley 2018). These preliminary data suggest that ROS-dependent endothelial Ca^{2+} signalling represent a promising tool to achieve therapeutic angiogenesis in ischemic disorders. Likewise, a more recent investigation confirmed that platelet lysate induced NOX4 activation in the mouse brain immortalized cell line, bEND5, thereby inducing $InsP_3$-induced ER Ca^{2+} release and SOCE (Martinotti et al 2019). This is in accordance with the fact that a mixture of growth factors, cytokines and chemokines can be locally administered to induce revascularization of ischemic tissues (Faris et al 2020b). Subsequently, the same group showed that H_2O_2 released by buckwheat honey triggers $InsP_3$-induced ER Ca^{2+} release followed by extracellular Ca^{2+} entry in the same cell line (Ranzato et al 2021). Honey-evoked Ca^{2+} influx was sensitive to econazole, an imidazole derivative that has long been known to affect SOCE (Moccia et al 2016).

Not surprisingly, local delivery of honey through cryogels, hydrogels, and electrospun scaffolds has been proposed as a promising strategy to stimulate wound healing and tissue reparation (Hixon et al 2019). Furthermore, it was demonstrated that transient administration of low-to-moderate doses of H_2O_2 (0.1-100 μM) may stimulate proliferation, migration, and tube formation in endothelial cells

from different vascular beds (Mu et al 2010, Wang et al 2020), while higher amounts promote endothelial cell death (Mu et al 2010).

Therefore, the regulated release of moderate doses of H_2O_2 from dynamic hydrogel matrices into injured tissues could locally stimulate proangiogenic Ca^{2+} signals in endothelial cells (Lee et al 2018, Park & Park 2018). As mentioned above, an additional alternative strategy to therapeutically exploit ROS-induced endothelial Ca^{2+} signalling consists in the optical stimulation of photosensitive conjugated polymers, which generate H_2O_2 upon exposure to visible light (Moccia et al 2020). This approach may prove extremely helpful to induce therapeutic angiogenesis in ischemic organs. Interestingly, it has been demonstrated that hypoxia-induced ROS production leads to TRPA1 activation in mouse cerebrovascular endothelial cells and the consequent TRPA1-mediated vasodilation contributes to arrest ischemic damage after stroke (Pires & Earley 2018). Accordingly, engagement of specific TRP channels via local release/production of appropriate amounts of ROS could produce more beneficial effects than expected in injured tissues.

2 AIM OF THE WORK

In this Thesis we aim to assess whether optical stimulation of ECFCs plated on rr-P3HT thin film induces Ca^{2+} signals through the ROS-dependent TRPV1 activation. In addition, the investigation focused on the subcellular distribution of TRPV1 and its role in the endogenous Ca^{2+} mobilization.

3 MATERIAL AND METHODS

3.1 POLYMER AND FILM PREPARATION

Regio-regular Poly-3-Hexyl-Thiophene (rr-P3HT) polymer (15,000–45,000 MW) was purchased from Sigma Aldrich (Merk Millipore, Darmstadt, Germany) and used without further purification. Therefore, rr-P3HT was dissolved in Chlorobenzene up to a final concentration of 20 mg/mL (Lodola et al 2019a). The solution was stirred at 65 °C for 6 hours. Glass substrates were carefully cleaned before use, by subsequent rinses in ultrasonic bath with deionized water, acetone, isopropanol (10 min each). rr-P3HT solution was then spin coated (1500 rpm for 1 min) on the glass coverslips, thereby obtaining a final thickness of 130 nm and an optical density of 0.6 (at the main absorption peak). Glass/rr-P3HT samples were thermally sterilized (2 h, 120 ◦C) and employed as cell culturing substrates.

3.2 ISOLATION AND CULTIVATION OF ECFCs

Blood samples (40 ml) collected in EDTA (ethylenediaminetetraacetic acid)-containing tubes were obtained from healthy human volunteers aged from 22 to 28 years old . The Institutional Review Board at “Istituto di Ricovero e Cura a Carattere Scientifico Policlinico San Matteo Foundation” in Pavia approved all protocols and specifically approved this study. Informed written consent was obtained according to the Declaration of Helsinki of 1975 as revised in 2008. To isolate ECFCs, MNCs were separated from peripheral blood by density gradient centrifugation on Lympholyte-M separation medium for 30 min at 400 g and washed twice in phosphate buffered saline (PBS) solution. A median of 36×10^6 MNCs (range 18–66) were plated on collagen I-coated 6 multiwell plates (Fisher Scientific, Göteborg, Sweden) in the presence of the Endothelial Cell Growth Medium MV 2 Ready-to-use (Promocell, Heidelberg, Germany) containing EBM-2, 5% FBS, recombinant human (rh) EGF, rh-VEGF 165, rh-FGF-B, rh-IGF-1, ascorbic acid, and hydrocortisone, and maintained at 37 °C in 5% CO_2 and humidified atmosphere. Discard of non-adherent cells was performed after 2 days; thereafter medium was changed each two days. The outgrowth of endothelial colonies from adherent MNCs was characterized by the formation of a cluster of cobblestone-appearing cells, resembling endothelial cells. That ECFC-derived colonies belonged to endothelial lineage was confirmed as described in (Dragoni et al 2011). Thereafter, ECFCs were detached through trypsinization and plated on control glass coverslips and rr-P3HT-coated coverslips to perform the subsequent experiments.

3.3 SOLUTIONS

Physiological salt solution (PSS) had the following composition (in mM): 150 NaCl, 6 KCl, 1.5 CaCl2, 1 MgCl2, 10 Glucose, 10 Hepes. In Ca^{2+}-free solution ($0Ca^{2+}$), Ca^{2+} was substituted with 2 mM NaCl, and 0.5 mM EGTA was added. Solutions were titrated to pH 7.4 with NaOH. The osmolality of PSS as measured with an osmometer (Wescor 5500, Logan, UT) was 338 mmol/kg.

3.4 FLUORESCENCE MICROSCOPY

Fluorescence microscope is an optical microscope employed to study fluorescent biological samples. In this Thesis work, we employed the secondary fluorescence emitted by fluorochromes, such as Fura-2/AM, which binds cytosolic Ca^{2+} ions . When enlightened, fluorochromes adsorb part of the radiation and in part they return it; the emitted radiation is featured by a lower energy and a higher wavelength. This is fundamental to understand the operative mechanism of the microscope. In this Thesis it has been used an epifluorescence microscope that is characterized by two light sources: a white lamp to watch the sample and find the region of interest, and a mercury-vapor lamp that emits in the low visible region and in the near UV. Microscope light path is enriched with lenses of a capacitors, which focus and condense the emitted rays and a pair of athermic filters that reduce the temperature of the beam to do not burn the sample. Finally, the dichroic mirror allows to separate the excitation light from the emitted one, thanks to the different wavelength mentioned above. Only the emitted radiation is able to reach the microscope oculars and it may be perceived by our eyes (**Figure 12**).

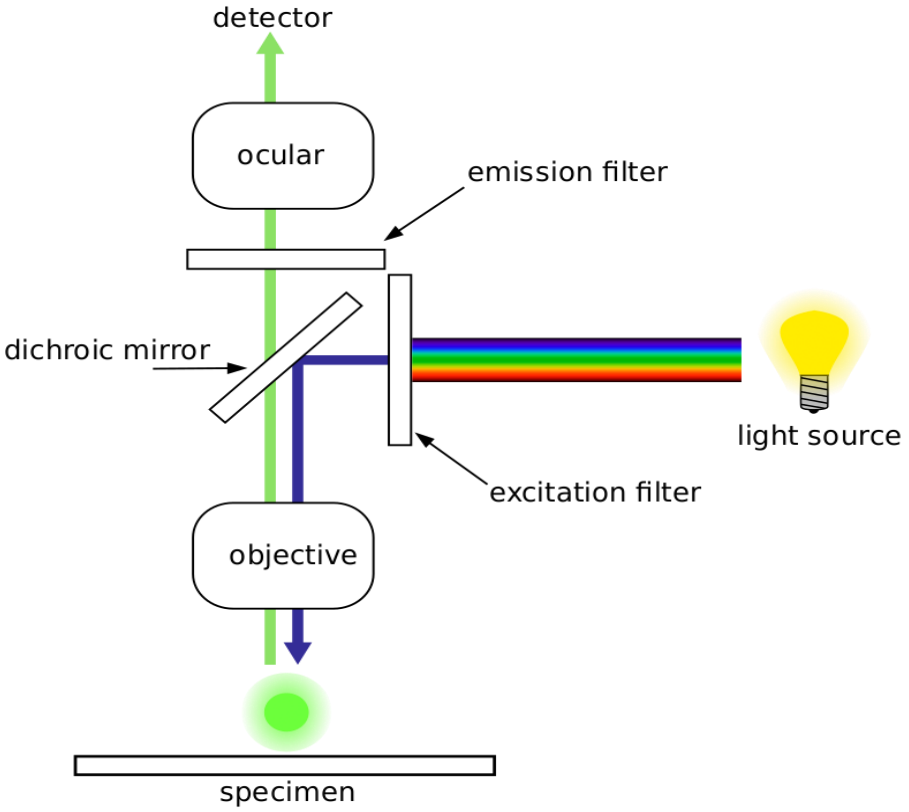

Figure 12 Epifluorescence microscope. Schematic representation of the components of a fluorescence microscope.

3.5 $[Ca^{2+}]_i$ MEASUREMENTS

ECFCs, plated either on rr-P3HT-coated or bare glass substrates, were loaded with 4 μM fura-2 acetoxymethyl ester (FURA-2/AM; 1 mM stock in dimethyl sulfoxide) in PSS for 10 minutes at 37 °C and 5% CO_2. After washing in PSS, the sample was fixed to the bottom of a Petri dish and the cells observed by an upright epifluorescence Axiolab microscope (Carl Zeiss, Oberkochen, Germany), usually equipped with a Zeiss × 40 Achroplan objective (water-immersion, 2.0 mm working distance, 0.9 numerical aperture). ECFCs were excited alternately at 340 and 380 nm, and the emitted light was detected at 510 nm. A first neutral density filter (1 or 0.3 optical density) reduced the overall intensity of the excitation light, and a second neutral density filter (optical density = 0.3) was coupled to the 380 nm filter to approach the intensity of the 340 nm light. A round diaphragm was used to increase the contrast. The excitation filters were mounted on a filter wheel (Lambda 10, Sutter Instrument, Novato, CA, USA). Custom software, working in the LINUX environment, was used to drive the camera (Extended-ISIS Camera, Photonic Science, Millham, UK) and the filter wheel, and to measure and plot on-line the fluorescence from 10 up to 40 rectangular "regions of interest" (ROI).

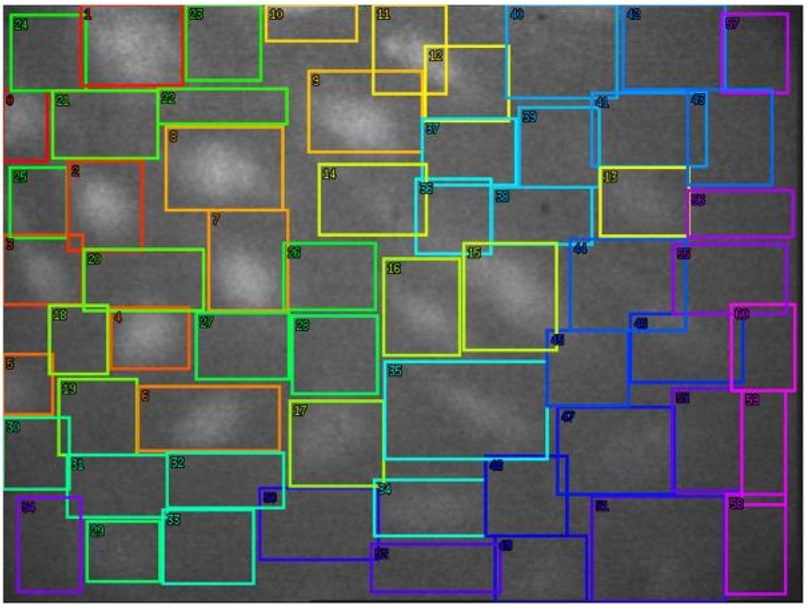

Figure 13 ECFCs loaded with FURA-2/AM and surrounded by ROIs observed with the fluorescence microscope.

Each ROI was identified by a number. Since cell borders were not clearly identifiable, a ROI may not include the whole cell or may include part of an adjacent cell. Adjacent ROIs never superimposed. To provide polymer photoexcitation, an external light emitting diode was employed (THORLABS M470L4-C5, Newton, New Jersey, USA), with spectral emission centred around 470 nm, which is far away from FURA-2/AM light absorption spectra, and photoexcitation impinging on the sample from the glass substrate side with a power density 0.6 mW/mm^2. Light pulses of different duration, in the range 2.5–20 sec, were used to optically stimulate the rr-P3HT polymer films as well as the uncovered, control glass substrates. During photoexcitation protocol, the acquisition system was off, and this is indicated by the corresponding upward/downward deflection of the Ca^{2+} tracings at the time of illumination. On/off switching time are in the order of ms, thus not interfering with the monitoring of $[Ca^{2+}]_i$ dynamics. $[Ca^{2+}]_i$ was monitored by measuring, for each ROI,

the ratio of the mean fluorescence emitted at 510 nm when exciting alternatively at 340 and 380 nm (F_{340}/F_{380}). An increase in $[Ca^{2+}]_i$ causes an increase in the ratio. Ratio measurements were performed and plotted on-line every 3 s and were never longer than 3600 sec. Mitochondrial Ca^{2+} concentration was measured by loading the cells with the specific fluorophore Rhodamine (Rhod-2/AM, 4 μM) for 30 min at 37 °C, 5% CO_2 saturated humidity and washed in PSS for 10 minutes. Rhod-2/AM fluorescence was measured by using the same equipment described for Ca^{2+} recordings but with a different filter set, i.e., excitation at 550 nm and emission at 580 nm wavelength. Again, off-line analysis was performed by using custom-made macros developed by Microsoft Office Excel software. In the figures, each Ca^{2+} tracing refers to an individual cell and is representative of at least three independent experiments. The experiments were performed at room temperature (22 °C).

3.6 rr-P3HT FLUORESCENCE EMISSION MEASUREMENTS

rr-P3HT coated glass coverslips were immersed in PSS extracellular medium and the fluorescence at the polymer surface was acquired in different field of views (excitation/emission wavelengths, 520/660 nm; integration time, 100 ms; binning: 2×2) using an upright microscope (Olympus BW63), equipped with a 20X water immersion objective and a sCMOS Camera (Prime BSI, Teledyne Photometrics; Tucson, Arizona, USA). Then, the FURA-2/AM optical excitation protocol, described in Section 2.4, was applied to the same field of views. Some fields were not treated as control. The rr-P3HT fluorescence emission was measured again in the same areas. The fluorescence intensity was evaluated over ROIs placed inside the treated/untreated regions, using ImageJ software. Mean values were averaged over 4 fields of view, over 3 statistically independent samples.

3.7 SDS-PAGE AND IMMUNOBLOTTING

Cells were lysed in ice-cold RIPA buffer (50 mM TRIS/HCl, pH 7.4, 150 mM NaCl, 1% Nonidet P40, 1 mM EDTA, 0.25% sodium deoxycholate, 0.1% SDS) added of protease (10 μg/mL Leu, 10 μg/mL Aprot, 1mM PMSF) and phosphatase (1mM Na_3VO_4 and 100 mM NaF) inhibitors. Upon protein quantification, the samples were dissociated by addition of half volume of SDS-sample buffer 3X (37.5 mM TRIS, pH 8.3, 288 mM glycine, 6% SDS, 30% glycerol, and 0.03% bromophenol blue), separated by SDS-PAGE on a 7.5% polyacrylamide gel, and transferred on a PVDF membrane. Detection of antigen was performed by using the different antibodies diluted 1:1000 in TBS (20 mM Tris, 500 mM NaCl, pH 7.5) containing 5% BSA and 0.1% Tween-20 in combination with the appropriate HRP-conjugated secondary antibodies (1:2000 in PBS plus 0.1% Tween-20). The following antibodies were used: anti-TRPV1 (ab3487) from ABCAM (Cambridge,UK) and anti-Tubulin (sc-32,293) from Santa Cruz Biotechnology (Dallas, Texas, USA) as equal loading control. The chemiluminescence reaction was performed using Immobilon Western (Millipore) and images were acquired by Chemidoc XRS (Bio-Rad, Segrate, Mi, Italy).

3.8 MITOCHONDRIAL ISOLATION AND IMMUNO BLOTTING

Mitochondrial and soluble fractions from ECFCs were isolated using the Qproteome Mitochondria Isolation Kit (37612; Qiagen). Proteinase K digestion was performed in solution as recommended by the manufacturer (Sigma Aldricht). For Western blotting we used precast gels (Bolt Invitrogen) to dissolve 10–40 μg of total cell lysate. Briefly, ECFCs were cultured for 5-7 days to obtain 5 million of cells. The crude mitochondria were isolated by following the protocol of Qproteome Mitochondria Isolation Kit (37612; Qiagen), the only modification was the addition of phosphatase inhibitors (1X PhosSTOP; Roche, Basilea Swizerland) to all required buffers. The two protein fractions compared along the work (cytosolic and mitochondria) were obtained in two different steps of the Qproteome kit. Cytosolic fraction was obtained after bland lysis of the cells (step 1 of protocol) and low-speed centrifugation (1000g for 10 minutes at 4°C). During this passage soluble proteins unbound are released, since the plasma membrane is compromised enough. On the contrary, all structures and organelles are maintained in the cells. We refer to this fraction as the "cytosolic fraction" and compare it with the mitochondria fraction obtained at the final step of the Qproteome protocol. The final products of the mitochondrial isolation and the complementary soluble/cytosolic components were quantified to determine accurately the protein concentration of each. Bradford reagent (B6916-500ML; Sigma Aldrich) was used along with a PerkinElmer LAMBDA Bio+ spectrophotometer. A predisposed amount of sample was dissolved in acrylamide gels (Invitrogen, Life Technologies Europe BV, Bleiswijk, ZUID-HOLLAND, Netherlands), and after transfer, the PVDF membranes were probed for TRPV1 and all the different organelle-specific markers. As control for mitochondrial successful isolation efficacy we used a TOMM20 antibody (ab56783; abcam), a Vinculin antibody (700062; Thermo Fisher Scientific, Waltham, Massachusetts, US) and a mixture of monoclonal antibodies recognizing several OXPHOS components (MS604-300; abcam). An antibody against GAPDH (sc-166574; Santa Cruz Biotechnology) was used as cytosolic marker. The GAPDH and OXPHOS antibodies were used separately and tested sequentially. HRP-conjugated secondary antibodies against rabbit (W401B) or mouse (W402B) were purchased from Promega (Madison, Wisconsin, US). Dilutions used for all primary antibodies were 1:1,000–1:3,000; dilutions for the secondary antibodies were 1:3,000–1:8,000.

3.9 GENE SILENCING

A selective siRNA, targeting human TRPV1, was purchased by Sigma-Aldrich Inc. MISSION esiRNA (hTRPV1, EHU073721). Scrambled siRNA was used as negative control (defined as Ctrl in the Figures). Briefly, once the monolayer cells had reached 50% confluency, the medium was removed, and the cells were added with Opti-MEM I reduced serum medium without antibiotics (Life Technologies Europe BV, Bleiswijk, ZUID-HOLLAND, Netherlands). siRNAs (100 nM final concentration) were diluted in Opti-MEM I reduced serum medium and mixed with Lipofectamine™ RNAiMAX transfection reagent (Invitrogen, Life Technologies) prediluted in Opti-MEM), according to the manufacturer's instructions. After 20 min incubation at room temperature, the mixes were added to the cells and incubated at 37 °C for 5 h. Transfection mixes were

then completely removed, and fresh culture media was added. The effectiveness of silencing was determined by immunoblotting (see **Figure 20**), and the silenced cells were used 48 h after transfection.

3.10 INTRACELLULAR REACTIVE OXYGEN SPECIES DETECTION

2′ ,7′ -dichlorodihydrofluorescein diacetate (H_2DCF-DA, purchased from Sigma Aldrich) was employed for intracellular detection of ROS. ECFCs cultured on rr-P3HT coated glass and glass control samples were photo-excited for 2.5 and 20 sec from glass side with a LED system (Thorlabs M470L3-C5, λ = 470 nm, P = 0.6 mW/mm2), thus employing the same parameters used for photoexcitation in $[Ca^{2+}]_i$ dynamics measurements. Subsequently, cells were incubated with the ROS probe for 30 min in PSS (10 μM). After careful wash-out of the excess probe from the extracellular medium, the fluorescence of the probes was recorded (excitation/emission wavelengths, 490/520 nm; integration time, 350 ms) with an upright microscope (Olympus BW63; Olympus Italia, Segrate (Mi), Italy), equipped with a 20X water immersion objective and a sCMOS Camera (Prime BSI, Teledyne Photometrics; Tucson, Arizona, USA). Variation of fluorescence intensity was evaluated over ROIs covering single cells areas, and reported values represent the average over multiple cells (n > 400) belonging to 3 statistically independent samples. Image processing was carried out with ImageJ and subsequently analysed with Origin Pro 2018.

3.11 STATISTICS

All the data have been collected from ECFCs deriving from at least three coverslips from three independent experiments. The amplitude of the maximum variation in $[Ca^{2+}]_i$ induced by optical stimulation was measured as the difference between the maximum increase in F_{340}/F_{380} ratio and the mean ratio of 1 min baseline before the onset of the Ca^{2+} response. The amplitude of the 1st Ca^{2+} transient of the intracellular Ca^{2+} oscillations was measured as the difference between the Ca^{2+} peak and mean ratio of 1 min baseline before the Ca^{2+} peak. Oscillation frequency was calculated by dividing the number of Ca^{2+} transients by the duration of the recording after the light stimulus (40–45 min). The amplitude of Ca^{2+} signals induced by chemical stimulation (i.e., apsaicin, H_2O_2, and NADH) was measured as the difference between the maximum variation in $[Ca^{2+}]_i$ and the mean ratio of 1 min baseline before the Ca^{2+} peak. The reduction of the mitochondrial Ca^{2+} concentration was evaluated by measuring the slope of the fluorescence intensity curve after the stimulation. Pooled data are given as mean±SEM and statistical significance (*P* value) was evaluated by the Student's *t*-test for unpaired observations and by the one-way ANOVA test followed by the post-hoc Dunnett's or Bonferroni test, as appropriate. Data are presented as mean ± SEM, while the number of cells analysed is indicated in histogram bars or in the text. For immunoblotting analysis, all reported figures are representative of at least three different experiments and the quantitative data are reported as mean ± SD. Comparison between control (Ctrl)and silenced (siTRPV1) cells was done using Student's *t*-test. *P*-values less than 0.05 were considered statistically significant.

3.12 CHEMICALS

FURA-2/AM was obtained from Invitrogen (Life Technologies). BTP-2 was purchased from Calbiochem (Merk Millipore, Darmstadt, Germany), Xestospongin C (XeC) was obtained from ABCAM (Cambridge, UK), while Nigericin and NED-19 were purchased from TOCRIS (Biotechne, Minneapolis, USA). All the other chemicals of analytical grade were obtained from Sigma Aldrich (Merk Millipore, Darmstadt, Germany).

4 RESULTS

4.1 OPTICAL EXCITATION OF rr-P3HT THIN FILMS INDUCES A COMPLEX INCREASE IN $[Ca^{2+}]_i$ IN CIRCULATING ECFCs

In the absence of photostimulation, circulating ECFCs loaded with the Ca^{2+}-sensitive fluorophore, FURA-2/AM (4 μM), did not display spontaneous Ca^{2+} oscillations, either when they were plated on uncoated glass coverslips or glass/P3HT samples (data not shown). Visible light pulses (wavelength excitation peak, 470 nm; photoexcitation density, 0.6 mW/mm^2) were provided by a LED source incident from the glass side (Lodola et al 2019a). Light pulses of different durations (2.5–20 sec) at the same photoexcitation density were delivered to ECFCs plated on rr-P3HT and loaded with FURA-2A/AM and the changes in $[Ca^{2+}]_i$ were measured after termination of the illumination protocol. The FURA-2/AM optical stimulation protocol, with excitation wavelengths at 340/380 nm, presents a negligible overlap with the rr-P3HT optical absorption (**Figure 14A**) and does not lead to degradation of the rr-P3HT thin film optical properties, as carefully verified by measuring its intrinsic fluorescence emission. No sizable differences were observed in the same region before and after exposure to the FURA-2/AM excitation (**Figure 14B**). A long-lasting increase in $[Ca^{2+}]_i$ was evoked in the majority of

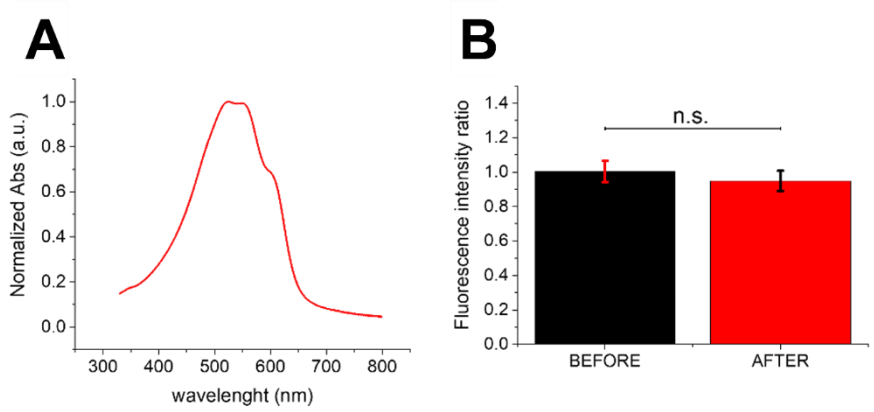

Figure 14 rr-P3HT fluorescence emission does not change after exposing rr-P3HT substrates to the 340/380 nm excitation protocol. **A.** rr-P3HT optical absorption spectrum, normalized to the peak maximum. **B.** Mean rr-P3HT fluorescence intensity ratio measured before and after the exposure of rr-P3HT films to the FURA-2/AM optical stimulation protocol (exc. 340/380 nm). The ratio is calculated by dividing the fluorescence of each treated region by the average fluorescence measured in the untreated rr-P3HT areas. Mean values were averaged over 4 fields of view, over 3 statistically independent samples. Data were compared using the nonparametric Mann-Whitney U-test (0.05 significance level). Error bars represent the standard deviation.

ECFCs subjected to photoexcitation for ≥ 2.5 sec (**Figure 15**). Upon 2.5 sec illumination (**Figure 15A**), almost half of ECFCs (60.95%, n = 167) displayed a slowly progressing increase in $[Ca^{2+}]_i$ to a plateau level, which remained stable above the baseline until the end of the recording (**Figure 15A**). We term this mode of Ca^{2+} signalling induced by photoexcitation as "not-oscillating" signal. In the remaining fraction of ECFCs (39.05%, n = 107), a 2.5 sec light pulse evoked complex Ca^{2+} waveforms (**Figure 15B**). The gradual rise in $[Ca^{2+}]_i$ was indeed overlapped by rapid Ca^{2+} spikes that terminated before the plateau level was achieved (**Figure 15B**). These fluctuations in $[Ca^{2+}]_i$ present the fast kinetics of

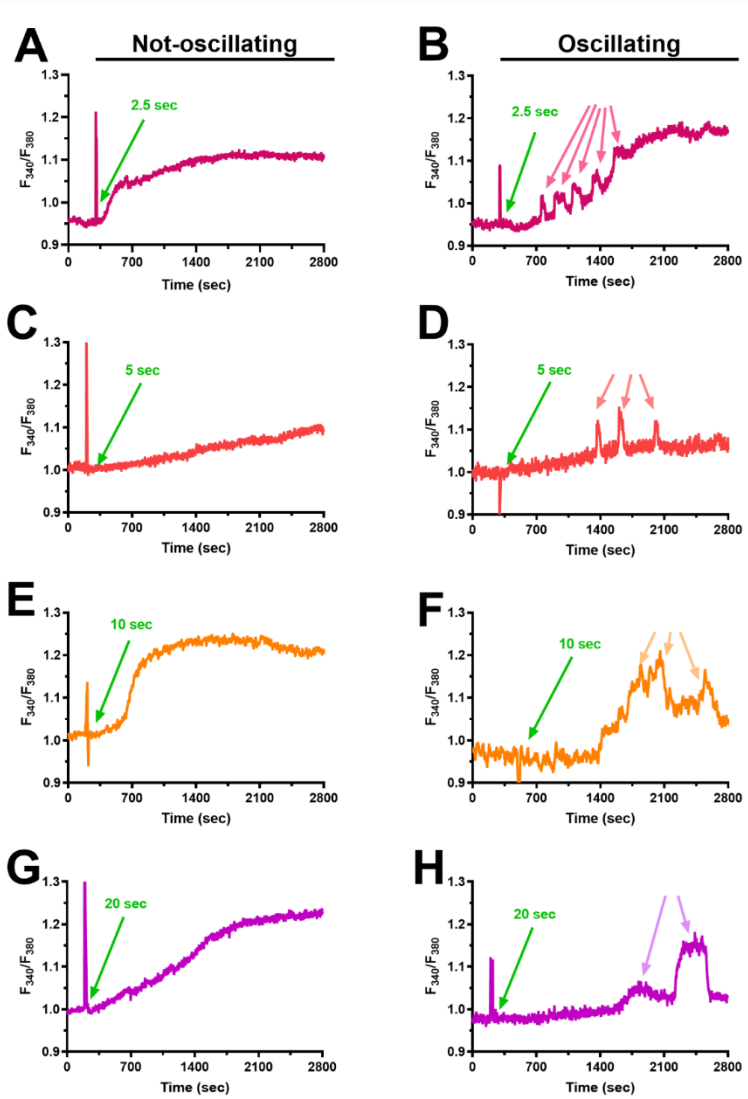

Figure 15 Optical stimulation of rr-P3HT thin films induces an increase in $[Ca^{2+}]_i$ in circulating ECFCs. **A.** 2.5 sec of light stimulation elicited an increase in $[Ca^{2+}]_i$ characterized by a slowly rising signal in ≈60% ECFCs. **B.** Ca^{2+} oscillations evoked by 2.5 sec of optical stimulation in ≈40% ECFCs. **C.** Slowly rising Ca^{2+} signal induced by 5 sec long light pulse in ≈77% ECFCs. **D.** ≈23% displayed oscillations evoked by 5 sec of light stimulation. **E.** 10 sec of optical stimulation evoked a plateauing increase in $[Ca^{2+}]_i$ in ≈86%. **F.** Ca^{2+} oscillations stimulated by 10 sec long light pulses in ≈14%. **G.** 20 sec of light stimulation elicited a plateauing increase in $[Ca^{2+}]_i$ in ≈94%. **H.** ≈6% ECFCs displayed Ca^{2+} oscillations in response to 20 sec light pulse long stimulation.

baseline Ca^{2+} spikes, but each of them falls to a $[Ca^{2+}]_i$ level that is increasingly above the resting baseline. Therefore, we term this mode of Ca^{2+} signalling induced by photoexcitation as "oscillating" (Thomas et al 1996). Notably, there was no significant difference in the amplitude of the plateau level above the resting baseline that was achieved by the $[Ca^{2+}]_i$ in "not-oscillating" vs. "oscillating" cells (0.199±0.011, n = 157, and 0.219±0.012, n = 107). The percentage of ECFCs displaying an oscillatory Ca^{2+} signal progressively decreased upon illumination with longer light pulses (5–20 sec). Intracellular Ca^{2+} oscillations appeared in 22.55% (n = 102), 14.45% (n = 152), and 5.63% (n = 142) ECFCs subjected to photoexcitation for, respectively, 5 sec, 10 sec, and 20 sec, with the remaining cells displaying a non-oscillating Ca^{2+} signal (**Figure 15**). Although the latency of the Ca^{2+} response was significantly (p <

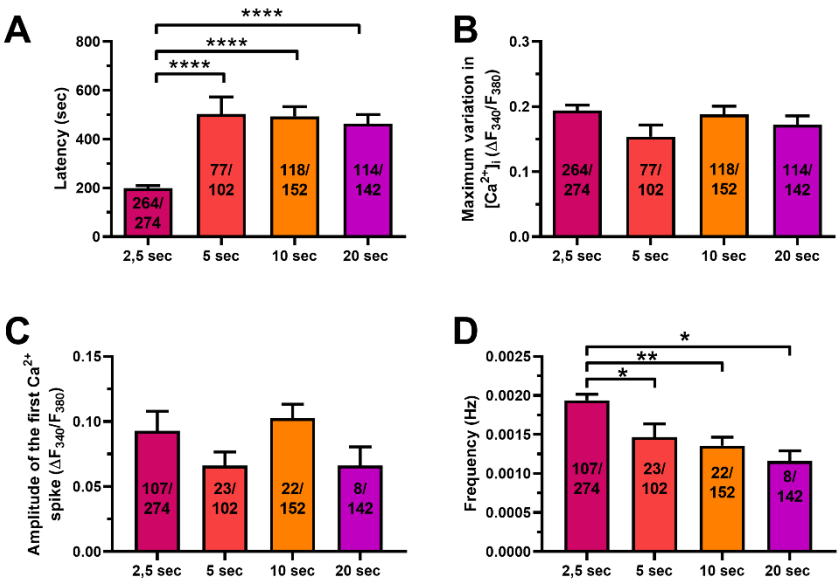

Figure 16 Statistical analysis of the intracellular Ca^{2+} signals evoked in ECFCs plated on rr-P3HT thin films by optical stimulation. **A.** Mean±SEM of the latency of the Ca^{2+} response evoked in ECFCs by light pulses of different durations. **B.** Mean±SEM of the amplitude of the plateau phase reached by $[Ca^{2+}]_i$ upon exposure to 2.5, 5, 10 and 20 sec light stimulation. **C.** Mean±SEM of the amplitude of the first Ca^{2+} spike evoked in oscillating ECFCs by light pulses of different durations. **D.** Mean±SEM of the frequency of Ca^{2+} oscillations evoked by light pulses of different durations. **** indicate $p < 0.0001$, ** indicate $p < 0.005$, and * indicates $p < 0.05$.

0.05) shorter in response to 2.5 sec light pulses (**Figure 16A**), the amplitude of the maximum variation that $[Ca^{2+}]_i$ achieved, either directly or after the oscillations, remained constant for each stimulus duration (**Figure 16B**). In oscillating ECFCs, the average amplitude of the first Ca^{2+} transient did not significantly change by varying the duration of photoexcitation (**Figure 16C**), while the oscillation frequency was significantly higher upon 2.5 sec long light pulses (**Figure 16D**). The onset of multiple patterns of intracellular Ca^{2+} signals upon polymer-mediated photoexcitation is therapeutically relevant as heterogeneous increases in $[Ca^{2+}]_i$ can stimulate pro-angiogenic activity in both vascular endothelial cells (Moccia et al 2019) and circulating ECFCs (Dragoni et al 2011, Lodola et al 2017a). Therefore, the bare impact of photoexcitation on intracellular Ca^{2+} dynamics was assessed by using control, glass substrates. Under these conditions, only a minority of ECFCs subjected to a 2.5 sec long light pulse displayed a slowly activating, non-oscillating Ca^{2+} signal (**Figure 17A** and **Figure 17B**, 20% vs. 95%), which displayed a significantly ($p < 0.05$) longer latency (**Figure 17C**) and a significantly lower peak amplitude (**Figure 17D**) as compared to the cells cultured on rr-P3HT. Intracellular Ca^{2+} oscillations were never induced by optical stimulation in ECFCs cultured on light-transparent substrates. Similar findings were obtained by increasing stimulus duration to 20 sec (**Figure 17E–Figure 17H**). Taken

together, these data indicate that polymer-mediated optical stimulation selectively results in an increase in $[Ca^{2+}]_i$, which can adopt multiple pro-angiogenic waveforms.

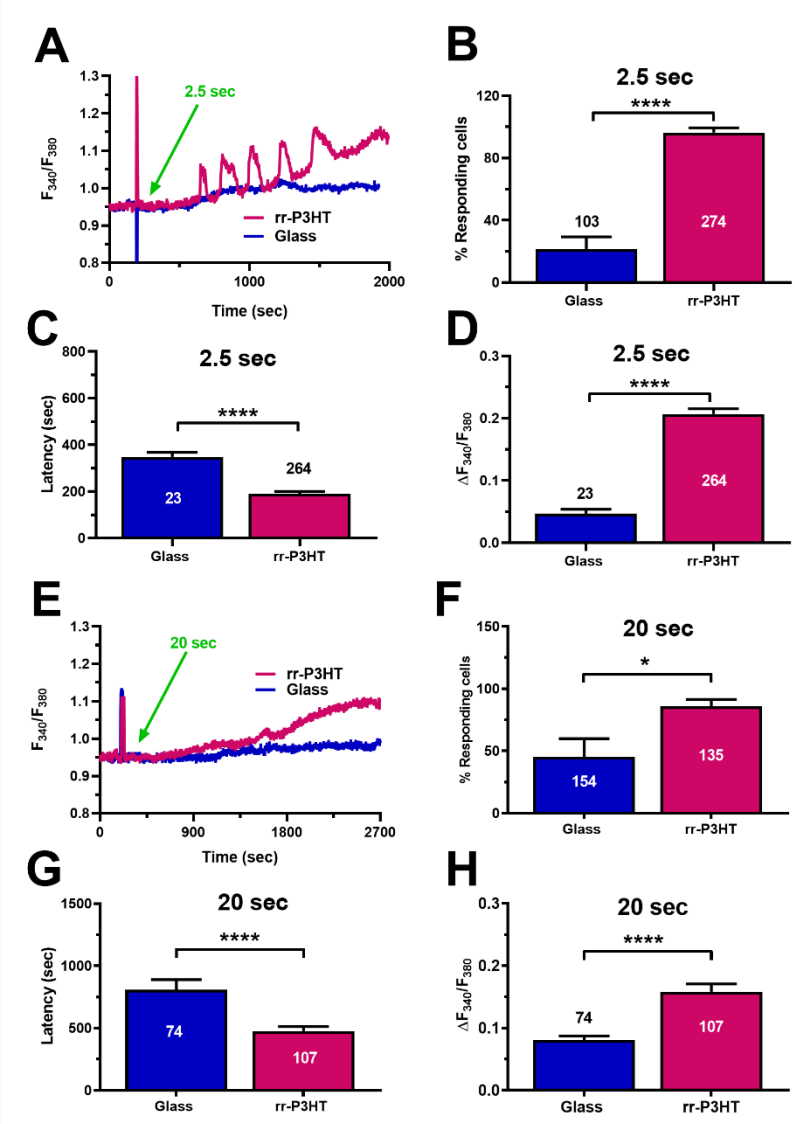

Figure 17 Optical stimulation of glass coverslips does not reliably induce long-lasting elevations in $[Ca^{2+}]_i$ in ECFCs. **A.** 2.5 sec light pulse photoexcitation induced a faster and higher Ca^{2+} response in ECFCs plated on rr-P3HT as compared to ECFCs plated on glass coverslips**. B.** Mean±SEM of the percentage of ECFCs displaying a Ca^{2+} response to 2.5 sec long light pulses in cells plated on glass coverslips and on rr-P3HT. **C.** Mean±SEM of the latency of the response evoked by 2.5 sec long light pulses in ECFCs, respectively, cultured on glass coverslips and rr-P3HT thin films. **D.** Mean±SEM of the amplitude of the Ca^{2+} responses to 2.5 sec long light pulses measured in ECFCs, respectively, cultured on glass coverslips and rr-P3HT thin films. **E**. 20 sec long light pulse evoked faster and higher intracellular Ca^{2+} signals in ECFCs plated on rr-P3HT compared to cells plated on glass coverslips. **F.** Mean±SEM of the percentage of ECFCs displaying a Ca^{2+} responses to 20 sec long light pulses in the presence of glass coverslips and rr-P3HT thin films. **G.** Mean±SEM of the latency of the response evoked by 10 sec long light pulses in ECFCs, respectively, cultured on glass coverslips and rr-P3HT thin films. **H.** Mean±SEM of the amplitude of the Ca^{2+} responses to 20 sec long light pulses measured in ECFCs, respectively, cultured on glass coverslips and rr-P3HT thin films. **** indicate $p < 0.0001$, while * indicates $p < 0.05$.

4.2 THE ROLE OF EXTRACELLULAR Ca^{2+} ENTRY IN THE Ca^{2+} RESPONSE EVOKED BY POLYMER-MEDIATED OPTICAL EXCITATION

Intracellular Ca^{2+} signalling in circulating ECFCs may be triggered by the opening of Ca^{2+}-permeable channels that are located either in the plasma membrane or in intracellular organelles (Moccia 2020). In order to assess the Ca^{2+} source that triggers the Ca^{2+} response to optical stimulation, ECFCs were loaded with FURA-2/AM and then subjected to 2.5 sec long light pulses upon removal of extracellular Ca^{2+} ($0Ca^{2+}$). **Figure 18A** shows that, under such conditions, photoexcitation did not elicit any robust increase in $[Ca^{2+}]_i$ over 300 sec, a time interval that is remarkably longer of the average latency of the Ca^{2+} response elicited by this protocol (i.e., 220.0 ± 11 sec, see **Figure 17A**). Restitution of extracellular Ca^{2+} to the perfusate resulted in a prompt increase in $[Ca^{2+}]_i$, which could display either a non-oscillatory (**Figure 18Aa**) or an oscillatory pattern (**Figure 18Ab**). The role of extracellular Ca^{2+} in maintaining the Ca^{2+} signal initiated by photoexcitation was then assessed by removing extracellular Ca^{2+} during the plateau phase. This manoeuvre caused a prompted and reversible reduction of $[Ca^{2+}]_i$ to the baseline (**Figure 18B**, non-oscillating response, and **Figure 18C**, oscillatory response). These data, therefore, demonstrate that extracellular Ca^{2+} entry is fundamental to trigger and maintain the Ca^{2+} response to polymer-mediated photoexcitation in circulating ECFCs.

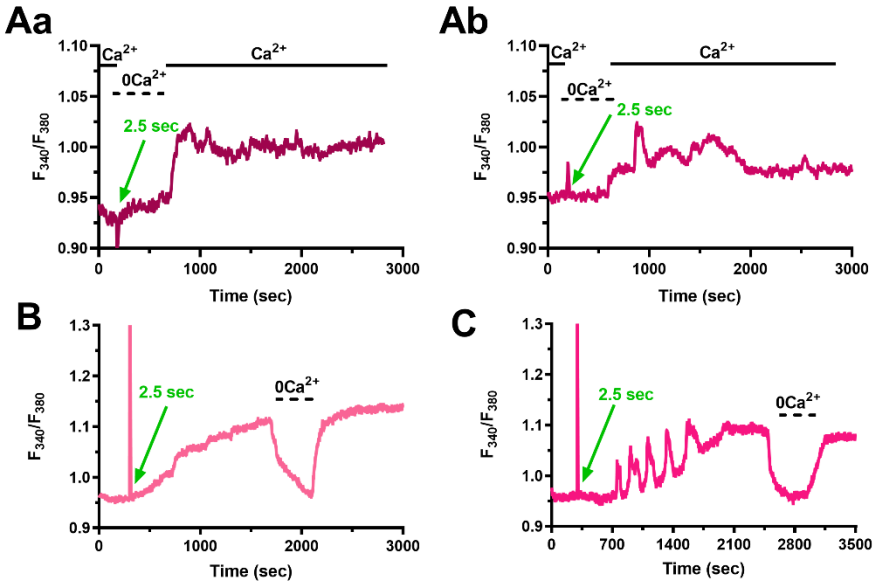

Figure 18 Extracellular Ca^{2+} entry triggers and maintains the Ca^{2+} response induced in ECFCs by photoexcitation of rr-P3HT thin films. **A.** ECFCs subjected to 2.5 sec long light pulses in the absence of extracellular Ca^{2+} did not show any increase in $[Ca^{2+}]_i$ over 300 sec. Restoration of extracellular Ca^{2+} in the bath resulted in a rapid increase in $[Ca^{2+}]_i$ that could display a plateauing (**Aa**) or an oscillatory pattern (**Ab**). **B.** Removal of extracellular Ca^{2+} during the plateau phase caused a prompted and reversible reduction of $[Ca^{2+}]_i$ to the baseline in plateauing cells. **C.** Removal of extracellular Ca^{2+} caused a prompted and reversible reduction of $[Ca^{2+}]_i$ to the baseline also in oscillating cells.

4.3 TRPV1 IS EXPRESSED AND IS FUNDAMENTAL TO INDUCE EXTRACELLULAR Ca^{2+} ENTRY IN ECFCs

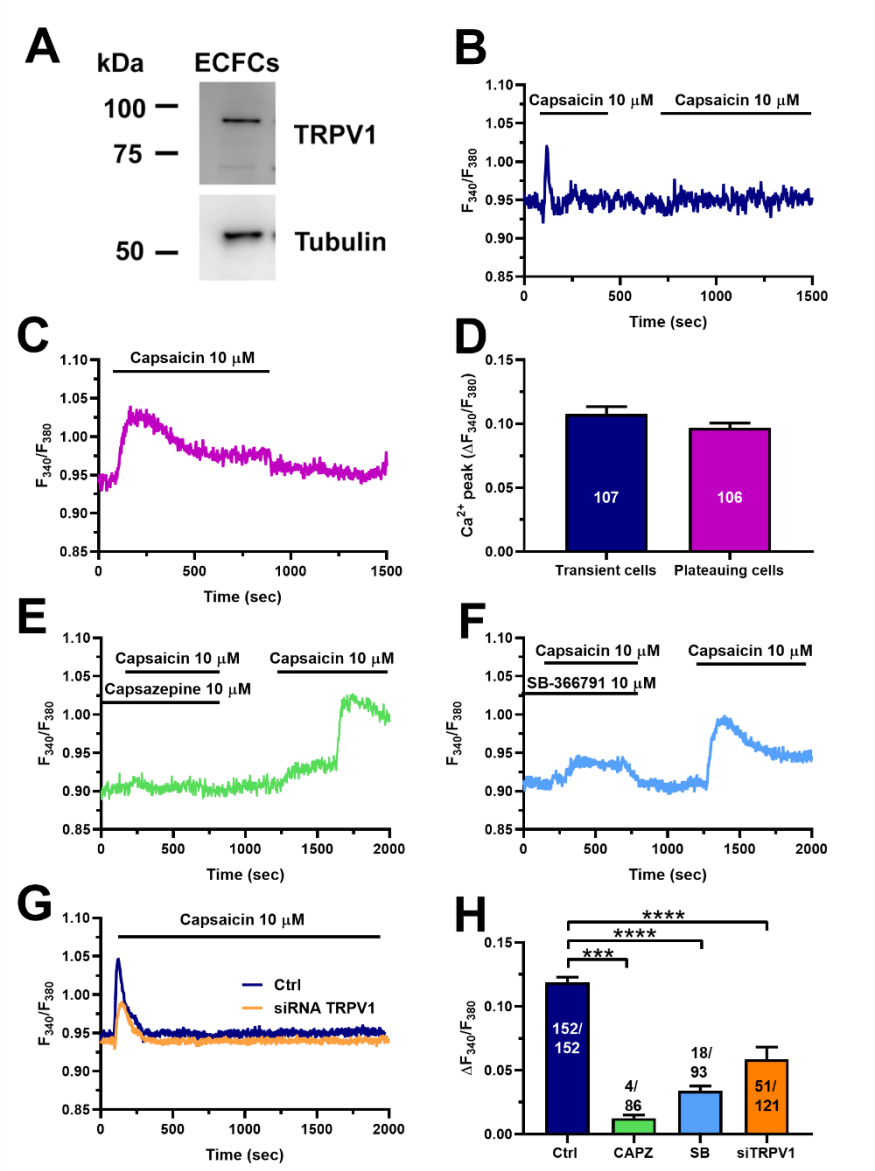

Figure 19 TRPV1 is expressed and induces extracellular Ca^{2+} entry in ECFCs. **A.** TRPV1 protein expression was detected by immunoblotting analysis in ECFCs. **B.** Capsaicin (10 µM), a selective TRPV1-agonist, induced a fast and transient increase in $[Ca^{2+}]_i$ in 107 of 213 cells. **C.** Capsaicin (10 µM) induced a biphasic Ca^{2+} signal, which decayed to the baseline upon the washout of the agonist from the perfusate, in 106 of 213 cells. **D.** Mean±SEM of the amplitude of the two different types of the Ca^{2+} response. **E.** The competitive TRPV1 antagonist, capsazepine (10 µM, 30 min), dramatically affected the amplitude of capsaicin-induced Ca^{2+} signals. Subsequent administration of capsaicin (10 µM), after washout of the antagonist, induced a prompted increase in $[Ca^{2+}]_i$. **F**. SB-366791 (10 µM, 30 min), a structurally different TRPV1 antagonist, strongly reduced the Ca^{2+} response induced by capsaicin (10 µM). **G.** Gene silencing of TRPV1 through the specific siTRPV1 significantly reduced the Ca^{2+} response to capsaicin (10 µM)**. H.** Mean±SEM of the amplitude of the capsaicin-induced Ca^{2+} response under the designated treatments, i.e., in the presence of capsazepine (CAPZ) or SB-366791 (SB) or upon gene silencing of TRPV1 (siTRPV1). **** indicate $p < 0.0001$, while *** indicate $p < 0.001$.

A recent investigation by our group provided the strong evidence that photoexcitation induced TRPV1-mediated depolarization in circulating ECFCs growing on rr-P3HT thin films (Lodola et al 2019a). This study, however, did not assess whether TRPV1 protein is expressed and mediates an increase in $[Ca^{2+}]_i$ in ECFCs. Immunoblotting revealed a major band of ≈100 kDa, which is the predicted molecular weight of TRPV1 (Caterina et al 1997) (**Figure 19A**). We then assessed the effect of capsaicin, a selective TRPV1 agonist (DelloStritto et al 2016a), on $[Ca^{2+}]_i$. Capsaicin (10 μM) evoked a fast Ca^{2+} transient in 107 out of 213 cells (50.2%) (**Figure 19B**). Subsequent delivery of this dietary agonist failed to evoke a detectable increase in $[Ca^{2+}]_i$ (**Figure 19B**), which suggests that the Ca^{2+} response to capsaicin rapidly desensitized in these cells (Faris et al 2020a). In the remaining 106 cells (49.8%), capsaicin (10 μM) induced a biphasic Ca^{2+} signal, which decayed to the baseline upon washout of the agonist from the bath (**Figure 19C**). The biphasic Ca^{2+} response to capsaicin consisted in an initial Ca^{2+} peak which then declined to a steady-state plateau level that persisted as long as the agonist was presented to the cells. This heterogeneous pattern of Ca^{2+} response to capsaicin has been reported in other cell types (Faris et al 2020a, Stueber et al 2017). However, there was no significant difference in the Ca^{2+} peak amplitude of the two distinct Ca^{2+} signals evoked by capsaicin (**Figure 19D**). In order to confirm that TRPV1 mediates an increase in $[Ca^{2+}]_i$, we probed the effects of two structurally unrelated compounds, such as capsazepine and SB-366,791, which are recognized as selective blockers of TRPV1 (Lodola et al 2017b, Lodola et al 2019a, Negri et al 2020). The Ca^{2+} response to capsaicin (10 μM) was reversibly blocked either by capsazepine (10 μM, 30 min) (**Figure 19E**) or by SB-366,791 (10 μM, 30 min) (**Figure 19F**). Furthermore, gene silencing of TRPV1 protein through a specific small interfering RNA (siTRPV1) also impaired capsaicin-induced intracellular Ca^{2+} signals in ECFCs (**Figure 19G**). The effectiveness of cell-trasfection to down-regulate TRPV1 expression has been confirmed by immunoblotting (**Figure 20**), whereas the impact of the pharmacological and genetic manipulation of TRPV1 has been summarized in **Figure 19H**). In aggregate, these findings demonstrate that TRPV1 is able to trigger an increase in $[Ca^{2+}]_i$ in circulating ECFCs.

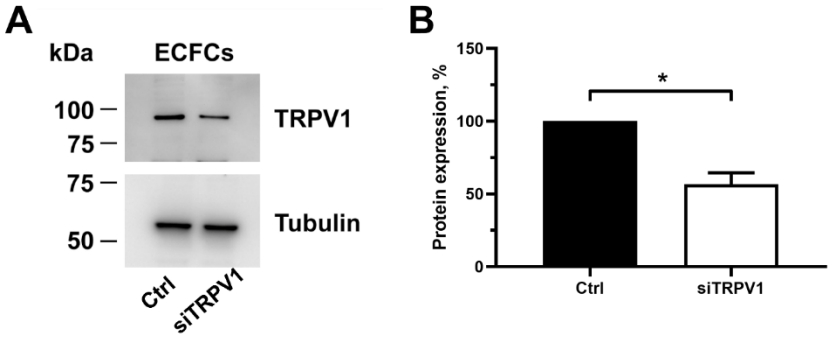

Figure 20 TRPV1 expression in ECFCs was significantly reduced by the siTRPV1-mediated gene silencing. **A.** Representative immunoblots of TRPV1 expression in control (Ctrl) and silenced (siTRPV1) ECFCs. Tubulin was used as equal loading control. The gel is representative of three. **B.** Quantification of the results performed by densitometric scanning reported as percentage of protein expression compared to control (Ctrl). Results are the Mean±SD of three different experiments. Student's t-test has been used for statistical comparison. * indicates $p < 0.05$.

4.4 TRPV1 TRIGGERS THE COMPLEX INCREASE IN $[Ca^{2+}]_i$ INDUCED BY POLYMER-MEDIATED OPTICAL EXCITATION IN ECFCs

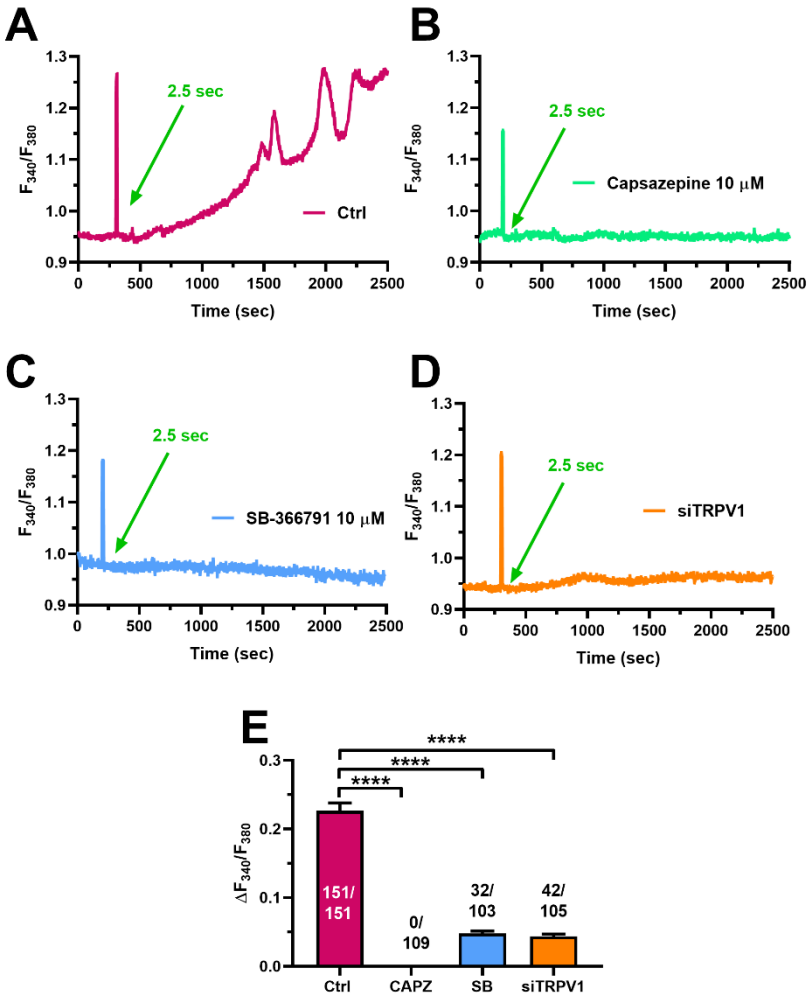

Figure 21 TRPV1 mediates light-induced Ca^{2+} signals in ECFCs plated on rr-P3HT thin films. **A.** 2.5 sec light pulse induced an oscillatory Ca^{2+} response in ECFCs plated on rr-P3HT and not pretreated with TRPV1 inhibitors. **B.** Pharmacological inhibition of TRPV1 with capsazepine (10 μM, 30 min) completely abrogated the Ca^{2+} response to optical stimulation. **C.** SB-366791 (10 μM, 30 min) strongly inhibited the Ca^{2+} signal induced by photoexcitation. **D.** Light-induced increase in $[Ca^{2+}]_i$ was dramatically reduced by gene silencing of TRPV1 through the specific siTRPV1. **E.** Mean±SEM of the amplitude of the Ca^{2+} response in cells under the designated treatments, i.e., in the presence of capsazepine (CAPZ) or SB-366791 (SB) or upon gene silencing of TRPV1 (siTRPV1). **** indicate $p < 0.0001$.

We exploited the pharmacological and genetic approach described above to assess whether TRPV1 initiates the Ca^{2+} response induced in ECFCs by the optical excitation of rr-P3HT thin films. **Figure 21A** shows the complex increases in $[Ca^{2+}]_i$ evoked by a 2.5 sec excitation pulse in ECFCs maintained under control conditions. The Ca^{2+} response to photoexcitation was suppressed by pharmacological blockade of TRPV1 with either capsazepine (10 μM, 30 min) (**Figure 21B**) or SB-366,791 (10 μM, 30 min) (**Figure 21C**). Likewise, genetic deletion of TRPV1 impaired light-induced intracellular Ca^{2+} signals in circulating ECFCs (**Figure 21D**). The statistical analysis of these data has been reported in

Figure 21E. Parallel recordings confirmed that the Ca^{2+} response to capsaicin (10 μM) was not dampened by culturing ECFCs on rr-P3HT thin films (**Figure 22**). Taken together, these findings demonstrate for the first time that TRPV1 activation triggers the complex increase in $[Ca^{2+}]_i$ induced by polymer-mediated optical excitation in circulating ECFCs.

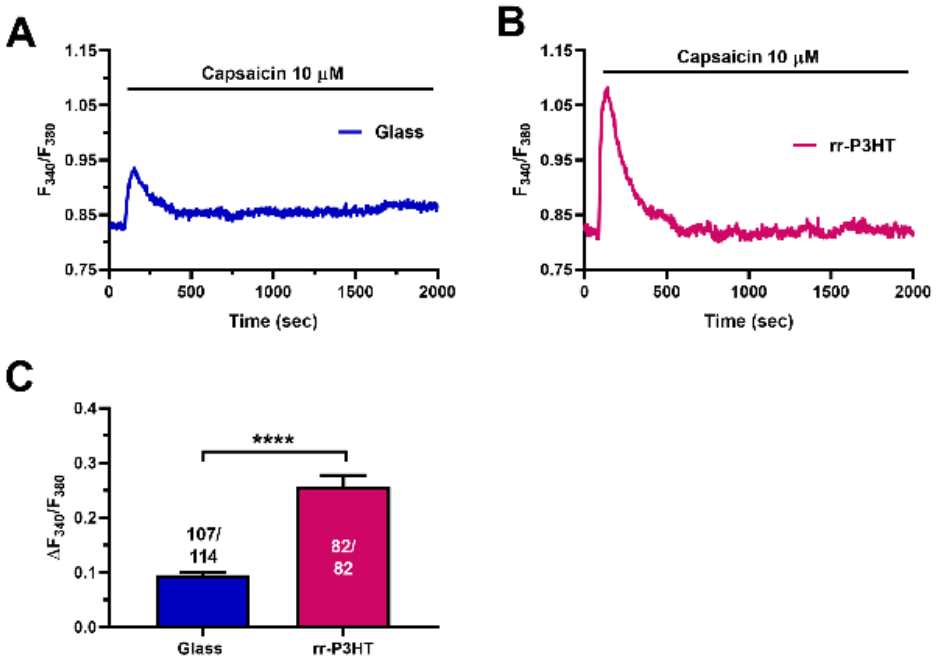

Figure 22 The Ca^{2+} response to capsaicin was not impaired by culturing ECFCs on rr-P3HT monolayers. **A.** Capsaicin-evoked Ca^{2+} response in ECFCs plated on glass coverslips. Capsaicin was administered at 10 μM. **B.** Capsaicin-induced Ca^{2+} signals in ECFCs plated on rr-P3HT thin films. Capsaicin was administered at 10 μM. **C.** Mean±SEM of the amplitude of capsaicin-induced Ca^{2+} signals upon the described conditions. **** indicate $p < 0.0001$.

4.5 THE PHOTOTRANSDUCTION MECHANISM: THE ROLE OF ROS IN THE Ca^{2+} RESPONSE TO POLYMER-MEDIATED OPTICAL EXCITATION OF rr-P3HT

A recent report by our groups suggested that the pro-angiogenic effect of rr-P3HT thin films is mainly mediated by ROS rather than heat (Lodola et al 2019a). To assess this issue, we first cultured ECFCs on a photoresist substrate (MicroPosit S1813), i.e., a fully electrically inert nanomaterial. Optical stimulation induced a Ca^{2+} response also under these conditions (**Figure 23A**). However, the percentage of responding cells (**Figure 23B**) was significantly ($p < 0.05$) lower, while the latency of the Ca^{2+} response (**Figure 23C**) was significantly ($p < 0.05$) longer, as compared to the Ca^{2+} signal recorded from ECFCs cultured on rr-P3HT thin films. Furthermore, the amplitude (**Figure 23D**) and duration (**Figure 23A**) of the Ca^{2+} response to optical excitation of S1813 were remarkably lower as compared to the increase in $[Ca^{2+}]_i$ evoked by light in the presence of rr-P3HT. Indeed, the Ca^{2+} response recorded in the absence of light-induced electrochemical reactions consisted in a transient elevation in $[Ca^{2+}]_i$ that rapidly recovered to the baseline (**Figure 23A**).

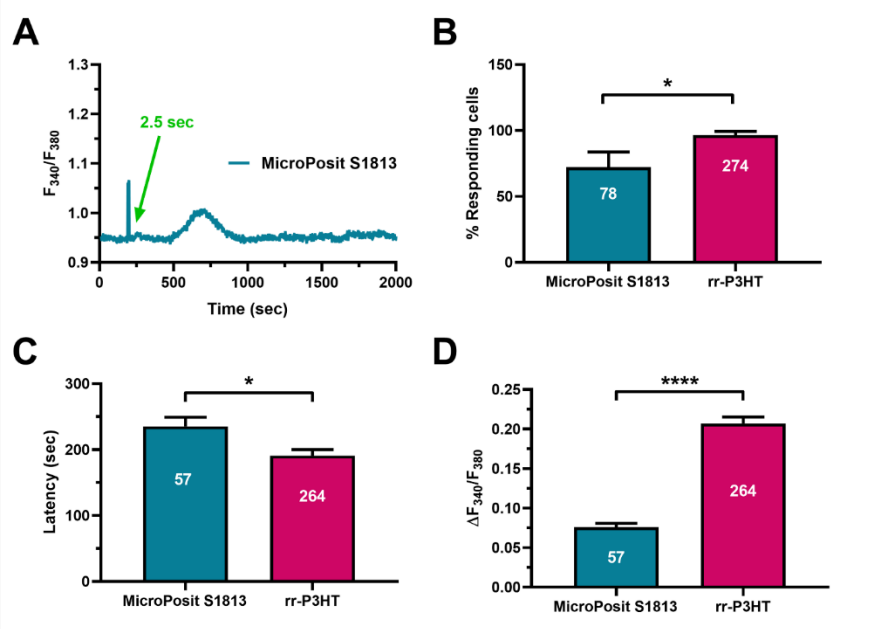

Figure 23 Optical stimulation of a photoresist nanomaterial does not reliably increase the $[Ca^{2+}]_i$ in ECFCs. **A**. Optical stimulation (2.5 sec light pulse) induced a delayed and transient increase in $[Ca^{2+}]_i$ in ECFCs plated on the photoresist material Microposit S1318**. B.** Mean±SEM of the percentage of ECFCs displaying a Ca^{2+} response to optical stimulation of ECFCs cultured on presence of MicroPosit S1813 and on rr-P3HT thin films, respectively. **C.** Mean±SEM of the latency of the Ca^{2+} response to optical stimulation of ECFCs cultured on MicroPosit S1813 and on rr-P3HT thin films, respectively. **D.** Mean±SEM of the amplitude of the Ca^{2+} response to optical stimulation in ECFCs cultured on MicroPosit S1813 and on rr-P3HT thin films, respectively. **** indicate $p < 0.0001$, * indicates $p < 0.05$.

Therefore, we next investigated ROS involvement in the onset of the long lasting Ca^{2+} response to light in circulating ECFCs plated on rr- P3HT thin films. ECFCs loaded with the cell-permeable fluorescent probe, H_2DCF-DA (10 μM), exhibited a significant ROS signal when exposed to 2.5 sec (**Figure 24A**) and 20 sec (**Figure 24B**) light pulses only in the presence, but not in the absence, of rr-P3HT. Considering that the main ROS produced by optical stimulation of rr-P3HT thin films is H_2O_2 (Bellani et al 2015, Bossio et al 2018), we repeated the intracellular ROS measurement in the presence of the

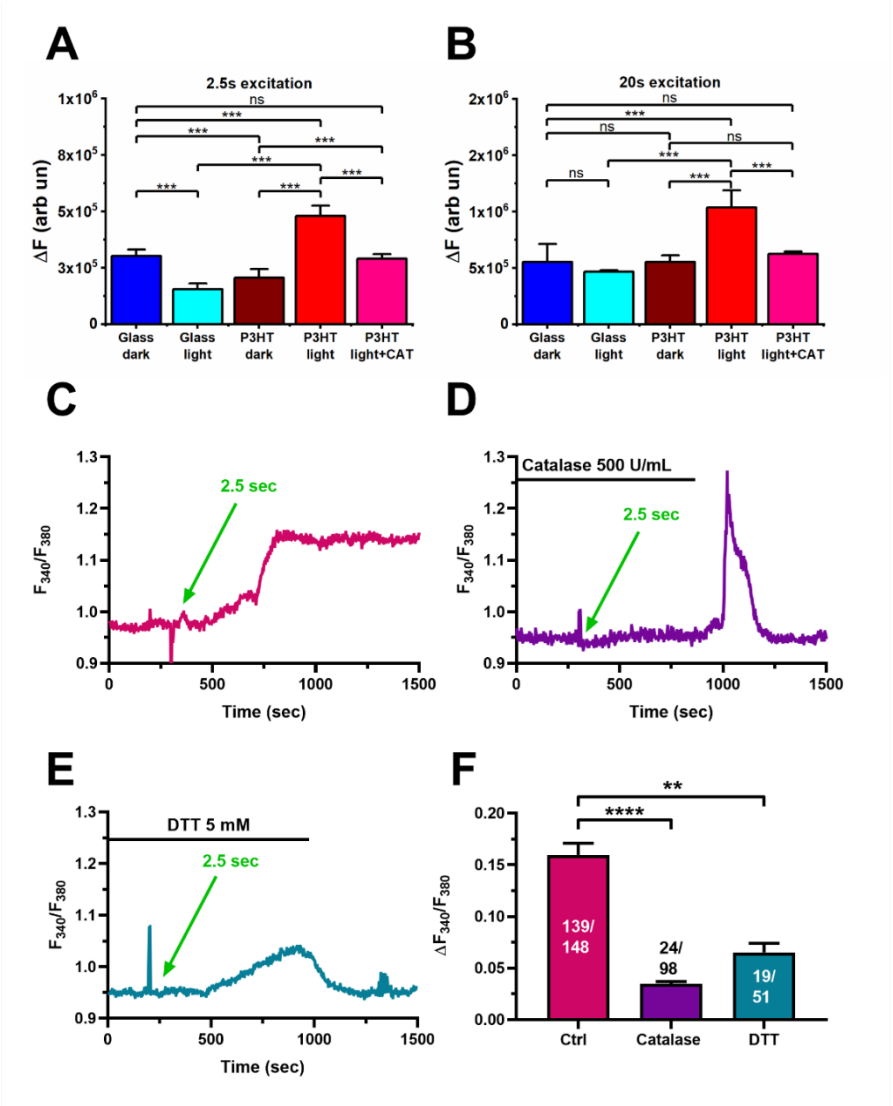

Figure 24 The crucial role of ROS in the light-induced Ca^{2+} response in ECFCs plated on rr-P3HT. **A.** ECFCs loaded with the cell-permeable fluorescent probe, H_2DCF-DA (10 μM), showed a significant increase in intracellular ROS concentration when exposed to 2.5 sec light pulses, in the presence of rr-P3HT. Conversely, the presence of the ROS scavenger, catalase (500 U/mL), strongly reduced the increase in H_2DCF-DA fluorescence. *** indicate $p < 0.001$. **B.** ECFCs stimulated with 20 sec light pulses, exhibited a similar ROS signal in the presence of rr-P3HT, which was significantly reduced in the presence of catalase**.** *** indicate $p < 0.001$. **C.** Ca^{2+} signal induced by 2.5 sec light pulse of optical stimulation of ECFCs cultured on rr-P3HT in the absence of ROS scavengers. **D.** The Ca^{2+} response to 2.5 sec long light pulses was significantly reduced by scavenging H_2O_2 production with catalase (500 U/mL). Washout of the scavenger resulted in a rebound and transient increase in $[Ca^{2+}]_i$. **E.** Dithiothreitol (DTT; 10 μM), a thiol-specific reducing compound, strongly reduced the Ca^{2+} response elicited by 2.5 sec long optical stimulation. **F.** Mean±SEM of the amplitude of light-induced Ca^{2+} signals in ECFCs plated on rr-P3HT under the designated treatments, i.e., in the presence of catalase, DTT, capsazepine (CAPZ), SB-366791 (SB) or upon gene silencing of TRPV1 (siTRPV1). **** indicate $p < 0.0001$.

H_2O_2 scavenger, catalase (500 U/mL). As expected, there was not a significant increase in H_2DCF-DA fluorescence under these conditions (**Figure 24A** and **Figure 24B**) (DelloStritto et al 2016a). In accord with this observation, scavenging H_2O_2 production with catalase (500 U/mL) significantly ($p < 0.0001$) reduced the Ca^{2+} response evoked in ECFCs by optical stimulation of rr-P3HT thin films (**Figure 24C** and **Figure 24D**). Washout of catalase from the bathing solution resulted in a rebound increase in $[Ca^{2+}]_i$ that rapidly declined to the baseline (**Figure 24D**). Furthermore, dithiothreitol (DTT) (5 mM) (**Figure 24E**), a thiol-specific reducing compound that is largely employed to reverse H_2O_2-mediated signalling (Chuang & Lin 2009, DelloStritto et al 2016a), potently inhibited light-induced intracellular Ca^{2+} signals (**Figure 24E**). The statistical analysis of these data has been shown in **Figure 24F**. These observations strongly suggest that H_2O_2 is crucial to the onset of the Ca^{2+} response to polymer-mediated optical excitation of rr-P3HT thin films.

4.6 H_2O_2 ACTIVATES TRPV1-MEDIATED INTRACELLULAR Ca^{2+} SIGNALS IN ECFCs

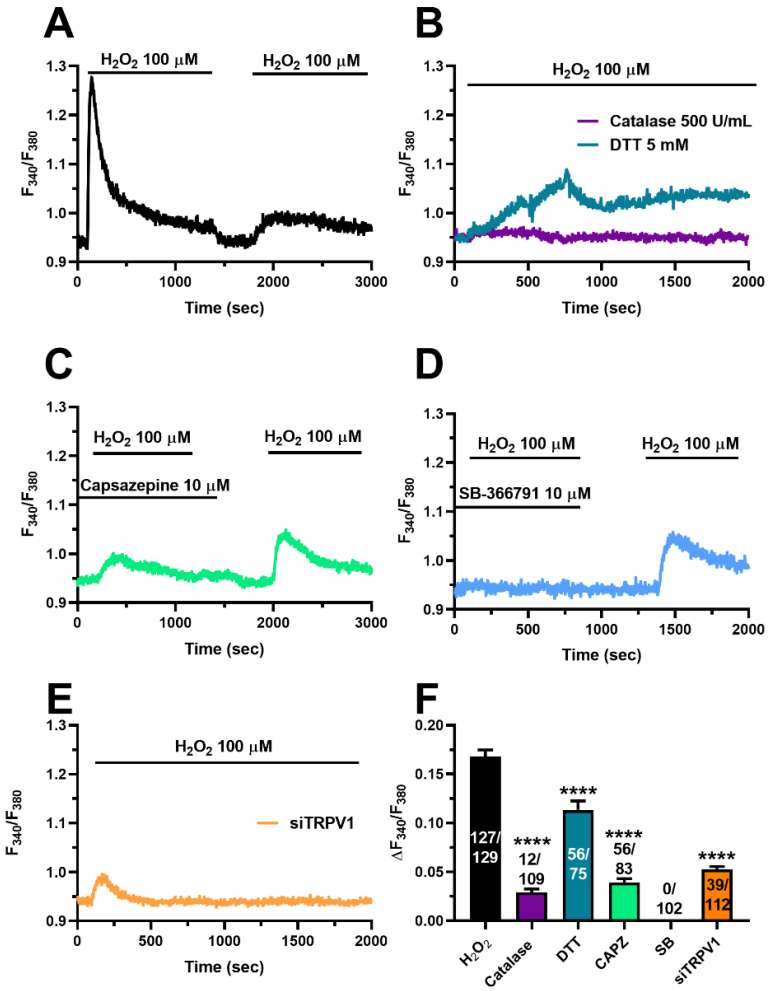

Figure 25 H_2O_2 triggers TRPV1-dependent intracellular Ca^{2+} signals in ECFCs. **A.** H_2O_2 (100 µM) induced a biphasic increase in $[Ca^{2+}]_i$, characterized by an intermediate plateau phase which decayed to the baseline level with the washout of the agonist. **B.** The Ca^{2+} response to H_2O_2 (100 µM) was significantly inhibited by the scavenger catalase (500 U/ml) and by DTT (10 µM). **C.** The selective TRPV1 antagonist, capsazepine (10 µM, 30 min), strongly reduced H_2O_2-induced intracellular Ca^{2+} signals. A further stimulation with H_2O_2 (100 µM) evoked a prompted increase in $[Ca^{2+}]_i$ after the washout of the inhibitor. **D.** SB-366791 (10 µM, 30 min), another specific TRPV1 inhibitor, completely abrogated H_2O_2-evoked Ca^{2+} signals in ECFCs. H_2O_2 was administered at 100 µM. **E.** Gene silencing of TRPV1 expression with the specific siTRPV1 also impaired H_2O_2-induced intracellular Ca^{2+} signals in ECFCs. H_2O_2 was administered at 100 µM. **F.** Mean±SEM of the amplitude of H_2O_2-induced Ca^{2+} signals under the designated treatments. **** indicate $p < 0.0001$.

In order to confirm the signalling role of ROS in polymer-mediated Ca^{2+} response to photoexcitation, we directly challenged ECFCs with H_2O_2. As previously reported for capsaicin, H_2O_2 (100 µM) evoked a fast Ca^{2+} transient in 108 out of 363 cells (30%) and a biphasic Ca^{2+} signal in the remaining 232 cells (64%) (**Figure 25A**). Similar to optical excitation, H_2O_2-induced Ca^{2+} signals were significantly ($p < 0.05$) inhibited by catalase (500 U/ml) and by DTT (5 mM) (**Figure 25B**). Furthermore, the Ca^{2+} response to H_2O_2 (100 µM) was significantly ($p < 0.05$) reduced by blocking TRPV1 with either capsazepine (10 µM, 30 min) (**Figure 25C**) or by SB-366,791 (10 µM, 30 min) (**Figure 25D**). Finally, genetic disruption of TRPV1 protein expression through the specific siTRPV1 also impaired H_2O_2-induced increase in $[Ca^{2+}]_i$ (**Figure 25E**). The statistical analysis of these data has been summarized in

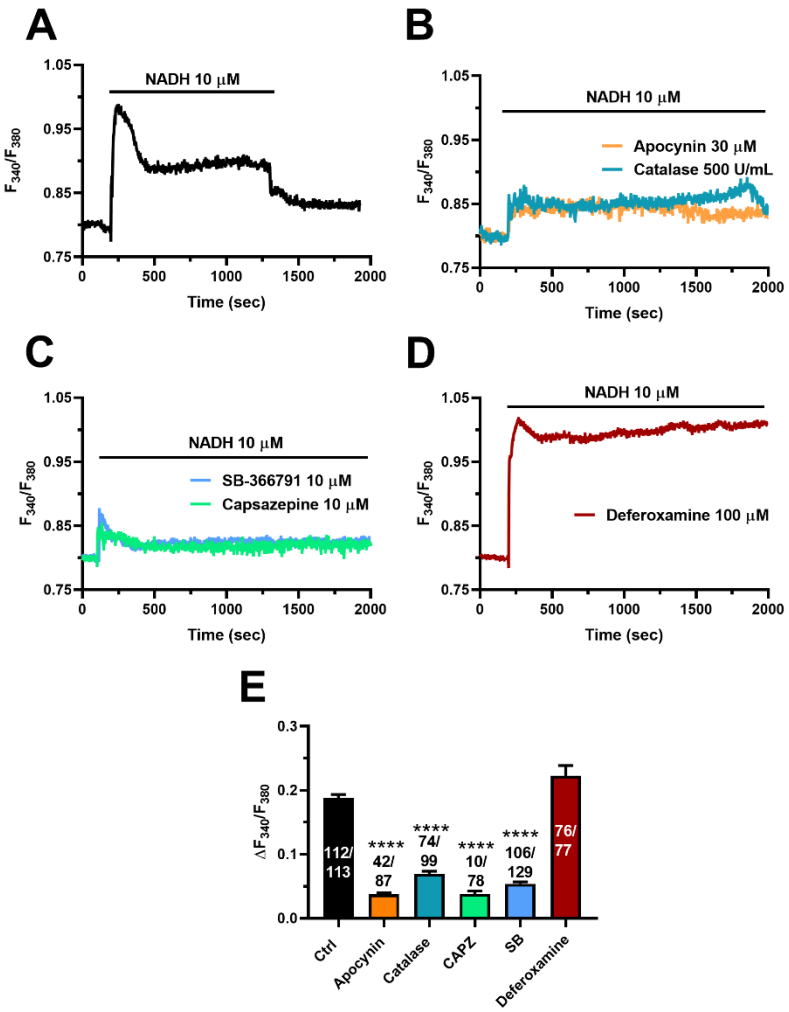

Figure 26 NOX-dependent H_2O_2 production induced TRPV1-dependent intracellular Ca^{2+} signals in ECFCs. **A.** NADH (10 µM) evoked a biphasic increase in $[Ca^{2+}]_i$, characterized by an initial peak followed by an intermediate plateau phase, which decayed to the baseline with the washout of the molecule. **B.** NADH-evoked Ca^{2+} signals were significantly inhibited by catalase (500 U/ml) and by pre-treating the cells with apocynin (30 µM, 5 min), a selective NOX inhibitor. NADH was administered at 10 µM. **C.** NADH-induced increase in $[Ca^{2+}]_i$ was strongly reduced by inhibiting TRPV1 with either capsazepine (10 µM, 30 min) or SB-366791 (10 µM, 30 min). NADH was administered at 10 µM. **D.** Deferoxamine (100 µM), which prevents the Fenton reaction by chelating Fe^{3+} and thus interferes with the subsequent lipid peroxidation, did not reduce the Ca^{2+} response to NADH (10 µM). **E.** Mean±SEM of the amplitude of NADH-induced Ca^{2+} signals under the designated treatments, i.e., apocynin, catalase, capsazepine (CAPZ), SB-366791 (SB), and deferoxamine. **** indicate $p < 0.0001$.

Figure 25F. Exogenous administration of NADH represents an additional strategy to investigate H_2O_2 signalling in endothelial cells (Sullivan et al 2015). NADH is converted by the membrane-bound enzyme, NOX, into O_2^-, which may be then dismutated to H_2O_2 either spontaneously or by superoxide dismutase (Song et al 2011). NADH (10 μM) evoked an increase in $[Ca^{2+}]_i$ that was inhibited by pre-treating the cells with apocynin (30 μM, 5 min) (**Figure 26A** and **Figure 26B**), a selective NOX inhibitor (Sullivan et al 2015). Furthermore, the Ca^{2+} response to NADH (10 μM) was significantly ($p < 0.0001$) reduced by catalase (500 U/ml) (**Figure 26A** and **Figure 26B**). This observation confirms that H_2O_2 generation is required by NADH to induce intracellular Ca^{2+} signals in ECFCs. Furthermore, NADH-evoked increase in $[Ca^{2+}]_i$ was dramatically attenuated by blocking TRPV1 with either capsazepine (10 μM, 30 min) (**Figure 26C**) or by SB-366,791 (10 μM, 30 min) (**Figure 26C**). In the presence of iron (Fe^{2+}), the Fenton reaction could degrade H_2O_2 into OH^- (Song et al 2011), which may also result in Ca^{2+} signalling via lipid peroxidation (Andersson et al 2008, Sullivan et al 2015). However, the Ca^{2+} response to NADH (10 μM) was not affected by deferoxamine (100 μM) (**Figure 26D**), which prevents the Fenton reaction by chelating ferric iron (Fe^{3+}) (Andersson et al 2008, Sullivan et al 2015). The statistical analysis of these data has been summarized in **Figure 8E**. In aggregate, these findings endorse the view that H_2O_2 produced upon optical excitation of rr-P3HT may induce intracellular Ca^{2+} signals by activating TRPV1 in circulating ECFCs.

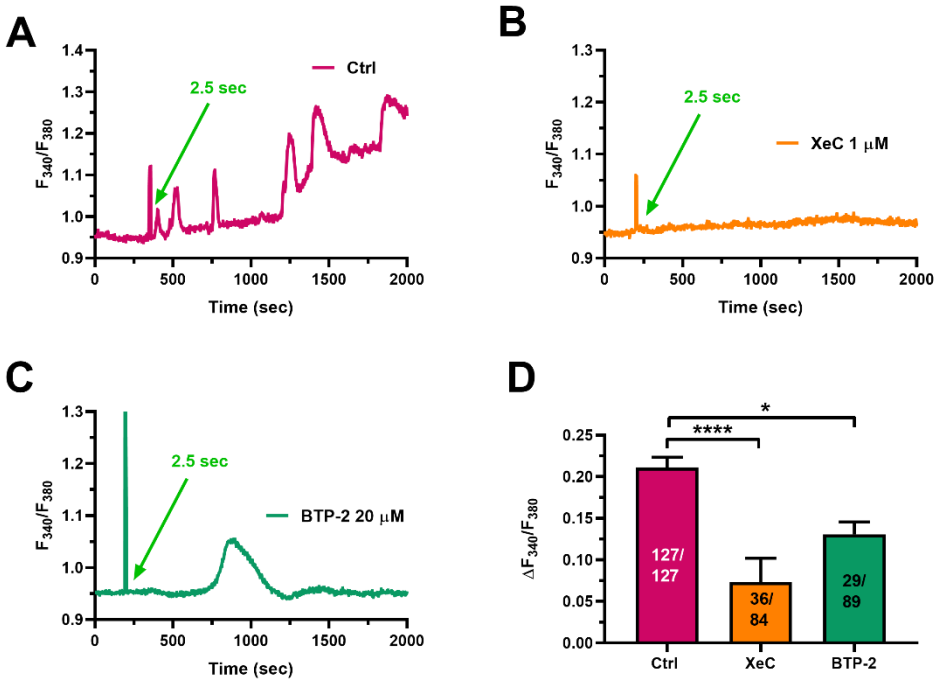

Figure 27 $InsP_3Rs$ and SOCE were involved in the Ca^{2+} response evoked by polymer-mediated optical excitation. **A.** 2.5 sec light pulse induced a robust increase in $[Ca^{2+}]_i$ in ECFCs plated on rr-P3HT thin films under control conditions. **B.** Light-induced Ca^{2+} signal was inhibited by blocking $InsP_3Rs$ with Xestospongin C (XeC; 1 μM, 10 min). **C.** Pre-treatment of cells with the selective SOCE inhibitor, BTP-2 (20 μM, 30 min), significantly reduced and shortened the Ca^{2+} response to optical stimulation. **D.** Mean±SEM of the amplitude of light-induced Ca^{2+} signals under the designated treatments. **** indicate $p < 0.0001$ and * indicates $p < 0.05$.

4.7 THE ROLE OF $InsP_3Rs$ AND SOCE IN THE Ca^{2+} RESPONSE EVOKED BY POLYMER-MEDIATED OPTICAL EXCITATION

The intracellular Ca^{2+} oscillations that arose in a significant fraction of ECFCs exposed to light stimuli in the presence of rr-P3HT resemble $InsP_3$-induced intracellular Ca^{2+} spikes from the ER (Dragoni et al 2011, Moccia et al 2021), which represents the largest endogenous Ca^{2+} store in vascular endothelial cells and ECFCs (Moccia et al 2021). In addition, $InsP_3Rs$ may also contribute to trigger slowly rising Ca^{2+} signals in response to extracellular stimulation (Gericke et al 1993). Notably, the pharmacological blockade of $InsP_3Rs$ with the selective inhibitor, XeC (1 μM, 10 min), prevented light-induced Ca^{2+} signals in the majority of ECFCs (100%, n = 127, and 42.8%, n = 84, in the absence and presence of XeC, respectively. Inspection of the Ca^{2+} tracings showed that, as compared to control cells (**Figure 27A**), the amplitude of the maximum variation in $[Ca^{2+}]_i$ was significantly ($p < 0.0001$) lower in the presence of XeC (**Figure 27B** and **Figure 27D**). $InsP_3$-induced ER Ca^{2+} mobilization, in turn, results in a massive depletion of ER Ca^{2+} levels, which activates a Ca^{2+}-entry pathway SOCE (Moccia et al 2012c). SOCE maintains long-lasting intracellular Ca^{2+} signals evoked by extracellular stimuli in vascular endothelial cells and ECFCs (Sanchez-Hernandez et al 2010). Of note, blocking SOCE with the pyrazole-derivative BTP-2 (20 μM, 30 min) (Lodola et al 2012, Sanchez-Hernandez et al 2010), reduced the percentage of ECFCs displaying a detectable Ca^{2+} response to light stimuli to 32.6% (n = 89). In these cells, BTP-2 converted the long-lasting increase in $[Ca^{2+}]_i$ evoked by optical excitation in a transient Ca^{2+} signal (**Figure 27C**), whose amplitude was significantly ($p < 0.5$) lower than the amplitude of the plateau phase recorded in control cells (**Figure 27D**). Collectively, therefore, these data suggest that SOCE activation upon the recruitment of $InsP_3Rs$ is an important molecular mechanism involved in extracellular Ca^{2+} entry in response to optical excitation, as more widely described in Section 5.4.

4.8 THE PLCβ SIGNALLING PATHWAY TRIGGERS AND SUSTAINS THE INTRACELLULAR Ca^{2+} RESPONSE EVOKED BY TRPV1: THE ROLE OF $InsP_3Rs$ AND SOCE

As showed in **Figure 19** and in **Figure 28A**, capsaicin (10 μM) mainly induced a biphasic Ca^{2+} signal in ECFCs plated on glass coverslips. The evidence that intracellular Ca^{2+} release was required to support the long-lasting Ca^{2+} response to optical excitation prompted us to assess whether, besides extracellular Ca^{2+} entry, TRPV1 activation was *per se* able to mobilize the intracellular Ca^{2+} pool. Therefore, to evaluate the involvement of TRPV1 in the endogenous Ca^{2+} mobilization, ECFCs were challenged with capsaicin (10 μM) in the absence of extracellular Ca^{2+} ($0Ca^{2+}$) (**Figure 28B**). Under these conditions, capsaicin evoked a transient increase in $[Ca^{2+}]_i$ that was characterized by a comparable amplitude as the

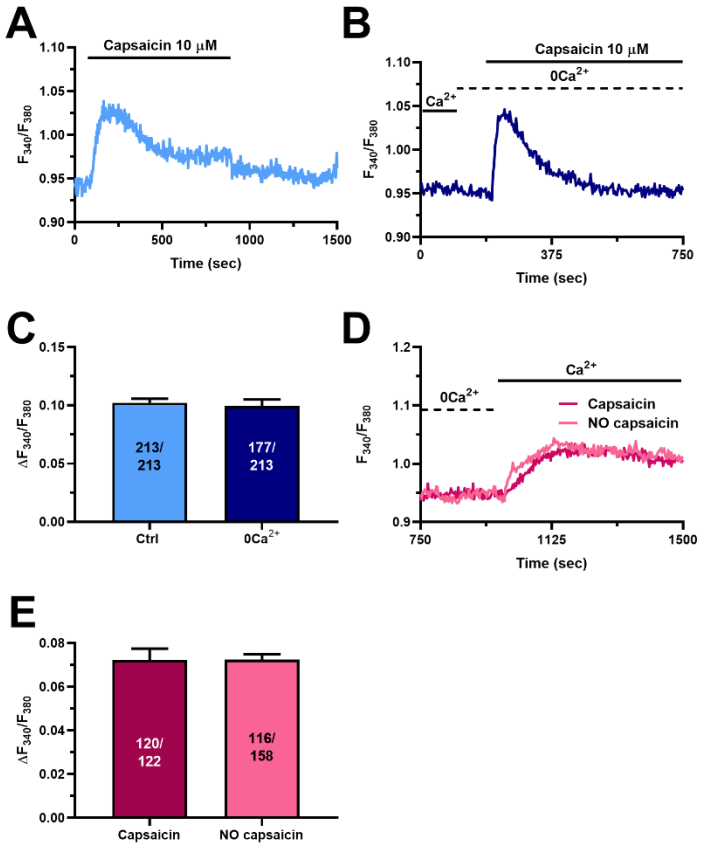

Figure 28 Capsaicin evoked intracellular Ca^{2+} mobilization and agonist-independent Ca^{2+} entry in ECFCs. **A.** Capsaicin (10 μM) induced a biphasic increase in $[Ca^{2+}]_i$ in the presence of extracellular Ca^{2+}. **B.** In the absence of extracellular Ca^{2+} ($0Ca^{2+}$), capsaicin induced a transient increase in $[Ca^{2+}]_i$, which was comparable to the signal amplitude obtained in the presence of extracellular Ca^{2+}.**C.** Mean ± SEM of the amplitude of capsaicin-evoked Ca^{2+} signals in control conditions and in $0Ca^{2+}$. **D.** The restoration of extracellular Ca^{2+} elicited a second raise in $[Ca^{2+}]_i$ both in the presence and in the absence of the agonist, the latter being is indicative of SOCE activation. **E.** Mean ± SEM of the amplitude of capsaicin-evoked extracellular Ca^{2+} entry in the presence and in the absence of capsaicin.

Ca^{2+} signal recorded in control experiments (**Figure 28A and Figure 28C**). In addition, the restoration of Ca^{2+} in the absence and in the presence of the agonist (**Figure 28D**), known as "Ca^{2+} add-back" protocol, induced a second raise in $[Ca^{2+}]_i$, which was comparable under the two different conditions (**Figure 28E**). These data suggest that the extracellular Ca^{2+} entry occurring after the endogenous Ca^{2+}

mobilization is mediated mainly by SOCE rather than by TRPV1, and it is consistent with the hypothesis of the intracellular TRPV1 localization.

To confirm the role of TRPV1 in the endogenous Ca^{2+} mobilization, ECFCs were incubated with capsazepine (10 μM, 30 min) and SB-366791 (10 μM, 30 min) and then stimulated with capsaicin under $0Ca^{2+}$ conditions (**Figure 29B**). The pharmacological manipulation significantly reduced the Ca^{2+} response recorder in control experiments (**Figure 29A**), by suggesting that TRPV1 may be expressed endogenously. Likewise, the Ca^{2+} response to capsaicin was significantly reduced by selectively blocking PLC activity with the amino-steroid U73122 (10 μM, 30 min) and by inhibiting $InsP_3Rs$ with

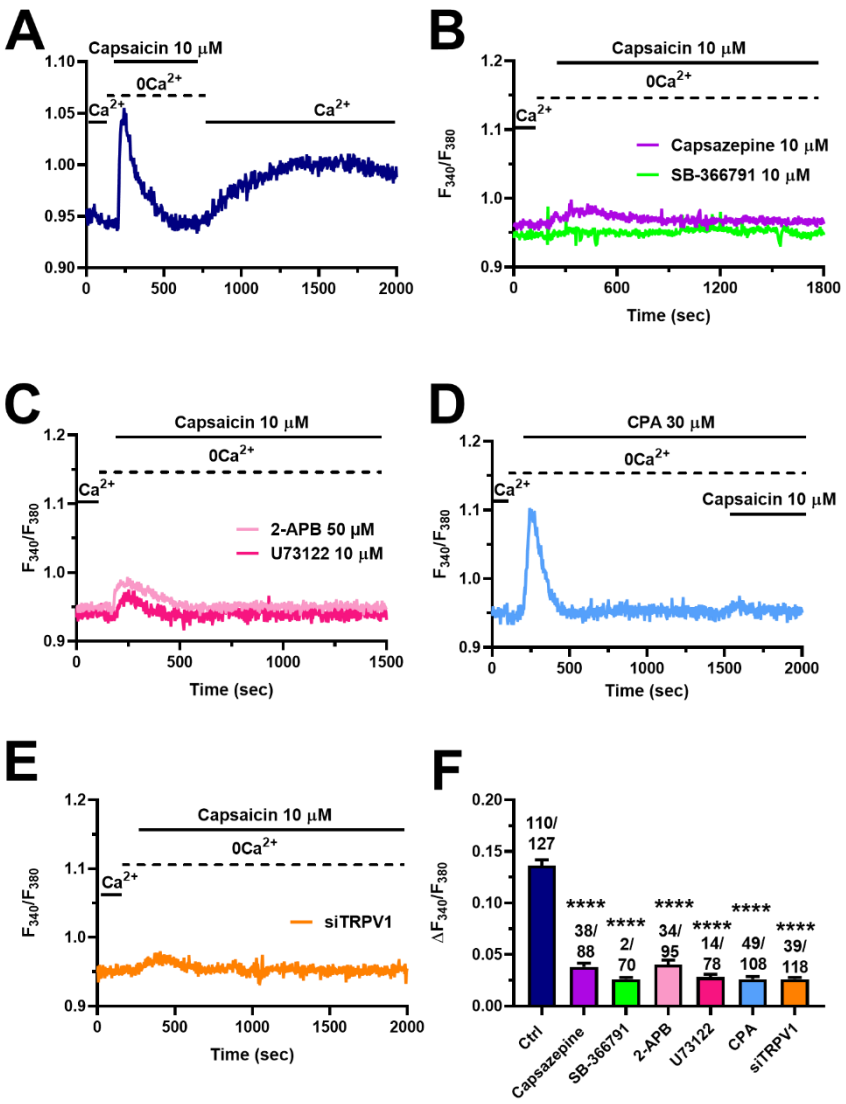

Figure 29 TRPV1-mediated endogenous Ca^{2+} mobilization induced by capsaicin requires ER-dependent Ca^{2+} release through $InsP_3Rs$. **A.** Capsaicin (10 μM) induced a transient increase in $[Ca^{2+}]_i$ in the absence of extracellular Ca^{2+}. The restoration of extracellular Ca^{2+} upon agonist washout induced a second increase in $[Ca^{2+}]_i$ that is indicative of SOCE. **B**. Capsazepine (10 μM, 30 min) and SB-366791 (10 μM, 30 min) inhibited the Ca^{2+} signal induced by capsaicin under $0Ca^{2+}$ condition. **C.** The Ca^{2+} response to capsaicin (10 μM) under $0Ca^{2+}$ conditions, was inhibited by U73122 (10 μM, 30 min), a selective PLC blocker. Moreover, the Ca^{2+} signal was inhibited by blocking $InsP_3Rs$ with 2-APB (50 μM, 30 min). **D.** Emptying the ER with CPA (30 μM, 15 min), a SERCA selective blocker, prevented the onset of the capsaicin-induced increase in $[Ca^{2+}]_i$. **E.** Gene silencing of TRPV1 expression with the specific siTRPV1 also impaired capsaicin-induced intracellular Ca^{2+} signals in ECFCs under $0Ca^{2+}$ conditions**. F.** Mean ± SEM of the amplitude of Ca^{2+} peak in cells under the designated treatments. **** indicate $p < 0.0001$.

2-APB (50 μM, 30 min) (**Figure 29C and Figure 29F**). These data clearly showed that the PLC/$InsP_3$ signalling cascade is involved in the intracellular Ca^{2+} release evoked by capsaicin. To further corroborate the hypothesis, we depleted the ER Ca^{2+} store with cyclopiazonic acid (CPA), which selectively inhibits SERCA activity (Dragoni et al 2011). As expected (Dragoni et al 2011), CPA (30 μM) caused a transient increase in $[Ca^{2+}]_i$ due to the ER Ca^{2+} release through the leakage channels and through several Ca^{2+} extrusion mechanisms (**Figure 29D**). Subsequent addition of capsaicin (10 μM) induced a significantly lower Ca^{2+} signal in a minor percentage of ECFCs (**Figure 29D and Figure 29F**), by confirming the role of ER Ca^{2+} mobilization in the response to capsaicin. Finally, the gene silencing of TRPV1 with the specific siTRPV1 significantly reduced the capsaicin-induced Ca^{2+} signals

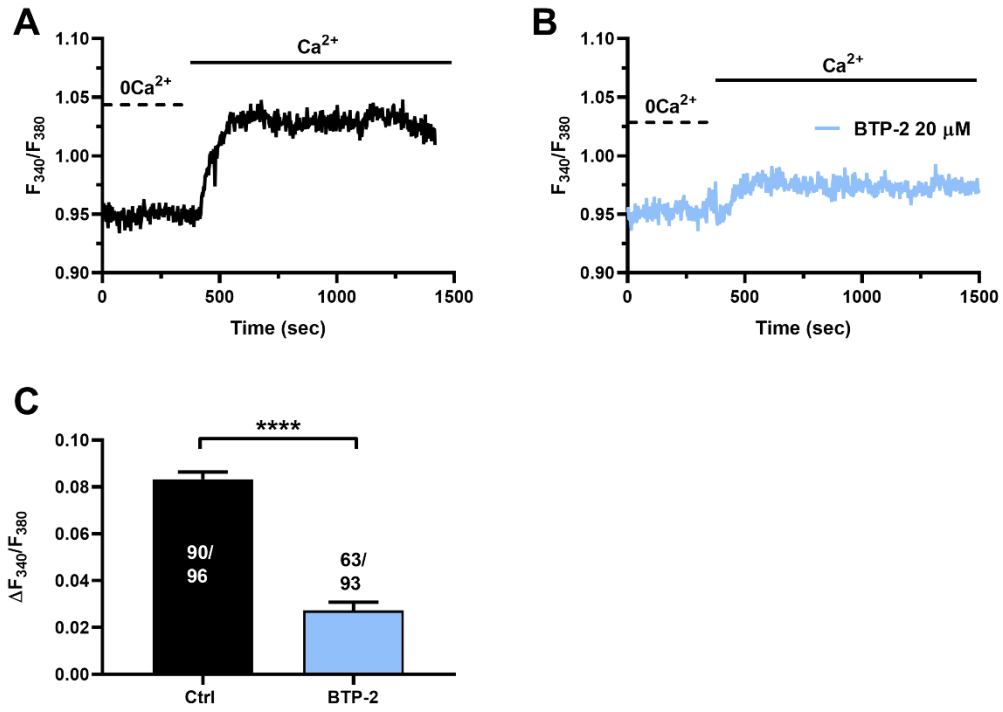

Figure 30 The Ca^{2+} response to capsaicin is sustained by SOCE. **A.** SOCE was activated by challenging ECFCs with capsaicin (10 μM) under $0Ca^{2+}$ conditions (not shown) followed by the restoration of extracellular Ca^{2+} to the recording solution in the absence of the agonist, which caused a second increase in $[Ca^{2+}]_i$ that was independent on agonist binding to the target channel. **B.** Reduced SOCE activation in the presence of the selective SOCE inhibitor, BTP-2 (20 μM, 20 min). **C.** Mean ± SEM of capsaicin-induced SOCE under the designated treatments. **** indicate $p < 0.0001$.

evoked under $0Ca^{2+}$ conditions (**Figure 29E and Figure 29F**), thereby further confirming a possible endogenous TRPV1 localization. SOCE is recruited upon $InsP_3R$-mediated ER Ca^{2+} depletion to refill the endogenous stores, as mentioned above. In order to assess the role of SOCE in Ca^{2+} entry upon TRPV1 activation, we exploited the "Ca^{2+} add back" protocol described for **Figure 28** (**Figure 30A**), The restoration of extracellular Ca^{2+} after the stimulation of ECFCs under $0Ca^{2+}$ conditions, and in the absence of the agonist, evoked a second increase in $[Ca^{2+}]_i$, which was significantly reduced by treating the cells with BTP-2 (20 μM, 20 min) (**Figure 30B and Figure 30C**). These data clearly demonstrate that TRPV1-induced Ca^{2+} signals are mediated by PLC activation and $InsP_3R$-mediated ER Ca^{2+} release followed by SOCE activation to sustain the Ca^{2+} response over the time.

4.9 H_2O_2 INDUCES THE ENDOGENOUS Ca^{2+} MOBILIZATION THROUGH THE PLC/$InsP_3$ SIGNALLING PATHWAY, ENDOGENOUS TRPV1-MEDIATED Ca^{2+} RELEASE AND SOCE ACTIVATION

As reported in **Figure 25A** and **Figure 31A** H_2O_2 induced a biphasic Ca^{2+} signal in ECFCs. In order to investigate whether ROS mediate intracellular Ca^{2+} release through TRPV1 activation, ECFCs were stimulated with H_2O_2 (100 μM) in the absence of extracellular Ca^{2+} ($0Ca^{2+}$). Under $0Ca^{2+}$ conditions, H_2O_2 was able to induce a transient increase in $[Ca^{2+}]_i$ (**Figure 31B**), which was significantly lower that the signal recorded in the control experiments (**Figure 31C**). In addition, restoration of extracellular Ca^{2+} induced a second increase in $[Ca^{2+}]_i$ both in the presence and in the absence of the agonist (**Figure 31D**). The amplitude of extracellular Ca^{2+} influx recorded under the two distinct conditions was

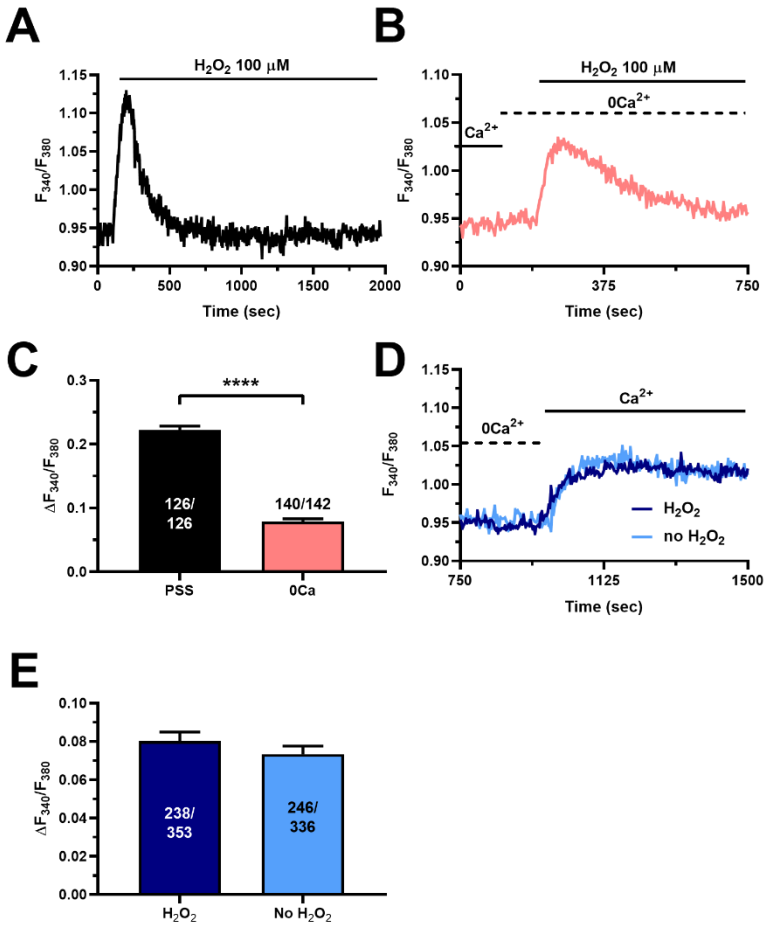

Figure 31 H_2O_2 evoked intracellular Ca^{2+} mobilization and agonist independent Ca^{2+} entry in ECFCs. **A.** H_2O_2 (100 μM) induced a biphasic increase in $[Ca^{2+}]_i$ in the presence of extracellular Ca^{2+}. **B.** In the absence of extracellular Ca^{2+} ($0Ca^{2+}$), H_2O_2 induced a transient increase in $[Ca^{2+}]_i$, which was significantly lower than the Ca^{2+} signals recorded in control experiments. **** indicates $p < 0.0001$. **C.** Mean ± SEM of the amplitude of H_2O_2-evoked Ca^{2+} signals in control conditions and under $0Ca^{2+}$ conditions. **D.** The restoration of extracellular Ca^{2+} resulted in a second raise in $[Ca^{2+}]i$ both in the presence and in the absence of the agonist, the latter being indicative of the activation of SOCE **E.** Mean ± SEM of the amplitude of H_2O_2-evoked Ca^{2+} signals under the designated treatments.

comparable (**Figure 31E**), thereby suggesting that, as observed with capsaicin, the main mechanism involved in the H_2O_2-mediated extracellular Ca^{2+} entry in ECFCs is SOCE.

The next step was to characterize the mechanisms underlying H_2O_2-dependent endogenous Ca^{2+} mobilization. In this view, the H_2O_2-induced increase in $[Ca^{2+}]_i$ occurring in the absence of extracellular Ca^{2+} (**Figure 32A**), was inhibited by the selective TRPV1 blocker, capsazepine (10 µM, 30 min) (**Figure 32B**). We then repeated the same pharmacological treatments used to investigate how capsaicin mobilizes endogenous Ca^{2+}. In this context, the Ca^{2+} response evoked by H_2O_2 (100 µM) in the absence of extracellular Ca^{2+} was inhibited by blocking PLC with U73122 (10 µM, 30 min) and $InsP_3Rs$ with 2-APB (50 µM, 30 min) (**Figure 32C**) and by depleting the ER Ca^{2+} reservoir with CPA (30 µM) (**Figure 32D**). The statistical analysis of these data is reported in **Figure 32E**. These results demonstrated that H_2O_2 stimulated endogenous TRPV1, which induced the intracellular Ca^{2+} release through PLC/$InsP_3Rs$ activation.

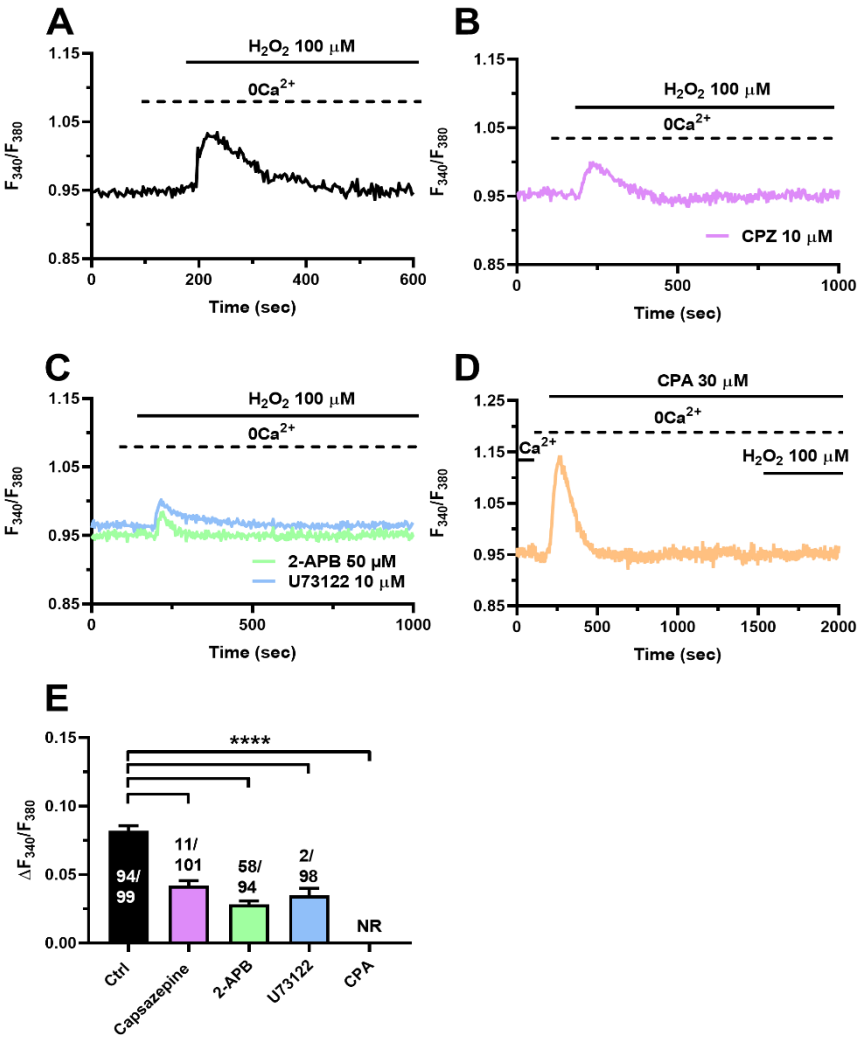

Figure 32 TRPV1-mediated endogenous Ca^{2+} mobilization induced by H_2O_2 requires ER-dependent Ca^{2+} release through $InsP_3Rs$. **A.** H_2O_2 (100 µM) induced a transient increase in $[Ca^{2+}]_i$ in the absence of extracellular Ca^{2+} ($0Ca^{2+}$) **B**. Capsazepine (10 µM, 30 min) inhibited the Ca^{2+} signal induced by H_2O_2 under $0Ca^{2+}$ conditions. **C.** The Ca^{2+} response to H_2O_2 (100 µM) under $0Ca^{2+}$ conditions was inhibited by U73122 (10 µM, 30 min), a selective PLC blocker. Moreover, the Ca^{2+} signal was inhibited by blocking $InsP_3Rs$ with 2-APB (50 µM, 30 min). **D.** Emptying the ER with CPA (30 µM, 15 min), a SERCA selective blocker, prevented the onset of the capsaicin-induced increase in $[Ca^{2+}]_i$. **E.** Mean ± SEM of the amplitude of Ca^{2+} peak in cells under the designated treatments. **** indicate $p < 0.0001$.

As reported for capsaicin, we then investigated the role of SOCE in the Ca^{2+} response to H_2O_2. For this reason, ECFCs were subjected to the "Ca^{2+} add-back" protocol (**Figure 33A**). The restoration of extracellular Ca^{2+} after the stimulation of ECFCs with H_2O_2 under $0Ca^{2+}$ conditions caused a second increase in $[Ca^{2+}]_i$, which was significantly reduced by BTP-2 (20 μM, 20 min) (**Figure 33B and Figure 33C**). These data showed that the Ca^{2+} signal induced by H_2O_2 is mediated by endogenous TRPV1 activation, requires the PLC/$InsP_3$ signalling pathway and is sustained by SOCE activation.

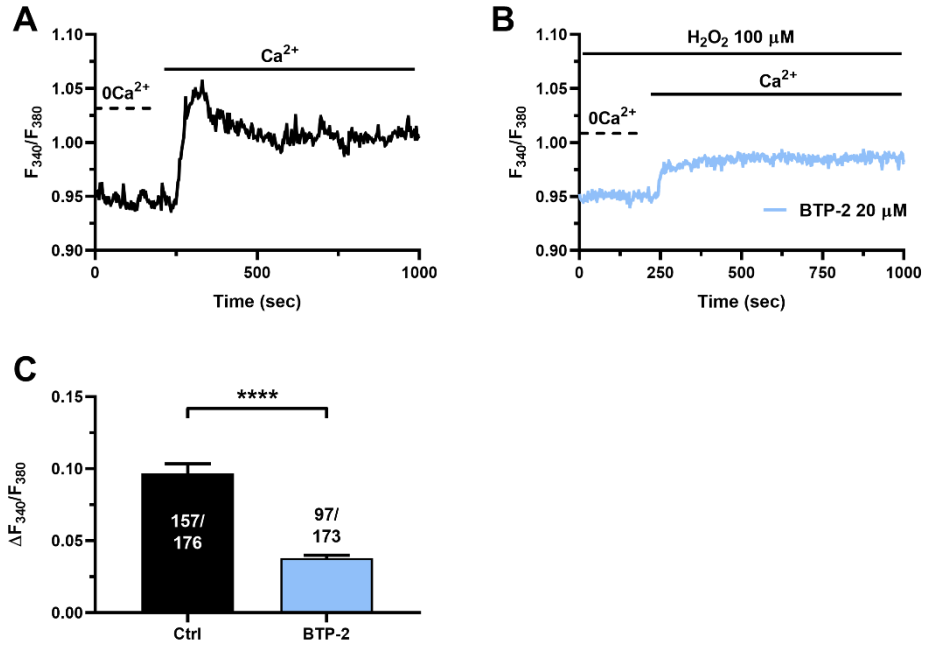

Figure 33 The Ca^{2+} response to H_2O_2 is sustained by SOCE. **A.** SOCE was activated by challenging ECFCs with H_2O_2 (100 μM) under $0Ca^{2+}$ conditions (not shown) followed by the restoration of extracellular Ca^{2+} to the recording bath, which caused a second increase in $[Ca^{2+}]_i$ indicative of SOCE. **B.** Evocation of SOCE in the presence of the selective SOCE inhibitor BTP-2 (20 μM, 20 min). **C.** Mean ± SEM of SOCE under the designated treatments. **** indicate $p < 0.0001$.

4.10 TRPV1 IS EXPRESSED IN MITOCHONDRIA IN ECFCs AND MEDIATES THE RELEASE OF MITOCHONDRIAL Ca^{2+}

A recent investigation demonstrated TRPV1 localization in the mitochondria of HUVECs (Otto et al 2020). Therefore, we isolated ECFC mitochondria as described in paragraph 3.8 of Material and methods, and we performed a western blot analysis to verify this hypothesis. As showed in **Figure 34**, TRPV1 is expressed in mitochondria, which present the specific marker TOMM20 (Nozawa et al 2021), and not in the cytosolic fraction, where the selective α-GAPDH marker was expressed. In addition, western blot revealed demonstrated that there was no α-Vinculin expression, a prove of the absence of membrane contamination in the mitochondrial fraction (**Figure 34**).

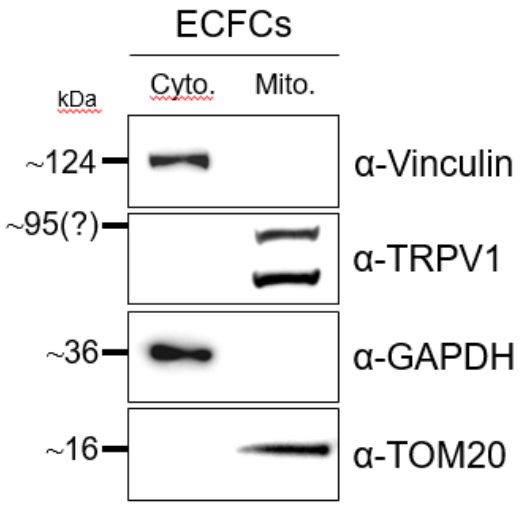

Figure 34 TRPV1 expression in ECFCs mitochondria. Western blot analysis demonstrated the expression of TRPV1 in the mitochondria and not in the cytosol. The mitochondrial α-TOMM20 marker was used as a positive control. On the contrary α-Vinculin and α-GAPDH were used as negative controls to demonstrate the efficacy of mitochondrial isolation. For instance, both of them were not found on the cell fraction represented by mitochondria.

In order to investigate the role of mitochondrial TRPV1 in the Ca^{2+} dynamics, we then performed Ca^{2+} imaging experiments by loading ECFCs with the mitochondrial Ca^{2+} fluorophore, Rhod-2/AM, as described in the Material and methods. ECFCs were challenged with capsaicin (10 μM) in the absence of extracellular Ca^{2+} to focus on endogenous Ca^{2+} mobilization. As showed in **Figure 35A**, capsaicin induced a robust reduction in the mitochondrial Ca^{2+} content, which was abrogated by the pharmacological treatment with the two specific TRPV1 inhibitors, capsazepine (10 μM, 30 min) and SB-366791 (10 μM, 30 min) (**Figure 35A and Figure 35B**). These data clearly showed that TRPV1 is expressed in ECFC mitochondria and mediates mitochondrial Ca^{2+} release, which could be in turn amplified by $InsP_3$-induced Ca^{2+} release from the ER and sustained over time by SOCE.

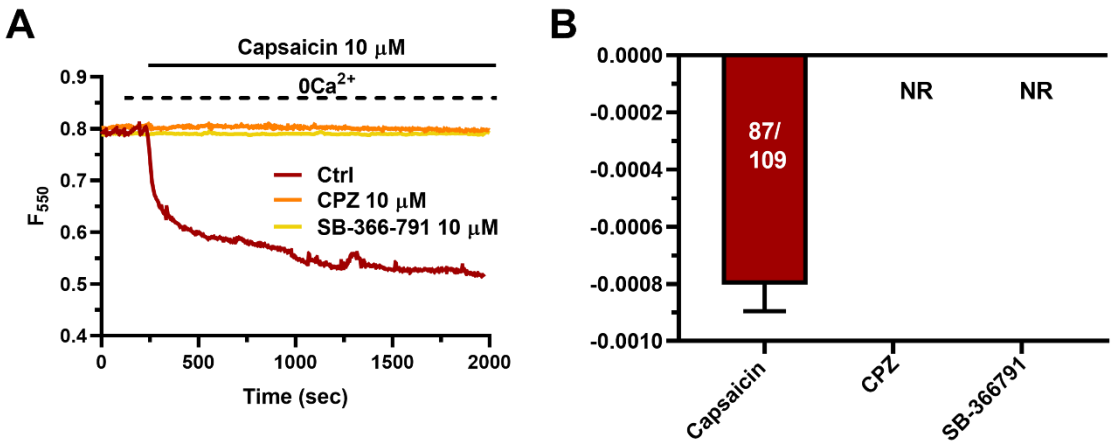

***Figure 35 Capsaicin induce mitochondrial Ca^{2+} release through TRPV1 activation*. A.** Capsaicin (10 μM), upon $0Ca^{2+}$ conditions, induced a robust reduction in Rhod-2/AM fluorescence, which is indicative of the reduction of Ca^{2+} levels in ECFC mitochondria. In addition, the two specific TRPV1 blockers capsazepine (10 μM, 30 min) and SB-366791 (10 μM, 30 min) abrogated the capsaicin-dependent effect. **B.** Mean ± SEM of the curve slope under the designated treatments.

5 DISCUSSION

Optical modulation through exogenous photoactive materials is emerging as a powerful, geneless, and minimally invasive tool able to control cellular activity and to rescue defective signalling pathways with unprecedented spatial resolution, potentially at the sub-cell organelles level, and with highly versatile temporal patterns. In this context, semiconducting conjugated polymers, such as rr-P3HT, have been proven to be highly reliable materials, able to effectively control cell functionality in several biomedical applications (Antognazza et al 2019, Antognazza et al 2015, Di Maria et al 2018, Moccia et al 2020). Nevertheless, the biological signal(s) whereby photostimulation of rr-P3HT, taken as a prototypical photoactive material, drive(s) cellular behaviours that are relevant for the recovery of specific lost functions are yet to be fully unravelled (Antognazza et al 2019, Di Maria et al 2018). Herein, we provided the first evidence that the non-selective cation channel, TRPV1, is activated by rr-P3HT-mediated optical excitation to induce an increase in $[Ca^{2+}]_i$ in circulating ECFCs, that represent the most suitable cellular substrate to induce therapeutic angiogenesis of ischemic tissues (Faris et al 2020b, O'Neill et al 2018, Paschalaki & Randi 2018). We further show that H_2O_2, which is produced at the interface between the rr-P3HT thin film and the cellular membrane (Antognazza et al 2019, Aziz et al 2020), is the main responsible for light-induced TRPV1 activation and extracellular Ca^{2+} entry. Moreover, we showed that TRPV1 is also expressed endogenously and, specifically, in mitochondria, where it mediates endogenous Ca^{2+} mobilization. Notably, other authors already demonstrated the intracellular TRPV1 localization in different cell types (Gallego-Sandin et al 2009, Lotteau et al 2013, Otto et al 2020, Pecze et al 2016a). These findings contribute to unravel the molecular mechanisms whereby optical excitation of rr-P3HT could stimulate circulating ECFCs to effect vascular regrowth in ischemic tissues.

5.1 OPTICAL EXCITATION OF rr-P3HT THIN FILMS CAUSES AN INCREASE IN $[Ca^{2+}]_i$ IN CIRCULATING ECFCs

Pro-angiogenic stimuli, such as VEGF (Lodola et al 2017a), SDF-1α, and the human amniotic fluid stem cell secretome (Balbi et al 2019), evoke different intracellular Ca^{2+} waveforms, such as intracellular Ca^{2+} oscillations and biphasic Ca^{2+} elevations in circulating ECFCs. Furthermore, a recent report from our group demonstrated that optical excitation (light power density 0.4 mW/mm^2) of rr-P3HT thin films stimulated ECFCs to proliferate and assemble into capillary-like networks (Lodola et al 2019a). The pro-angiogenic effect of optical excitation was abrogated by pre-treating the cells with BAPTA-AM, a membrane-permeable buffer of intracellular Ca^{2+} levels (Lodola et al 2019a). This observation hinted at a crucial role played by Ca^{2+} signalling in polymer-mediated photoexcitation of ECFCs' pro-angiogenic activity (Moccia et al 2020, Negri et al 2020). We now confirmed this hypothesis by showing that a similar protocol of photostimulation (i.e., light power density 0.6 mW/mm^2) of ECFCs cultured on rr-P3HT thin films induced an increase in $[Ca^{2+}]_i$ that could adopt multiple patterns. Around half of ECFCs subjected to 2.5 sec light pulses displayed a delayed, slow increase in $[Ca^{2+}]_i$. The remaining half of

ECFCs presented intracellular Ca^{2+} oscillations, consisting of repeated Ca^{2+} transients overlapping the slowly developing $[Ca^{2+}]_i$ rise. Interestingly, pro-angiogenic cues, which stimulate long-lasting processes, such as endothelial cell proliferation, migration, and tube formation, usually evoke quite heterogeneous intracellular Ca^{2+} signatures (Moccia et al 2019, Noren et al 2016, Yokota et al 2015). For instance, VEGF-induced intracellular Ca^{2+} oscillations stimulate ECFC proliferation and in vitro *tubulogenesis* through the nuclear translocation of the Ca^{2+}-sensitive transcription factor, NF-κB (Dragoni et al 2011, Lodola et al 2017a), as also observed in circulating ECFCs challenged with the human amniotic fluid stem cell secretome (Balbi et al 2019, Balducci et al 2021). On the other hand, SDF-1α was found to promote ECFC migration, both in vitro and in vivo, by eliciting biphasic Ca^{2+} signals in ECFCs that recruited ERK and PI_3K/Akt (Zuccolo et al 2018). Likewise, early work revealed that insulin-like growth factor 2 could induce postnatal vasculogenesis by eliciting a non-oscillatory Ca^{2+} signal in circulating ECFCs (Maeng et al 2009). A recent investigation from our group revealed that rr-P3HT-mediated optical excitation of ECFCs stimulated proliferation and *tubulogenesis* through the Ca^{2+}-dependent recruitment of NF-κB (Lodola et al 2019a). Although the photoexcitation protocols employed in the two studies are slightly different (chronic exposure to pulsed illumination in (Lodola et al 2019a), single light pulses here), these findings suggest that light-induced intracellular Ca^{2+} oscillations could preferentially induce ECFCs to proliferate and assembly into capillary-like structure, whereas the non-oscillatory elevation in $[Ca^{2+}]_i$ could rather be coupled to the Ca^{2+}-dependent motility machinery. This hypothesis is further corroborated by the recent evidence that VEGF may trigger distinct functional responses in vascular endothelial cells depending on the pattern of the Ca^{2+} response, whereas intracellular Ca^{2+} oscillations and biphasic Ca^{2+} signals selectively lead to proliferation and migration, respectively (Noren et al 2016). Photoexcitation of ECFCs cultured on bare glass substrate did not reliably increase the $[Ca^{2+}]_i$. In agreement with this and previous observations (Lodola et al 2019a), photobiomodulation mediated by endogenous chromophores is able to elicit endothelial signalling only at wavelengths longer than 625 nm (Peplow et al 2010). This is, therefore, the first evidence that optical stimulation of rr-P3HT thin layers by visible light induces intracellular Ca^{2+} signals in a cellular model with a potentially high therapeutic relevance (Faris et al 2020b). Furthermore, our observations are consistent with previous reports showing that photocatalytic activity of rr-P3HT nanoparticles internalized within the cytoplasm caused an increase in $[Ca^{2+}]_i$ in HEK-293 cells (Bossio et al 2018), which was not due to physiological signalling and not to unwanted dismantling of the Ca^{2+} handling machinery (Zucchetti et al 2017).

5.2 TRPV1-DEPENDENT Ca^{2+} ENTRY IS FUNDAMENTAL IN THE ONSET OF Ca^{2+} SIGNALS EVOKED BY OPTICAL EXCITATION OF rr-P3HT THIN FILMS

Recent work from our group demonstrated that photoexcitation of circulating ECFCs growing on rr-P3HT thin films increases ECFC proliferation and *in vitro tubulogenesis* through a Ca^{2+}-dependent

mechanism. (Lodola et al 2019a). In this view, TRPV1 was the most likely candidate to trigger the Ca^{2+} response to photoexcitation. In agreement with this hypothesis, we first found that extracellular Ca^{2+} entry was strictly required both to trigger the Ca^{2+} signal and to maintain the increase in $[Ca^{2+}]_i$ observed in all ECFCs subjected to light stimulation. The following pieces of evidence demonstrate that TRPV1 provides the main pathway to sustain the influx of Ca^{2+} evoked by photoexcitation. First, TRPV1 protein was abundantly expressed in circulating ECFCs, as previously observed in UCB-derived ECFCs (Hofmann et al 2014). The size of TRPV1 protein in ECFCs is within the same range as that described in peripheral nociceptors, i.e., 100 kDa (Caterina et al 1997), whereas, in other cell types, it can undergo post-translational modifications that induce significant alterations in the molecular weight (≈75 kDa) (Kedei et al 2001, Veldhuis et al 2012). Second, capsaicin, a selective TRPV1 agonist (Caterina et al 1997, DelloStritto et al 2016a, Faris et al 2020a), caused an increase in $[Ca^{2+}]_i$ that was dampened by two structurally distinct TRPV1 blockers, such as capsazepine and SB-366791 (DelloStritto et al 2016a, Lodola et al 2017b, Negri et al 2020). Third, the genetic deletion of TRPV1 protein with a selective siTRPV1 strongly inhibited capsaicin-induced intracellular Ca^{2+} signals. The efficacy of this construct to downregulate extracellular Ca^{2+} entry through TRPV1 has already been proved in metastatic colorectal cancer cells (Faris et al 2020b). Fourth, the pharmacological (with capsazepine or SB-366,791) and genetic (with the selective siTRPV1) blockade of TRPV1 significantly inhibited light-induced intracellular Ca^{2+} signals in ECFCs cultured on rr-P3HT thin films. These findings provide the first evidence that TRPV1 may effectively translate optical excitation of a photosensitive organic semiconductor, such as rr-P3HT, in an increase in $[Ca^{2+}]_i$. It is worth pointing out that TRPV1 is emerging as the ideal target of other nanotechnological strategies. For instance, TRPV1 can also be activated by magnetic nanoparticles exposed to alternating magnetic fields and thereby elicit neuronal activity within the ventral tegmental area in mouse brain (Chen et al 2015). Furthermore, near infrared light-dependent stimulation of gold nanorods restored the visual function in a mouse model of degenerative blindness upon viral-mediated delivery of TRPV1 in retinal cones (Nelidova et al 2020). Therefore, TRPV1 activation could represent the molecular mechanism onto which multiple nanotechnological solutions converge to rescue defective Ca^{2+} signalling, e.g., in neurons, or to stimulate pro-angiogenic Ca^{2+} signals, e.g., in circulating ECFCs.

5.3 THE PRIMARY ROLE OF ROS IN TRPV1 ACTIVATION UPON OPTICAL EXCITATION OF rr-P3HT THIN FILMS

TRPV1 is a polymodal channel that may effectively integrate the two main biologically relevant signals generated by the photocatalytic activity of rr-P3HT thin films (Caterina et al 1997, Lodola et al 2017b, Negri et al 2020), i.e., the local increase in temperature and in H_2O_2 levels at the interface between the substrate and the cell membrane (Bellani et al 2015, Bossio et al 2018). TRPV1 may indeed serve as a sensor for noxious heat (>42 °C) (Caterina et al 1997) and is also directly activated by H_2O_2 (DelloStritto

et al 2016a, Gryszel et al 2018). Elucidation of the phototransduction mechanisms showed that ROS, but not heat, were responsible for light-induced ECFC proliferation and in vitro *tubulogenesis* in the presence of rr-P3HT thin films (Lodola et al 2019a). This study further highlights the interplay among photoelectrochemical activity, ROS generation, TRPV1 activation and modulation of $[Ca^{2+}]_i$. In accord, optical excitation of a photoresist substrate that does not undergo the photoelectrochemical reaction, did not reliably increase the $[Ca^{2+}]_i$ in circulating ECFCs. Furthermore, this Ca^{2+} signal only exhibited a transient duration, presented a longer latency and was remarkably lower as compared to rr-P3HT-mediated Ca^{2+} responses. This finding is consistent with our previous report that the global increase in temperature upon light exposure does not reach the thermal threshold required for TRPV1 activation by heat (≈38 °C vs. 42 °C) (Lodola et al 2017b). We cannot rule out the possibility that the local elevation in temperature at the interface between the photoresist nanomaterial and some ECFCs may activate TRPV1; however, this thermal signal does not suffice to induce the long-lasting increase in $[Ca^{2+}]_i$ that regularly arises upon optical excitation of rr-P3HT. Second, a robust increase in intracellular ROS levels occurs in ECFCs growing on rr-P3HT thin films, but not on glass substrates, and subjected to 2.5 sec and 20 sec long light pulses. Although H_2DCF-DA does not selectively detect H_2O_2 (Gomes et al 2005), the increase in ROS production induced by photoexcitation of rr-P3HT was abrogated by scavenging H_2O_2 with catalase (DelloStritto et al 2016a, Martinotti et al 2019). In agreement with these observations, the increase in $[Ca^{2+}]_i$ induced by polymer-mediated optical excitation was abrogated by catalase and significantly reduced by DTT, which is commonly employed to reverse H_2O_2-dependent TRPV1 activation by reducing the thiol groups involved in channel opening (Chuang & Lin 2009, DelloStritto et al 2016a). To further corroborate the gating role played by H_2O_2 in the TRPV1- mediated Ca^{2+} response to photoexcitation, we adopted two different strategies. Acute H_2O_2 exposure caused an increase in $[Ca^{2+}]_i$ that was abrogated by catalase and strongly decreased by DTT. Furthermore, H_2O_2-induced intracellular Ca^{2+} signals were reversibly inhibited by the pharmacological (with capsazepine or SB-366791) and genetic (with the selective siTRPV1) deletion of TRPV1. H_2O_2 was known to elevate the $[Ca^{2+}]_i$ (Hu et al 1998, Zheng & Shen 2005) and to activate TRPV1-mediated transmembrane currents (DelloStritto et al 2016a) in vascular endothelial cells. However, this is the first evidence that TRPV1 contributes to H_2O_2-induced intracellular Ca^{2+} signals in the endothelial lineage. In a next set of experiments, circulating ECFCs were challenged with NADH, the substrate of NOX enzymes, which catalyse the transfer of an electron from NAD(P)H to O_2, thereby generating the O_2^- (Pires & Earley 2017, Sullivan et al 2015). O_2^- can then be dismutated into H_2O_2, which, in the presence of Fe^{2+}, can in turn be degraded to OH^- through the Fenton reaction (Pires & Earley 2017, Sullivan et al 2015). A recent report identified NOX4 as the major NOX isoform expressed in ECFCs (Hakami et al 2017). Herein, we found that NADH induced an increase in $[Ca^{2+}]_i$ that was significantly attenuated by blocking NOX activity with apocynin and scavenging extracellular H_2O_2 with catalase. In agreement with these observations, the Ca^{2+} response to NADH was hindered by blocking TRPV1 with either capsazepine or SB-366,791. Furthermore, preventing the Fenton reaction with deferoxamine enhanced, rather than

decreasing, NADH-induced intracellular Ca^{2+} signals in ECFCs. This observation is consistent with the notion that OH^--induced peroxidation of membrane lipids may somehow inhibit TRPV1 activity in microvascular endothelial cells (DelloStritto et al 2016b). These findings, therefore, collectively hint at H_2O_2 as the biological signal gating TRPV1 in the plasma membrane of ECFCs upon optical excitation of rr-P3HT thin films. Since H_2O_2 is crucial to stimulate extracellular Ca^{2+} entry in photoexcited ECFCs, we cannot rule out the possibility that other ROS-sensitive TRP channels, such as TRPM2 and TRPA1 (Pires & Earley 2017). However, TRPA1 is seemingly expressed only in brain microvascular endothelial cells, in which Ca^{2+} entry is gated by lipid peroxidation (Sullivan et al 2015), thereby suggesting that this TRP isoform is not involved in rr-P3HT-mediated increase in $[Ca^{2+}]_i$ in ECFCs. TRPM2, in turn, has been shown to trigger ROS-sensitive endothelial Ca^{2+} signals in multiple vascular beds (Ding et al 2021). TRPM2 activation is, however, secondary to H_2O_2-induced mitochondrial production of ADP ribose and may be sustained over time by the accompanying binding of Ca^{2+}; therefore, TRPM2 is unlikely to be the primary target of H_2O_2 on the plasma membrane upon its diffusion across the phospholipid bilayer. Nevertheless, investigations are underway in our group to assess whether TRPA1 and TRPM2 somehow contribute to the residual Ca^{2+} response arising in ECFCs following the pharmacological (with capsazepine and SB-366,791) and genetic (with the specific siTRPV1) blockade of TRPV1.

5.4 THE ROLE OF $InsP_3Rs$ AND SOCE IN THE Ca^{2+} RESPONSE TO OPTICAL STIMULATION

The complex increase in $[Ca^{2+}]_i$ evoked by visible light in a remarkable fraction (≈50%) of ECFCs growing on rr-P3HT thin films encompasses fast Ca^{2+} transients that could overlap the slowly developing rise in $[Ca^{2+}]_i$. These repetitive Ca^{2+} oscillations are strongly reminiscent of the $InsP_3$-induced Ca^{2+} release events that are often elicited by growth factors in both vascular endothelial cells (Noren et al 2016) and ECFCs (Balbi et al 2019). This observation led us to speculate about $InsP_3R$ engagement by TRPV1. Indeed, extracellular Ca^{2+} entry across the plasma membrane may recruit ER-embedded $InsP_3Rs$ through the mechanism of CICR in vascular endothelial cells (Morgan & Jacob 1996). Furthermore, H_2O_2 may enhance $InsP_3R$ sensitivity to ambient $[InsP_3]$ and thereby mobilize ER Ca^{2+} (Joseph 2010), as also shown in endothelial cells from multiple vascular districts (Zheng & Shen 2005). For instance, the direct application of H_2O_2 under $0Ca^{2+}$ conditions induced a transient increase in $[Ca^{2+}]_i$, indicative of endogenous Ca^{2+} mobilization. However, since capsaicin exerted the same effect, we speculated on the endogenous expression of TRPV1, which will be discussed in the next paragraph. ECFCs express all the three $InsP_3R$ subtypes ($InsP_3R1$–3), while they lack RyRs (Moccia et al 2018b), which represent the canonical target for CICR. Quite surprisingly, XeC, a selective blocker of $InsP_3Rs$, did not only abolish the intracellular Ca^{2+} oscillations; it also strongly dampened the global Ca^{2+} response evoked in ECFCs by the photoexcitation of rr-P3HT thin films. This unexpected finding led us to hypothesize the involvement of an additional Ca^{2+} entry pathway, i.e., SOCE, which is activated

downstream of $InsP_3Rs$ (Moccia et al 2012c). SOCE is mediated by the physical interaction between STIM1, the sensor of ER Ca^{2+} concentration, and the Ca^{2+}-permeable channels, Orai1 and TRPC1 on the plasma membrane (Lodola et al 2012, Moccia et al 2012c). SOCE develops over seconds to ten of seconds upon $InsP_3$-dependent depletion of the ER Ca^{2+} pool and sustains the long-lasting duration of the Ca^{2+} signals evoked in ECFCs by pro-angiogenic cues (Dragoni et al 2011). Of note, pre-treating the cells with BTP-2, a selective blocker of SOCE in ECFCs (Moccia et al 2012c), extended the latency, reduced the amplitude and strongly curtailed the duration of the Ca^{2+} response to optical excitation, which adopted a transient pattern. These findings provide the first evidence that $InsP_3Rs$ and SOCE may participate to the phototransduction mechanisms whereby optical modulation of rr-P3HT thin films controls cellular activity.

5.5 UNEXPECTED EVIDENCE THAT H_2O_2 ACTIVATES ENDOGENOUS, RATHER THAN PLASMALEMMAL, TRPV1

The evidence that TRPV1-mediated Ca^{2+} response to optical stimulation requires $InsP_3$-induced ER Ca^{2+} release is somehow reminiscent of earlier studies reporting that TRPV1 can also be located in endogenous organelles, such as ER cisternae and mitochondria (Lotteau et al 2013, Otto et al 2020, Pecze et al 2016a, Pecze et al 2016b). In order to address this compelling issue, we directly stimulated ECFCs plated on glass coverslips with H_2O_2 and capsaicin in the absence of extracellular Ca^{2+}. First of all, we showed that both the agonists were able to induce an increase in $[Ca^{2+}]_i$ also under $0Ca^{2+}$ conditions, by confirming a role of TRPV1 in the endogenous Ca^{2+} mobilization. In addition, a second bump in the Ca^{2+} levels was recorded when the extracellular Ca^{2+} concentration was restored. Then, we restored the extracellular Ca^{2+}, either in the presence and in the absence of the agonist, in order to investigate the role of TRPV1 and SOCE in the molecular mechanism. Notably, the amplitude of the recorded Ca^{2+} signals was comparable under the two conditions thereby suggesting that extracellular Ca^{2+} entry is mainly mediated by SOCE. Indeed, if plasmalemmal TRPV1 was involved in the extracellular Ca^{2+} entry, the second increase in $[Ca^{2+}]_i$ after extracellular Ca^{2+} levels restoration, would be higher in the presence of the agonist.

We have originally hypothesized that TRPV1 is expressed on the plasma membrane where it mediates Na^+ and Ca^{2+} entry (Lodola et al., 2019); however, the data present in this thesis suggest that TRPV1 is expressed also endogenously. For this reason, we repeated the same experiments by pre-treating ECFCs with capsazepine, the specific TRPV1 antagonist, and we applied capsaicin or H_2O_2 in the absence of extracellular Ca^{2+}. As we supposed, the Ca^{2+} response was significantly reduced. Although, the intracellular TRPV1 localization remained to be clarified, the first idea was to investigate the involvement of $InsP_3Rs$ and ER Ca^{2+} release. For this reason, ECFCs were pharmacologically manipulated by inhibiting PLC activity with U73122 and $InsP_3Rs$ with 2-APB, which were able to significantly reduce the Ca^{2+} signals induced by both, capsaicin and H_2O_2, upon $0Ca^{2+}$ conditions. Moreover, the depletion of ER Ca^{2+} reservoir through the SERCA inhibition with CPA confirmed the

role of ER in the endogenous Ca^{2+} mobilization induced by capsaicin and H_2O_2. TRPV1-mediated Ca^{2+} release induces CICR. Notably, several pieces of evidence reported TRPV1 expression in the ER membranes in different cell types (e.g. rat nociceptive neurons (Karai et al 2004), breast (Lozano et al 2018) and prostate (Pecze et al 2016b) cancer cell lines). Endogenous TRPV1-dependent Ca^{2+} efflux from the ER or from the mitochondria may be amplified by $InsP_3Rs$ through the CICR mechanism (Moccia et al 2012b). Finally, the "Ca^{2+} add back" protocol confirmed that either capsaicin or H_2O_2 were able to mediate extracellular Ca^{2+} entry following the ER pool depletion, and it was significantly reduced by BTP-2, an established SOCE inhibitor. These data support the notion that SOCE is the main mechanism involved in extracellular Ca^{2+} entry in ECFCs and it may be involved in the Ca^{2+} response to TRPV1 stimulation (Moccia et al 2014a, Moccia et al 2019). Notably, it seems that TRPV1 is not directly involved in the extracellular Ca^{2+} entry. Conversely, it mediates intracellular store depletion and the consequent SOCE activation (Moccia et al 2014a). Not surprisingly, the same behaviour has been described for TRPM8 in the prostate cancer (Thebault et al 2005). These data support the previous result that enlightened the importance of $InsP_3Rs$ and SOCE, obtained in ECFCs plated on rr-P3HT and stimulated by light.

Nevertheless it is important to recall that H_2O_2 may directly sensitize $InsP_3Rs$ (Zheng & Shen 2005) and activate PLC (Hong et al 2006) thereby emphasizing the recorded TRPV1-mediated effect.

5.6 ENDOGENOUS EXPRESSION OF TRPV1: MITOCHONDRIA AS A GOLDEN SNITCH

A recent investigation demonstrated that TRPV1 is expressed in endothelial mitochondria (Otto et al 2020). The authors demonstrated that TRPV1 colocalizes with mitochondria through immunohistochemistry experiments, in addition cell fractionation confirmed the greatest TRPV1 expression in these organelles (Otto et al 2020). For this reason, we isolated ECFC mitochondria, and we tested the presence of the polymodal channel. As expected, TRPV1 was found in the mitochondria and not in the cytosol. Thereafter, to understand the role of the protein in the mitochondrial Ca^{2+} dynamics, ECFCs were charged with the selective Ca^{2+} fluorophore Rhod-2/AM and stimulated with capsaicin in the absence of extracellular Ca^{2+}. Upon these conditions, the agonist induced an immediate reduction in Rhod-2/AM fluorescence, which is indicative of the reduction of the mitochondrial Ca^{2+} content. The most likely explanation is that Ca^{2+} permeate TRPV1 and leaves the mitochondria by following the concentration gradient, for instance the cytosolic [Ca^{2+}] is 100 nM. In accord, the pharmacological inhibition of TRPV1 with capsazepine and SB-366791 prevented the fluorescence decay induced by capsaicin. An alternative hypothesis would be that TRPV1 may participate to the constitution of the permeability transition pore, however future work is needed to verify the assumption. It has long been known that MAMs permit the physical interaction with the ER, by allowing the Ca^{2+} trafficking between the two organelles (Kerkhofs et al 2018, Morciano et al 2018). Therefore, the

presence of MAMs may explain how the mitochondrial Ca^{2+} release mediated by TRPV1 stimulated the $InsP_3R$-dependent ER Ca^{2+} release through CICR mechanism.

In this investigation, rr-P3HT was employed as a thin film, however the future direction is to use conjugated polymers in nanoparticles form, as they are easier to administer and functionalize. In this view, the endogenous TRPV1 expression would be an additional advantage, since the nanoparticles are internalized in endothelial cells and optical stimulation-induced ROS production occurs directly in the cytosol (Bossio et al 2018, Lodola et al 2017b).

5.7 PUTTING ALL THE PIECES TOGETHER: THE PROPOSED MECHANISM

Based upon these novel observations, we can now revise the model that have recently suggested to explain how H_2O_2 and TRPV1 trigger the intracellular Ca^{2+} signals that drive light-induced ECFC proliferation and tube formation. H_2O_2 produced at the interface between rr-P3HT thin films and the extracellular solution may freely permeate through the plasma membrane (Pires & Earley 2017) and oxidize the cysteine-thiol groups that are located in the cytosolic carboxy- and amino-terminal tails of TRPV1 (Chuang & Lin 2009). This in turn results in a kinetically slow increase in $[Ca^{2+}]_i$ that is likely to reflect the rate of H_2O_2 production and accumulation beneath the cytosolic membrane leaflet. The real-time measurement of light-induced increases in cytosolic H_2O_2 by using electrochemical probes is currently underway (Malferrari et al 2019). We initially demonstrated that extracellular Ca^{2+} entry is strictly required to initiate the Ca^{2+} response to optical stimulation; however, the data presented in this thesis showed that TRPV1 per se in unlikely to mediate Ca^{2+} influx across the plasma membrane. Conversely, compelling evidence suggests that TRPV1 is mainly located in mitochondria, thereby triggering Ca^{2+} release from the ER through the CICR and indirectly recruiting SOCE, which therefore stands out as the most important mechanism driving Ca^{2+} entry upon TRPV1 activation. (**Figure 36**). The influx of Ca^{2+} may in turn contribute to sensitize $InsP_3Rs$ to ambient $[InsP_3]$, a process that could also be directly promoted by H_2O_2 reaching the bulk cytosol (Zheng & Shen 2005). Notably, the unpredictable occurrence of ER Ca^{2+} spikes could reflect differences in ambient $[InsP_3]$ within different sub-regions of the same cell and/or among different ECFCs, which might therefore result in different sensitivities to $InsP_3$-induced Ca^{2+} release. In other words, upon TRPV1-mediated mitochondrial Ca^{2+} release, some compartments of the ER could discharge in a less-synchronous manner (low ambient $[InsP_3]$) and contribute to the slowly

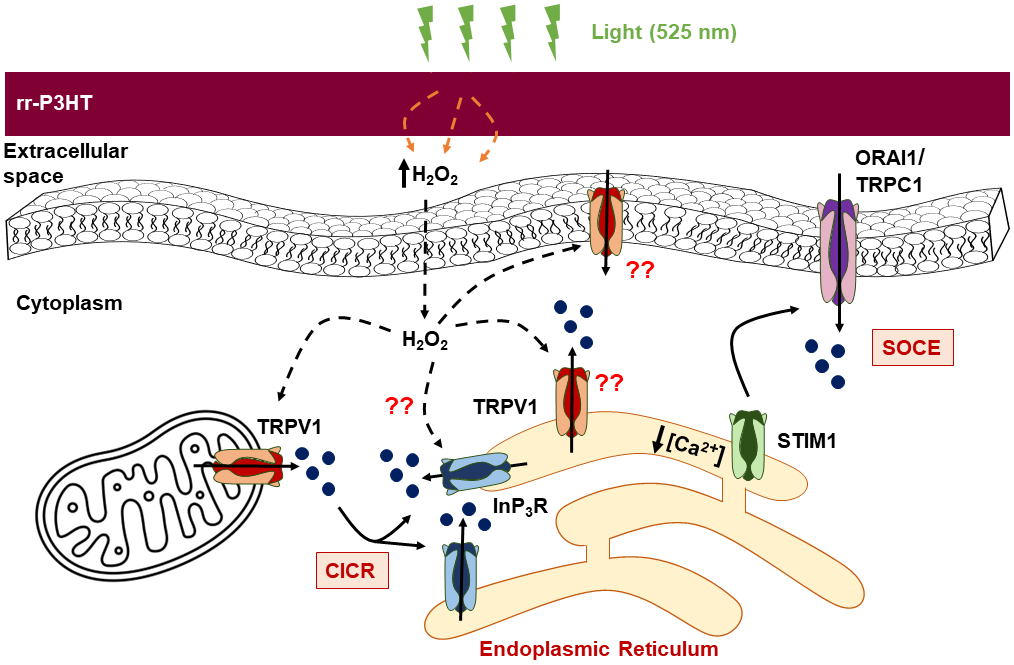

Figure 36 Schematic representation of the molecular mechanisms leading to the Ca^{2+} response to visible excitation in circulating ECFCs plated on rr-P3HT thin films. Optical stimulation of ECFCs plated on rr-P3HT induced the production of H_2O_2 between the thin film and the cell membrane. H_2O_2 permeates the cell membrane and in turn, activates mitochondrial TRPV1, thereby leading to intracellular Ca^{2+} release that promotes the Ca^{2+}-dependent recruitment of $InsP_3Rs$ on ER membrane. The following release of intraluminal Ca^{2+} leads to a dramatic reduction in ER Ca^{2+} concentration ($[Ca^{2+}]_i$), which leads to the STIM1-dependent activation of SOCE through Orai1 and TRPC1 channels on the plasma membrane.

rising Ca^{2+} signal. Other sub-regions of the ER could instead result in the well synchronized events of Ca^{2+} release that underlie fast Ca^{2+} spikes (high ambient [$InsP_3$]). This biphasic mode of $InsP_3R$ signalling depending upon ambient [$InsP_3$] has been proposed to mediate the intracellular Ca^{2+} oscillations evoked in non-excitable cells (Parekh & Penner 1995), including vascular endothelial cells (Gericke et al 1993), by the thiol oxidizing reagent, thimerosal. Alternately, intracellular Ca^{2+} oscillations could arise depending on whether H_2O_2 recruits PLC (Hong et al 2006), the membrane receptor responsible for $InsP_3$ cleavage from PIP_2, which could locally boost $InsP_3$ synthesis and induce fast events of ER Ca^{2+} release. A feature of the Ca^{2+} response to optical excitation of rr-P3HT thin films that deserves to be addressed is that the latency of the signal increases while the percentage and frequency of oscillating cells decrease at longer light pulses. Excessive H_2O_2 levels could indirectly dampen endothelial $InsP_3Rs$ by depolarizing the mitochondrial membrane potential (Zhang et al 2019). Therefore, upon exposure to light pulses longer than 2.5 sec, $InsP_3R$-mediated ER Ca^{2+} release could be somehow hindered by the larger H_2O_2 production, thereby delaying the slow increase in $[Ca^{2+}]_i$ evoked by TRPV1 and progressively lowering the probability that Ca^{2+} oscillations arise. The assessment of this hypothesis requires a quantitatively more precise measurement of ROS and H_2O_2 upon exposure to increasingly longer light stimuli and the evaluation of $InsP_3R$ inhibition by high H_2O_2 concentrations.

6 CONCLUSION

The present work provided the first evidence that TRPV1 translates optical excitation of rr-P3HT thin films in a long lasting Ca^{2+} signal in a therapeutically relevant cell model, such as circulating ECFCs. This increase in $[Ca^{2+}]_i$ in turn mediate ECFCs' angiogenic activity *in vitro* (Lodola et al 2019a) and could thereby favour therapeutic angiogenesis *in vivo*, although this latter hypothesis remains to be experimentally probed. H_2O_2 plays a central role in TRPV1 activation by light, as confirmed by multiple approaches. Contrary to our previous hypothesis (Negri et al., 2022), TRPV1 is expressed endogenously, specifically in the mitochondria, where it mediates endogenous Ca^{2+} mobilization. The mitochondrial-derived Ca^{2+} in turn activates $InsP_3Rs$ on the ER through CICR thereby leading to ER Ca^{2+} depletion and the following SOCE activation (**Figure 36**). The proof-of-concept that photostimulation of rr-P3HT induces TRPV1-mediated Ca^{2+} signals in a therapeutically relevant cell model will broaden the application of organic semiconductors to the treatment of diseases associated to defective Ca^{2+} dynamics, including heart failure (Berridge 2006), neurodegenerative (McDaid et al 2020) and muscular (Silva-Rojas et al 2020) disorders. Furthermore, optical stimulation of rr-P3HT thin films could provide a reliable strategy to mitigate Ca^{2+}-dependent endothelial dysfunction in a plethora of CVDs (Peters et al 2022, Wilson et al 2020)

7 BIBLIOGRAFY

Abdullaev IF, Bisaillon JM, Potier M, Gonzalez JC, Motiani RK, Trebak M. 2008. Stim1 and Orai1 mediate CRAC currents and store-operated calcium entry important for endothelial cell proliferation. *Circ Res* 103: 1289-99

Ahern GP, Wang X, Miyares RL. 2006. Polyamines are potent ligands for the capsaicin receptor TRPV1. *J Biol Chem* 281: 8991-5

Aird WC. 2005. Spatial and temporal dynamics of the endothelium. *J Thromb Haemost* 3: 1392-406

Alansary D, Schmidt B, Dorr K, Bogeski I, Rieger H, et al. 2016. Thiol dependent intramolecular locking of Orai1 channels. *Sci Rep* 6: 33347

Alvarado MG, Thakore P, Earley S. 2021. Transient Receptor Potential Channel Ankyrin 1: A Unique Regulator of Vascular Function. *Cells* 10

Andersson DA, Gentry C, Moss S, Bevan S. 2008. Transient receptor potential A1 is a sensory receptor for multiple products of oxidative stress. *Journal of Neuroscience* 28: 2485-94

Andrikopoulos P, Eccles SA, Yaqoob MM. 2017. Coupling between the TRPC3 ion channel and the NCX1 transporter contributed to VEGF-induced ERK1/2 activation and angiogenesis in human primary endothelial cells. *Cell Signal* 37: 12-30

Aneiros E, Cao L, Papakosta M, Stevens EB, Phillips S, Grimm C. 2011. The biophysical and molecular basis of TRPV1 proton gating. *EMBO J* 30: 994-1002

Antigny F, Jousset H, Konig S, Frieden M. 2011. Thapsigargin activates Ca(2)+ entry both by store-dependent, STIM1/Orai1-mediated, and store-independent, TRPC3/PLC/PKC-mediated pathways in human endothelial cells. *Cell Calcium* 49: 115-27

Antognazza MR, Abdel Aziz I, Lodola F. 2019. Use of Exogenous and Endogenous Photomediators as Efficient ROS Modulation Tools: Results and Perspectives for Therapeutic Purposes. *Oxid Med Cell Longev* 2019: 2867516

Antognazza MR, Di Paolo M, Ghezzi D, Mete M, Di Marco S, et al. 2016. Characterization of a Polymer-Based, Fully Organic Prosthesis for Implantation into the Subretinal Space of the Rat. *Adv Healthc Mater* 5: 2271-82

Antognazza MR, Martino N, Ghezzi D, Feyen P, Colombo E, et al. 2015. Shedding Light on Living Cells. *Adv Mater* 27: 7662-9

Appendino G, Minassi A, Pagani A, Ech-Chahad A. 2008. The role of natural products in the ligand deorphanization of TRP channels. *Curr Pharm Des* 14: 2-17

Aromolaran AS, Zima AV, Blatter LA. 2007. Role of glycolytically generated ATP for CaMKII-mediated regulation of intracellular Ca2+ signaling in bovine vascular endothelial cells. *Am J Physiol Cell Physiol* 293: C106-18

Asahara T, Murohara T, Sullivan A, Silver M, van der Zee R, et al. 1997. Isolation of putative progenitor endothelial cells for angiogenesis. *Science* 275: 964-7

Ashraf S, Bell S, O'Leary C, Canning P, Micu I, et al. 2019. CAMKII as a therapeutic target for growth factor-induced retinal and choroidal neovascularization. *JCI Insight* 4: pii: 122442

Au P, Daheron LM, Duda DG, Cohen KS, Tyrrell JA, et al. 2008. Differential in vivo potential of endothelial progenitor cells from human umbilical cord blood and adult peripheral blood to form functional long-lasting vessels. *Blood* 111: 1302-5

Avdonin PV, Rybakova EY, Avdonin PP, Trufanov SK, Mironova GY, et al. 2019. VAS2870 Inhibits Histamine-Induced Calcium Signaling and vWF Secretion in Human Umbilical Vein Endothelial Cells. *Cells* 8

Az-ma T, Saeki N, Yuge O. 1999. Cytosolic Ca2+ movements of endothelial cells exposed to reactive oxygen intermediates: role of hydroxyl radical-mediated redox alteration of cell-membrane Ca2+ channels. *Br J Pharmacol* 126: 1462-70

Aziz IA, Malferrari M, Roggiani F, Tullii G, Rapino S, Antognazza MR. 2020. Light-Triggered Electron Transfer between a Conjugated Polymer and Cytochrome C for Optical Modulation of Redox Signaling. *Iscience* 23

Balbi C, Lodder K, Costa A, Moimas S, Moccia F, et al. 2019. Reactivating endogenous mechanisms of cardiac regeneration via paracrine boosting using the human amniotic fluid stem cell secretome. *Int J Cardiol* 287: 87-95

Banno K, Yoder MC. 2018. Tissue regeneration using endothelial colony-forming cells: promising cells for vascular repair. *Pediatr Res* 83: 283-90

Banno K, Yoder MC. 2019. Endothelial Stem and Progenitor Cells for Regenerative Medicine. *Curr Stem Cell Rep* 5: 101-08

Bansaghi S, Golenar T, Madesh M, Csordas G, RamachandraRao S, et al. 2014. Isoform- and species-specific control of inositol 1,4,5-trisphosphate (IP3) receptors by reactive oxygen species. *J Biol Chem* 289: 8170-81

Basile DP, Yoder MC. 2014. Circulating and tissue resident endothelial progenitor cells. *J Cell Physiol* 229: 10-6

Bellani S, Ghadirzadeh A, Meda L, Savoini A, Tacca A, et al. 2015. Hybrid Organic/Inorganic Nanostructures for Highly Sensitive Photoelectrochemical Detection of Dissolved Oxygen in Aqueous Media. *Adv Funct Mater* 25: 4531-38

Benfenati V, Martino N, Antognazza MR, Pistone A, Toffanin S, et al. 2014. Photostimulation of whole-cell conductance in primary rat neocortical astrocytes mediated by organic semiconducting thin films. *Adv Healthc Mater* 3: 392-9

Bennis Y, Sarlon-Bartoli G, Guillet B, Lucas L, Pellegrini L, et al. 2012. Priming of late endothelial progenitor cells with erythropoietin before transplantation requires the CD131 receptor subunit and enhances their angiogenic potential. *J Thromb Haemost* 10: 1914-28

Berra-Romani R, Faris P, Negri S, Botta L, Genova T, Moccia F. 2019. Arachidonic Acid Evokes an Increase in Intracellular Ca(2+) Concentration and Nitric Oxide Production in Endothelial Cells from Human Brain Microcirculation. *Cells* 8

Berridge MJ. 2006. Remodelling Ca2+ signalling systems and cardiac hypertrophy. *Biochem Soc T* 34: 228-31

Berridge MJ. 2007. Inositol trisphosphate and calcium oscillations. *Biochem Soc Symp*: 1-7

Berridge MJ. 2009. Inositol trisphosphate and calcium signalling mechanisms. *Biochim Biophys Acta* 1793: 933-40

Berridge MJ, Bootman MD, Roderick HL. 2003. Calcium signalling: Dynamics, homeostasis and remodelling. *Nat Rev Mol Cell Biol* 4: 517-29

Berrout J, Jin M, O'Neil RG. 2012. Critical role of TRPP2 and TRPC1 channels in stretch-induced injury of blood-brain barrier endothelial cells. *Brain Res* 1436: 1-12

Bhardwaj R, Hediger MA, Demaurex N. 2016. Redox modulation of STIM-ORAI signaling. *Cell Calcium* 60: 142-52

Birnbaumer L. 2009. The TRPC class of ion channels: a critical review of their roles in slow, sustained increases in intracellular Ca(2+) concentrations. *Annu Rev Pharmacol Toxicol* 49: 395-426

Bogeski I, Kummerow C, Al-Ansary D, Schwarz EC, Koehler R, et al. 2010. Differential redox regulation of ORAI ion channels: a mechanism to tune cellular calcium signaling. *Sci Signal* 3: ra24

Boscolo E, Mulliken JB, Bischoff J. 2011. VEGFR-1 mediates endothelial differentiation and formation of blood vessels in a murine model of infantile hemangioma. *Am J Pathol* 179: 2266-77

Bossio C, Aziz IA, Tullii G, Zucchetti E, Debellis D, et al. 2018. Photocatalytic Activity of Polymer Nanoparticles Modulates Intracellular Calcium Dynamics and Reactive Oxygen Species in HEK-293 Cells. *Front Bioeng Biotech* 6

Brandes RP, Weissmann N, Schroder K. 2014. Nox family NADPH oxidases: Molecular mechanisms of activation. *Free Radic Biol Med* 76: 208-26

Brandman O, Liou J, Park WS, Meyer T. 2007. STIM2 is a feedback regulator that stabilizes basal cytosolic and endoplasmic reticulum Ca2+ levels. *Cell* 131: 1327-39

Breton-Romero R, Lamas S. 2014. Hydrogen peroxide signaling in vascular endothelial cells. *Redox Biol* 2: 529-34

Brouet A, Sonveaux P, Dessy C, Balligand JL, Feron O. 2001. Hsp90 ensures the transition from the early Ca2+-dependent to the late phosphorylation-dependent activation of the endothelial nitric-oxide synthase in vascular endothelial growth factor-exposed endothelial cells. *J Biol Chem* 276: 32663-9

Burger D, Vinas JL, Akbari S, Dehak H, Knoll W, et al. 2015. Human endothelial colony-forming cells protect against acute kidney injury: role of exosomes. *Am J Pathol* 185: 2309-23
Burgoyne JR, Mongue-Din H, Eaton P, Shah AM. 2012. Redox signaling in cardiac physiology and pathology. *Circ Res* 111: 1091-106
Cai H. 2005a. Hydrogen peroxide regulation of endothelial function: origins, mechanisms, and consequences. *Cardiovasc Res* 68: 26-36
Cai H. 2005b. NAD(P)H oxidase-dependent self-propagation of hydrogen peroxide and vascular disease. *Circ Res* 96: 818-22
Cao E, Liao M, Cheng Y, Julius D. 2013. TRPV1 structures in distinct conformations reveal activation mechanisms. *Nature* 504: 113-8
Carmeliet P, Jain RK. 2011. Molecular mechanisms and clinical applications of angiogenesis. *Nature* 473: 298-307
Caterina MJ, Julius D. 2001. The vanilloid receptor: a molecular gateway to the pain pathway. *Annu Rev Neurosci* 24: 487-517
Caterina MJ, Schumacher MA, Tominaga M, Rosen TA, Levine JD, Julius D. 1997. The capsaicin receptor: a heat-activated ion channel in the pain pathway. *Nature* 389: 816-24
Chen R, Romero G, Christiansen MG, Mohr A, Anikeeva P. 2015. Wireless magnetothermal deep brain stimulation. *Science* 347: 1477-80
Chen Z, Li B, Dong Q, Qian C, Cheng J, Wang Y. 2018. Repetitive Transient Ischemia-Induced Cardiac Angiogenesis is Mediated by Camkii Activation. *Cell Physiol Biochem* 47: 914-24
Cheng W, Sun C, Zheng J. 2010. Heteromerization of TRP channel subunits: extending functional diversity. *Protein Cell* 1: 802-10
Cheng W, Yang F, Takanishi CL, Zheng J. 2007. Thermosensitive TRPV channel subunits coassemble into heteromeric channels with intermediate conductance and gating properties. *J Gen Physiol* 129: 191-207
Chidgey J, Fraser PA, Aaronson PI. 2016. Reactive oxygen species facilitate the EDH response in arterioles by potentiating intracellular endothelial Ca(2+) release. *Free Radic Biol Med* 97: 274-84
Ching LC, Chen CY, Su KH, Hou HH, Shyue SK, et al. 2012. Implication of AMP-activated protein kinase in transient receptor potential vanilloid type 1-mediated activation of endothelial nitric oxide synthase. *Mol Med* 18: 805-15
Ching LC, Kou YR, Shyue SK, Su KH, Wei J, et al. 2011. Molecular mechanisms of activation of endothelial nitric oxide synthase mediated by transient receptor potential vanilloid type 1. *Cardiovasc Res* 91: 492-501
Chuang HH, Lin S. 2009. Oxidative challenges sensitize the capsaicin receptor by covalent cysteine modification. *Proc Natl Acad Sci U S A* 106: 20097-102
Chung AS, Ferrara N. 2011. Developmental and pathological angiogenesis. *Annu Rev Cell Dev Biol* 27: 563-84
Cioffi DL, Barry C, Stevens T. 2010. Store-operated calcium entry channels in pulmonary endothelium: the emerging story of TRPCS and Orai1. *Adv Exp Med Biol* 661: 137-54
Cioffi DL, Wu S, Chen H, Alexeyev M, St Croix CM, et al. 2012. Orai1 determines calcium selectivity of an endogenous TRPC heterotetramer channel. *Circ Res* 110: 1435-44
Cosens DJ, Manning A. 1969. Abnormal electroretinogram from a Drosophila mutant. *Nature* 224: 285-7
Costa TJ, Barros PR, Arce C, Santos JD, da Silva-Neto J, et al. 2021. The homeostatic role of hydrogen peroxide, superoxide anion and nitric oxide in the vasculature. *Free Radic Biol Med* 162: 615-35
d'Audigier C, Cochain C, Rossi E, Guerin CL, Bieche I, et al. 2015. Thrombin receptor PAR-1 activation on endothelial progenitor cells enhances chemotaxis-associated genes expression and leukocyte recruitment by a COX-2-dependent mechanism. *Angiogenesis* 18: 347-59
Daneva Z, Marziano C, Ottolini M, Chen YL, Baker TM, et al. 2021. Caveolar peroxynitrite formation impairs endothelial TRPV4 channels and elevates pulmonary arterial pressure in pulmonary hypertension. *Proc Natl Acad Sci U S A* 118

Daskoulidou N, Zeng B, Berglund LM, Jiang H, Chen GL, et al. 2015. High glucose enhances store-operated calcium entry by upregulating ORAI/STIM via calcineurin-NFAT signalling. *J Mol Med (Berl)* 93: 511-21

DelloStritto DJ, Connell PJ, Dick GM, Fancher IS, Klarich B, et al. 2016a. Differential regulation of TRPV1 channels by H2O2: implications for diabetic microvascular dysfunction. *Basic Res Cardiol* 111: 21

DelloStritto DJ, Sinharoy P, Connell PJ, Fahmy JN, Cappelli HC, et al. 2016b. 4-Hydroxynonenal dependent alteration of TRPV1-mediated coronary microvascular signaling. *Free Radic Biol Med* 101: 10-19

Derek V, Rand D, Migliaccio L, Hanein Y, Glowacki ED. 2020. Untangling Photofaradaic and Photocapacitive Effects in Organic Optoelectronic Stimulation Devices. *Front Bioeng Biotech* 8

Di Giuro CML, Shrestha N, Malli R, Groschner K, van Breemen C, Fameli N. 2017. Na (+)/Ca(2+) exchangers and Orai channels jointly refill endoplasmic reticulum (ER) Ca(2+) via ER nanojunctions in vascular endothelial cells. *Pflugers Arch* 469: 1287-99

Di Maria F, Lodola F, Zucchetti E, Benfenati F, Lanzani G. 2018. The evolution of artificial light actuators in living systems: from planar to nanostructured interfaces. *Chem Soc Rev* 47: 4757-80

Di Nezza F, Zuccolo E, Poletto V, Rosti V, De Luca A, et al. 2017. Liposomes as a Putative Tool to Investigate NAADP Signaling in Vasculogenesis. *J Cell Biochem* 118: 3722-29

Ding R, Yin YL, Jiang LH. 2021. Reactive Oxygen Species-Induced TRPM2-Mediated Ca(2+) Signalling in Endothelial Cells. *Antioxidants (Basel)* 10

Djonov V, Baum O, Burri PH. 2003. Vascular remodeling by intussusceptive angiogenesis. *Cell Tissue Res* 314: 107-17

Doan TN, Gentry DL, Taylor AA, Elliott SJ. 1994. Hydrogen peroxide activates agonist-sensitive Ca(2+)-flux pathways in canine venous endothelial cells. *Biochem J* 297 (Pt 1): 209-15

Doucette CD, Hilchie AL, Liwski R, Hoskin DW. 2013. Piperine, a dietary phytochemical, inhibits angiogenesis. *J Nutr Biochem* 24: 231-9

Dragoni S, Guerra G, Fiorio Pla A, Bertoni G, Rappa A, et al. 2015a. A functional Transient Receptor Potential Vanilloid 4 (TRPV4) channel is expressed in human endothelial progenitor cells. *J Cell Physiol* 230: 95-104

Dragoni S, Laforenza U, Bonetti E, Lodola F, Bottino C, et al. 2011. Vascular endothelial growth factor stimulates endothelial colony forming cells proliferation and tubulogenesis by inducing oscillations in intracellular Ca2+ concentration. *Stem Cells* 29: 1898-907

Dragoni S, Laforenza U, Bonetti E, Lodola F, Bottino C, et al. 2013. Canonical transient receptor potential 3 channel triggers vascular endothelial growth factor-induced intracellular Ca2+ oscillations in endothelial progenitor cells isolated from umbilical cord blood. *Stem Cells Dev* 22: 2561-80

Dragoni S, Reforgiato M, Zuccolo E, Poletto V, Lodola F, et al. 2015b. Dysregulation of VEGF-induced proangiogenic Ca2+ oscillations in primary myelofibrosis-derived endothelial colony-forming cells. *Exp Hematol* 43: 1019-30 e3

Dragoni S, Turin I, Laforenza U, Potenza DM, Bottino C, et al. 2014. Store-operated Ca2+ entry does not control proliferation in primary cultures of human metastatic renal cellular carcinoma. *Biomed Res Int* 2014: 739494

Dreher D, Junod AF. 1995. Differential effects of superoxide, hydrogen peroxide, and hydroxyl radical on intracellular calcium in human endothelial cells. *J Cell Physiol* 162: 147-53

Drummond GR, Sobey CG. 2014. Endothelial NADPH oxidases: which NOX to target in vascular disease? *Trends Endocrinol Metab* 25: 452-63

Du J, Ma X, Shen B, Huang Y, Birnbaumer L, Yao X. 2014. TRPV4, TRPC1, and TRPP2 assemble to form a flow-sensitive heteromeric channel. *Faseb J* 28: 4677-85

Earley S, Brayden JE. 2015. Transient receptor potential channels in the vasculature. *Physiol Rev* 95: 645-90

Eckstein M, Vaeth M, Aulestia FJ, Costiniti V, Kassam SN, et al. 2019. Differential regulation of Ca(2+) influx by ORAI channels mediates enamel mineralization. *Sci Signal* 12

Eichmann A, Yuan L, Moyon D, Lenoble F, Pardanaud L, Breant C. 2005. Vascular development: from precursor cells to branched arterial and venous networks. *Int J Dev Biol* 49: 259-67

Ejneby MS, Migliaccio L, Gicevicius M, Derek V, Jakesova M, et al. 2020. Extracellular Photovoltage Clamp Using Conducting Polymer-Modified Organic Photocapacitors. *Adv Mater Technol-Us* 5

Elliott SJ, Doan TN. 1993. Oxidant stress inhibits the store-dependent Ca(2+)-influx pathway of vascular endothelial cells. *Biochem J* 292 (Pt 2): 385-93
Elrod JW, Duranski MR, Langston W, Greer JJ, Tao L, et al. 2006. eNOS gene therapy exacerbates hepatic ischemia-reperfusion injury in diabetes: a role for eNOS uncoupling. *Circ Res* 99: 78-85
Entcheva E, Kay MW. 2021. Cardiac optogenetics: a decade of enlightenment. *Nat Rev Cardiol* 18: 349-67
Esposito B, Gambara G, Lewis AM, Palombi F, D'Alessio A, et al. 2011. NAADP links histamine H1 receptors to secretion of von Willebrand factor in human endothelial cells. *Blood* 117: 4968-77
Evangelista AM, Thompson MD, Bolotina VM, Tong X, Cohen RA. 2012. Nox4- and Nox2-dependent oxidant production is required for VEGF-induced SERCA cysteine-674 S-glutathiolation and endothelial cell migration. *Free Radic Biol Med* 53: 2327-34
Faehling M, Kroll J, Fohr KJ, Fellbrich G, Mayr U, et al. 2002. Essential role of calcium in vascular endothelial growth factor A-induced signaling: mechanism of the antiangiogenic effect of carboxyamidotriazole. *Faseb J* 16: 1805-7
Faris P, Ferulli F, Vismara M, Tanzi M, Negri S, et al. 2020a. Hydrogen Sulfide-Evoked Intracellular Ca(2+) Signals in Primary Cultures of Metastatic Colorectal Cancer Cells. *Cancers (Basel)* 12
Faris P, Negri S, Perna A, Rosti V, Guerra G, Moccia F. 2020b. Therapeutic Potential of Endothelial Colony-Forming Cells in Ischemic Disease: Strategies to Improve their Regenerative Efficacy. *Int J Mol Sci* 21
Faris P, Pellavio G, Ferulli F, Di Nezza F, Shekha M, et al. 2019. Nicotinic Acid Adenine Dinucleotide Phosphate (NAADP) Induces Intracellular Ca(2+) Release through the Two-Pore Channel TPC1 in Metastatic Colorectal Cancer Cells. *Cancers (Basel)* 11: pii: E542
Faris P, Shekha M, Montagna D, Guerra G, Moccia F. 2018. Endolysosomal Ca(2+) Signalling and Cancer Hallmarks: Two-Pore Channels on the Move, TRPML1 Lags Behind! *Cancers (Basel)* 11
Favia A, Desideri M, Gambara G, D'Alessio A, Ruas M, et al. 2014. VEGF-induced neoangiogenesis is mediated by NAADP and two-pore channel-2-dependent Ca2+ signaling. *Proc Natl Acad Sci U S A* 111: E4706-15
Ferlauto L, Leccardi MJIA, Chenais NAL, Gillieron SCA, Vagni P, et al. 2018. Design and validation of a foldable and photovoltaic wide-field epiretinal prosthesis. *Nature Communications* 9
Feyen P, Colombo E, Endeman D, Nova M, Laudato L, et al. 2016. Light-evoked hyperpolarization and silencing of neurons by conjugated polymers. *Sci Rep* 6: 22718
Finkel T. 2012. Signal transduction by mitochondrial oxidants. *J Biol Chem* 287: 4434-40
Fischer C, Schneider M, Carmeliet P. 2006. Principles and therapeutic implications of angiogenesis, vasculogenesis and arteriogenesis. *Handb Exp Pharmacol*: 157-212
Florea AM, Varghese E, McCallum JE, Mahgoub S, Helmy I, et al. 2017. Calcium-regulatory proteins as modulators of chemotherapy in human neuroblastoma. *Oncotarget* 8: 22876-93
Forstermann U, Munzel T. 2006. Endothelial nitric oxide synthase in vascular disease: from marvel to menace. *Circulation* 113: 1708-14
Foskett JK, White C, Cheung KH, Mak DO. 2007. Inositol trisphosphate receptor Ca2+ release channels. *Physiol Rev* 87: 593-658
Fujinaga H, Fujinaga H, Watanabe N, Kato T, Tamano M, et al. 2016. Cord blood-derived endothelial colony-forming cell function is disrupted in congenital diaphragmatic hernia. *Am J Physiol Lung Cell Mol Physiol* 310: L1143-54
Fujisawa T, Tura-Ceide O, Hunter A, Mitchell A, Vesey A, et al. 2019. Endothelial Progenitor Cells Do Not Originate From the Bone Marrow. *Circulation* 140: 1524-26
Fukai T, Ushio-Fukai M. 2020. Cross-Talk between NADPH Oxidase and Mitochondria: Role in ROS Signaling and Angiogenesis. *Cells* 9
Furuhashi M. 2020. New insights into purine metabolism in metabolic diseases: role of xanthine oxidoreductase activity. *Am J Physiol Endocrinol Metab* 319: E827-E34
Galeano-Otero I, Del Toro R, Khatib AM, Rosado JA, Ordonez-Fernandez A, Smani T. 2021. SARAF and Orai1 Contribute to Endothelial Cell Activation and Angiogenesis. *Front Cell Dev Biol* 9: 639952
Galione A. 2015. A primer of NAADP-mediated Ca(2+) signalling: From sea urchin eggs to mammalian cells. *Cell Calcium* 58: 27-47

Gallego-Sandin S, Rodriguez-Garcia A, Alonso MT, Garcia-Sancho J. 2009. The Endoplasmic Reticulum of Dorsal Root Ganglion Neurons Contains Functional TRPV1 Channels. *Journal of Biological Chemistry* 284: 32591-601

Gaudet R. 2008. TRP channels entering the structural era. *J Physiol* 586: 3565-75

Gees M, Colsoul B, Nilius B. 2010. The role of transient receptor potential cation channels in Ca2+ signaling. *Cold Spring Harb Perspect Biol* 2: a003962

Gericke M, Droogmans G, Nilius B. 1993. Thimerosal induced changes of intracellular calcium in human endothelial cells. *Cell Calcium* 14: 201-7

Geron M, Hazan A, Priel A. 2017. Animal Toxins Providing Insights into TRPV1 Activation Mechanism. *Toxins (Basel)* 9

Ghezzi D, Antognazza MR, Dal Maschio M, Lanzarini E, Benfenati F, Lanzani G. 2011. A hybrid bioorganic interface for neuronal photoactivation. *Nat Commun* 2: 166

Gibhardt CS, Cappello S, Bhardwaj R, Schober R, Kirsch SA, et al. 2020. Oxidative Stress-Induced STIM2 Cysteine Modifications Suppress Store-Operated Calcium Entry. *Cell Rep* 33: 108292

Go YM, Jones DP. 2008. Redox compartmentalization in eukaryotic cells. *Biochim Biophys Acta* 1780: 1273-90

Goel M, Sinkins WG, Schilling WP. 2002. Selective association of TRPC channel subunits in rat brain synaptosomes. *J Biol Chem* 277: 48303-10

Goldenberg NM, Wang L, Ranke H, Liedtke W, Tabuchi A, Kuebler WM. 2015. TRPV4 Is Required for Hypoxic Pulmonary Vasoconstriction. *Anesthesiology* 122: 1338-48

Goldie LC, Nix MK, Hirschi KK. 2008. Embryonic vasculogenesis and hematopoietic specification. *Organogenesis* 4: 257-63

Gomes A, Fernandes E, Lima JL. 2005. Fluorescence probes used for detection of reactive oxygen species. *J Biochem Biophys Methods* 65: 45-80

Gorlach A, Bertram K, Hudecova S, Krizanova O. 2015. Calcium and ROS: A mutual interplay. *Redox Biol* 6: 260-71

Gough DR, Cotter TG. 2011. Hydrogen peroxide: a Jekyll and Hyde signalling molecule. *Cell Death Dis* 2: e213

Graier WF, Hoebel BG, Paltauf-Doburzynska J, Kostner GM. 1998. Effects of superoxide anions on endothelial Ca2+ signaling pathways. *Arterioscler Thromb Vasc Biol* 18: 1470-9

Greenberg HZE, Carlton-Carew SRE, Khan DM, Zargaran AK, Jahan KS, et al. 2017. Heteromeric TRPV4/TRPC1 channels mediate calcium-sensing receptor-induced nitric oxide production and vasorelaxation in rabbit mesenteric arteries. *Vascul Pharmacol* 96-98: 53-62

Gremmels H, de Jong OG, Hazenbrink DH, Fledderus JO, Verhaar MC. 2017. The Transcription Factor Nrf2 Protects Angiogenic Capacity of Endothelial Colony-Forming Cells in High-Oxygen Radical Stress Conditions. *Stem Cells International* 2017

Griffin MF, Butler PE, Seifalian AM, Kalaskar DM. 2015. Control of stem cell fate by engineering their micro and nanoenvironment. *World J Stem Cells* 7: 37-50

Groschner K, Shrestha N, Fameli N. 2017. Cardiovascular and Hemostatic Disorders: SOCE in Cardiovascular Cells: Emerging Targets for Therapeutic Intervention. *Adv Exp Med Biol* 993: 473-503

Groschner LN, Waldeck-Weiermair M, Malli R, Graier WF. 2012. Endothelial mitochondria--less respiration, more integration. *Pflugers Arch* 464: 63-76

Grupe M, Myers G, Penner R, Fleig A. 2010. Activation of store-operated I(CRAC) by hydrogen peroxide. *Cell Calcium* 48: 1-9

Gryszel M, Sytnyk M, Jakesova M, Romanazzi G, Gabrielsson R, et al. 2018. General Observation of Photocatalytic Oxygen Reduction to Hydrogen Peroxide by Organic Semiconductor Thin Films and Colloidal Crystals. *ACS Appl Mater Interfaces* 10: 13253-57

Guo BC, Wei J, Su KH, Chiang AN, Zhao JF, et al. 2015. Transient receptor potential vanilloid type 1 is vital for (-)-epigallocatechin-3-gallate mediated activation of endothelial nitric oxide synthase. *Mol Nutr Food Res* 59: 646-57

Guo Z, Grimm C, Becker L, Ricci AJ, Heller S. 2013. A novel ion channel formed by interaction of TRPML3 with TRPV5. *PLoS One* 8: e58174

Guo ZY, Zhang YH, Xie GQ, Liu CX, Zhou R, Shi W. 2016. Down-regulation of Homer1 attenuates t-BHP-induced oxidative stress through regulating calcium homeostasis and ER stress in brain endothelial cells. *Biochem Biophys Res Commun* 477: 970-76

Guven H, Shepherd RM, Bach RG, Capoccia BJ, Link DC. 2006. The number of endothelial progenitor cell colonies in the blood is increased in patients with angiographically significant coronary artery disease. *J Am Coll Cardiol* 48: 1579-87

Hache G, Garrigue P, Bennis Y, Stalin J, Moyon A, et al. 2016. ARA290, a Specific Agonist of Erythropoietin/CD131 Heteroreceptor, Improves Circulating Endothelial Progenitors' Angiogenic Potential and Homing Ability. *Shock* 46: 390-7

Hakami NY, Ranjan AK, Hardikar AA, Dusting GJ, Peshavariya HM. 2017. Role of NADPH Oxidase-4 in Human Endothelial Progenitor Cells. *Front Physiol* 8: 150

Hardie RC. 1992. Whole-Cell Recordings of the Light-Induced Current in Dissociated Drosophila Photoreceptors. *J Physiol-London* 446: P325-P25

Hare JM. 2004. Nitroso-redox balance in the cardiovascular system. *N Engl J Med* 351: 2112-4

Hawkins BJ, Irrinki KM, Mallilankaraman K, Lien YC, Wang Y, et al. 2010. S-glutathionylation activates STIM1 and alters mitochondrial homeostasis. *J Cell Biol* 190: 391-405

Heil M, Eitenmuller I, Schmitz-Rixen T, Schaper W. 2006. Arteriogenesis versus angiogenesis: similarities and differences. *J Cell Mol Med* 10: 45-55

Heinke J, Patterson C, Moser M. 2012. Life is a pattern: vascular assembly within the embryo. *Front Biosci (Elite Ed)* 4: 2269-88

Henschke PN, Elliott SJ. 1995. Oxidized glutathione decreases luminal Ca2+ content of the endothelial cell ins(1,4,5)P3-sensitive Ca2+ store. *Biochem J* 312 (Pt 2): 485-9

Herbert SP, Stainier DY. 2011. Molecular control of endothelial cell behaviour during blood vessel morphogenesis. *Nat Rev Mol Cell Biol* 12: 551-64

Hernandez-Lopez R, Chavez-Gonzalez A, Torres-Barrera P, Moreno-Lorenzana D, Lopez-DiazGuerrero N, et al. 2017. Reduced proliferation of endothelial colonyforming cells in unprovoked venous thromboembolic disease as a consequence of endothelial dysfunction. *Plos One* 12

Hertle DN, Yeckel MF. 2007. Distribution of inositol-1,4,5-trisphosphate receptor isotypes and ryanodine receptor isotypes during maturation of the rat hippocampus. *Neuroscience* 150: 625-38

Hidalgo C, Donoso P. 2008. Crosstalk between calcium and redox signaling: from molecular mechanisms to health implications. *Antioxid Redox Signal* 10: 1275-312

Hixon KR, Klein RC, Eberlin CT, Linder HR, Ona WJ, et al. 2019. A Critical Review and Perspective of Honey in Tissue Engineering and Clinical Wound Healing. *Adv Wound Care (New Rochelle)* 8: 403-15

Hofmann NA, Barth S, Waldeck-Weiermair M, Klec C, Strunk D, et al. 2014. TRPV1 mediates cellular uptake of anandamide and thus promotes endothelial cell proliferation and network-formation. *Biol Open* 3: 1164-72

Hofmann T, Schaefer M, Schultz G, Gudermann T. 2002. Subunit composition of mammalian transient receptor potential channels in living cells. *Proc Natl Acad Sci U S A* 99: 7461-6

Holzmann C, Kilch T, Kappel S, Dorr K, Jung V, et al. 2015. Differential Redox Regulation of Ca(2)(+) Signaling and Viability in Normal and Malignant Prostate Cells. *Biophys J* 109: 1410-9

Hong JH, Moon SJ, Byun HM, Kim MS, Jo H, et al. 2006. Critical role of phospholipase C gamma 1 in the generation of H2O2-evoked [Ca2+](i) oscillations in cultured rat cortical astrocytes. *Journal of Biological Chemistry* 281: 13057-67

Hu Q, Corda S, Zweier JL, Capogrossi MC, Ziegelstein RC. 1998. Hydrogen peroxide induces intracellular calcium oscillations in human aortic endothelial cells. *Circulation* 97: 268-75

Hu Q, Yu ZX, Ferrans VJ, Takeda K, Irani K, Ziegelstein RC. 2002. Critical role of NADPH oxidase-derived reactive oxygen species in generating Ca2+ oscillations in human aortic endothelial cells stimulated by histamine. *J Biol Chem* 277: 32546-51

Hu Q, Zheng G, Zweier JL, Deshpande S, Irani K, Ziegelstein RC. 2000. NADPH oxidase activation increases the sensitivity of intracellular Ca2+ stores to inositol 1,4,5-trisphosphate in human endothelial cells. *J Biol Chem* 275: 15749-57

Huang SM, Bisogno T, Trevisani M, Al-Hayani A, De Petrocellis L, et al. 2002. An endogenous capsaicin-like substance with high potency at recombinant and native vanilloid VR1 receptors. *Proc Natl Acad Sci U S A* 99: 8400-5

Ihori H, Nozawa T, Sobajima M, Shida T, Fukui Y, et al. 2016. Waon therapy attenuates cardiac hypertrophy and promotes myocardial capillary growth in hypertensive rats: a comparative study with fluvastatin. *Heart Vessels* 31: 1361-9

Incalza MA, D'Oria R, Natalicchio A, Perrini S, Laviola L, Giorgino F. 2018. Oxidative stress and reactive oxygen species in endothelial dysfunction associated with cardiovascular and metabolic diseases. *Vascul Pharmacol* 100: 1-19

Ingram DA, Mead LE, Moore DB, Woodard W, Fenoglio A, Yoder MC. 2005. Vessel wall-derived endothelial cells rapidly proliferate because they contain a complete hierarchy of endothelial progenitor cells. *Blood* 105: 2783-6

Ingram DA, Mead LE, Tanaka H, Meade V, Fenoglio A, et al. 2004. Identification of a novel hierarchy of endothelial progenitor cells using human peripheral and umbilical cord blood. *Blood* 104: 2752-60

Inoue K, Xiong ZG. 2009. Silencing TRPM7 promotes growth/proliferation and nitric oxide production of vascular endothelial cells via the ERK pathway. *Cardiovasc Res* 83: 547-57

Jarajapu YP, Hazra S, Segal M, Li Calzi S, Jadhao C, et al. 2014. Vasoreparative dysfunction of CD34+ cells in diabetic individuals involves hypoxic desensitization and impaired autocrine/paracrine mechanisms. *PLoS One* 9: e93965

Joo HJ, Song S, Seo HR, Shin JH, Choi SC, et al. 2015. Human endothelial colony forming cells from adult peripheral blood have enhanced sprouting angiogenic potential through up-regulating VEGFR2 signaling. *Int J Cardiol* 197: 33-43

Joseph SK. 2010. Role of thiols in the structure and function of inositol trisphosphate receptors. *Curr Top Membr* 66: 299-322

Joseph SK, Nakao SK, Sukumvanich S. 2006. Reactivity of free thiol groups in type-I inositol trisphosphate receptors. *Biochem J* 393: 575-82

Joseph SK, Young MP, Alzayady K, Yule DI, Ali M, et al. 2018. Redox regulation of type-I inositol trisphosphate receptors in intact mammalian cells. *J Biol Chem* 293: 17464-76

Kang KT, Lin RZ, Kuppermann D, Melero-Martin JM, Bischoff J. 2017. Endothelial colony forming cells and mesenchymal progenitor cells form blood vessels and increase blood flow in ischemic muscle. *Sci Rep* 7: 770

Karai LJ, Russell JT, Iadarola MJ, Olah Z. 2004. Vanilloid receptor 1 regulates multiple calcium compartments and contributes to Ca2+-induced Ca2+ release in sensory neurons. *Journal of Biological Chemistry* 279: 16377-87

Kedei N, Szabo T, Lile JD, Treanor JJ, Olah Z, et al. 2001. Analysis of the native quaternary structure of vanilloid receptor 1. *J Biol Chem* 276: 28613-9

Keighron C, Lyons CJ, Creane M, O'Brien T, Liew A. 2018. Recent Advances in Endothelial Progenitor Cells Toward Their Use in Clinical Translation. *Front Med (Lausanne)* 5: 354

Kelley EE, Khoo NK, Hundley NJ, Malik UZ, Freeman BA, Tarpey MM. 2010. Hydrogen peroxide is the major oxidant product of xanthine oxidase. *Free Radic Biol Med* 48: 493-8

Kerkhofs M, Bittremieux M, Morciano G, Giorgi C, Pinton P, et al. 2018. Emerging molecular mechanisms in chemotherapy: Ca(2+) signaling at the mitochondria-associated endoplasmic reticulum membranes. *Cell Death Dis* 9: 334

Khaddaj Mallat R, Mathew John C, Kendrick DJ, Braun AP. 2017. The vascular endothelium: A regulator of arterial tone and interface for the immune system. *Crit Rev Clin Lab Sci* 54: 458-70

Kim C, Kim JY, Kim JH. 2008. Cytosolic phospholipase A(2), lipoxygenase metabolites, and reactive oxygen species. *BMB Rep* 41: 555-9

Kim I, Moon SO, Kim SH, Kim HJ, Koh YS, Koh GY. 2001. Vascular endothelial growth factor expression of intercellular adhesion molecule 1 (ICAM-1), vascular cell adhesion molecule 1 (VCAM-1), and E-selectin through nuclear factor-kappa B activation in endothelial cells. *J Biol Chem* 276: 7614-20

Kim K, Yoo H, Lee EK. 2022. New Opportunities for Organic Semiconducting Polymers in Biomedical Applications. *Polymers (Basel)* 14

Kim MS, Kim YK, Cho KH, Chung JH. 2006. Infrared exposure induces an angiogenic switch in human skin that is partially mediated by heat. *Br J Dermatol* 155: 1131-8

Kohler R, Brakemeier S, Kuhn M, Degenhardt C, Buhr H, et al. 2001. Expression of ryanodine receptor type 3 and TRP channels in endothelial cells: comparison of in situ and cultured human endothelial cells. *Cardiovasc Res* 51: 160-8

Komici K, Faris P, Negri S, Rosti V, Garcia-Carrasco M, et al. 2020. Systemic lupus erythematosus, endothelial progenitor cells and intracellular Ca(2+) signaling: A novel approach for an old disease. *J Autoimmun* 112: 102486

Kurusamy S, Lopez-Maderuelo D, Little R, Cadagan D, Savage AM, et al. 2017. Selective inhibition of plasma membrane calcium ATPase 4 improves angiogenesis and vascular reperfusion. *J Mol Cell Cardiol* 109: 38-47

Kuzhikandathil EV, Wang H, Szabo T, Morozova N, Blumberg PM, Oxford GS. 2001. Functional analysis of capsaicin receptor (vanilloid receptor subtype 1) multimerization and agonist responsiveness using a dominant negative mutation. *J Neurosci* 21: 8697-706

Lambert AJ, Brand MD. 2009. Reactive oxygen species production by mitochondria. *Methods Mol Biol* 554: 165-81

Landmesser U, Spiekermann S, Preuss C, Sorrentino S, Fischer D, et al. 2007. Angiotensin II induces endothelial xanthine oxidase activation: role for endothelial dysfunction in patients with coronary disease. *Arterioscler Thromb Vasc Biol* 27: 943-8

Lanzani G, Antognazza MR, Martino N, Ghezzi D, Benfenati F. 2015. Controlling Cell Functions by Light. *I Ieee Embs C Neur E*: 603-06

Lee JH, Lee SH, Choi SH, Asahara T, Kwon SM. 2015. The sulfated polysaccharide fucoidan rescues senescence of endothelial colony-forming cells for ischemic repair. *Stem Cells* 33: 1939-51

Lee M, Spokes KC, Aird WC, Abid MR. 2010. Intracellular Ca2+ can compensate for the lack of NADPH oxidase-derived ROS in endothelial cells. *Febs Lett* 584: 3131-6

Lee Y, Son JY, Kang JI, Park KM, Park KD. 2018. Hydrogen Peroxide-Releasing Hydrogels for Enhanced Endothelial Cell Activities and Neovascularization. *ACS Appl Mater Interfaces* 10: 18372-79

Lepage PK, Boulay G. 2007. Molecular determinants of TRP channel assembly. *Biochem Soc Trans* 35: 81-3

Lewis RS. 2020. Store-Operated Calcium Channels: From Function to Structure and Back Again. *Cold Spring Harb Perspect Biol* 12

Li H, Forstermann U. 2013. Uncoupling of endothelial NO synthase in atherosclerosis and vascular disease. *Curr Opin Pharmacol* 13: 161-7

Li J, Cubbon RM, Wilson LA, Amer MS, McKeown L, et al. 2011. Orai1 and CRAC channel dependence of VEGF-activated Ca2+ entry and endothelial tube formation. *Circ Res* 108: 1190-8

Li J, Duan H, Pu K. 2019. Nanotransducers for Near-Infrared Photoregulation in Biomedicine. *Adv Mater* 31: e1901607

Li Q, Youn JY, Cai H. 2015. Mechanisms and consequences of endothelial nitric oxide synthase dysfunction in hypertension. *J Hypertens* 33: 1128-36

Liao M, Cao E, Julius D, Cheng Y. 2013. Structure of the TRPV1 ion channel determined by electron cryo-microscopy. *Nature* 504: 107-12

Lin RZ, Moreno-Luna R, Li D, Jaminet SC, Greene AK, Melero-Martin JM. 2014. Human endothelial colony-forming cells serve as trophic mediators for mesenchymal stem cell engraftment via paracrine signaling. *Proc Natl Acad Sci U S A* 111: 10137-42

Lin Y, Weisdorf DJ, Solovey A, Hebbel RP. 2000. Origins of circulating endothelial cells and endothelial outgrowth from blood. *J Clin Invest* 105: 71-7

Lock JT, Sinkins WG, Schilling WP. 2012. Protein S-glutathionylation enhances Ca2+-induced Ca2+ release via the IP3 receptor in cultured aortic endothelial cells. *J Physiol* 590: 3431-47

Lodola F, Laforenza U, Bonetti E, Lim D, Dragoni S, et al. 2012. Store-operated Ca2+ entry is remodelled and controls in vitro angiogenesis in endothelial progenitor cells isolated from tumoral patients. *PLoS One* 7: e42541

Lodola F, Laforenza U, Cattaneo F, Ruffinatti FA, Poletto V, et al. 2017a. VEGF-induced intracellular Ca^{2+} oscillations are down-regulated and do not stimulate angiogenesis in breast cancer-derived endothelial colony forming cells. *Oncotarget* 8: 95223-46

Lodola F, Martino N, Tullii G, Lanzani G, Antognazza MR. 2017b. Conjugated polymers mediate effective activation of the Mammalian Ion Channel Transient Receptor Potential Vanilloid 1. *Sci Rep* 7: 8477

Lodola F, Rosti V, Tullii G, Desii A, Tapella L, et al. 2019a. Conjugated polymers optically regulate the fate of endothelial colony-forming cells. *Sci Adv* 5: eaav4620

Lodola F, Vurro V, Crasto S, Di Pasquale E, Lanzani G. 2019b. Optical Pacing of Human-Induced Pluripotent Stem Cell-Derived Cardiomyocytes Mediated by a Conjugated Polymer Interface. *Adv Healthc Mater* 8: e1900198

Lotteau S, Ducreux S, Romestaing C, Legrand C, Van Coppenolle F. 2013. Characterization of functional TRPV1 channels in the sarcoplasmic reticulum of mouse skeletal muscle. *PLoS One* 8: e58673

Lounsbury KM, Hu Q, Ziegelstein RC. 2000. Calcium signaling and oxidant stress in the vasculature. *Free Radic Biol Med* 28: 1362-9

Lozano C, Cordova C, Marchant I, Zuniga R, Ochova P, et al. 2018. Intracellular aggregated TRPV1 is associated with lower survival in breast cancer patients. *Breast Cancer (Dove Med Press)* 10: 161-68

Ma X, Cheng KT, Wong CO, O'Neil RG, Birnbaumer L, et al. 2011. Heteromeric TRPV4-C1 channels contribute to store-operated Ca(2+) entry in vascular endothelial cells. *Cell Calcium* 50: 502-9

Ma X, Qiu S, Luo J, Ma Y, Ngai CY, et al. 2010. Functional role of vanilloid transient receptor potential 4-canonical transient receptor potential 1 complex in flow-induced Ca2+ influx. *Arterioscler Thromb Vasc Biol* 30: 851-8

Madreiter-Sokolowski CT, Thomas C, Ristow M. 2020. Interrelation between ROS and Ca(2+) in aging and age-related diseases. *Redox Biol* 36: 101678

Maeng YS, Choi HJ, Kwon JY, Park YW, Choi KS, et al. 2009. Endothelial progenitor cell homing: prominent role of the IGF2-IGF2R-PLCbeta2 axis. *Blood* 113: 233-43

Malferrari M, Becconi M, Rapino S. 2019. Electrochemical monitoring of reactive oxygen/nitrogen species and redox balance in living cells. *Anal Bioanal Chem* 411: 4365-74

Malli R, Frieden M, Osibow K, Graier WF. 2003. Mitochondria efficiently buffer subplasmalemmal Ca2+ elevation during agonist stimulation. *J Biol Chem* 278: 10807-15

Malli R, Frieden M, Trenker M, Graier WF. 2005. The role of mitochondria for Ca2+ refilling of the endoplasmic reticulum. *J Biol Chem* 280: 12114-22

Mancardi D, Pla AF, Moccia F, Tanzi F, Munaron L. 2011. Old and new gasotransmitters in the cardiovascular system: focus on the role of nitric oxide and hydrogen sulfide in endothelial cells and cardiomyocytes. *Curr Pharm Biotechnol* 12: 1406-15

Marsakova L, Barvik I, Zima V, Zimova L, Vlachova V. 2017. The First Extracellular Linker Is Important for Several Aspects of the Gating Mechanism of Human TRPA1 Channel. *Front Mol Neurosci* 10: 16

Martino N, Bossio C, Vaquero Morata S, Lanzani G, Antognazza MR. 2016. Optical Control of Living Cells Electrical Activity by Conjugated Polymers. *J Vis Exp*: e53494

Martino N, Feyen P, Porro M, Bossio C, Zucchetti E, et al. 2015. Photothermal cellular stimulation in functional bio-polymer interfaces. *Sci Rep* 5: 8911

Martino N, Ghezzi D, Benfenati F, Lanzani G, Antognazza MR. 2013. Organic semiconductors for artificial vision. *J Mater Chem B* 1: 3768-80

Martinotti S, Laforenza U, Patrone M, Moccia F, Ranzato E. 2019. Honey-Mediated Wound Healing: H(2)O(2) Entry through AQP3 Determines Extracellular Ca(2+) Influx. *Int J Mol Sci* 20

Massa M, Campanelli R, Bonetti E, Ferrario M, Marinoni B, Rosti V. 2009. Rapid and large increase of the frequency of circulating endothelial colony-forming cells (ECFCs) generating late outgrowth endothelial cells in patients with acute myocardial infarction. *Exp Hematol* 37: 8-9

Mauge L, Sabatier F, Boutouyrie P, D'Audigier C, Peyrard S, et al. 2014. Forearm ischemia decreases endothelial colony-forming cell angiogenic potential. *Cytotherapy* 16: 213-24

Maya-Vetencourt JF, Di Marco S, Mete M, Di Paolo M, Ventrella D, et al. 2020. Biocompatibility of a Conjugated Polymer Retinal Prosthesis in the Domestic Pig. *Front Bioeng Biotechnol* 8: 579141

Maya-Vetencourt JF, Ghezzi D, Antognazza MR, Colombo E, Mete M, et al. 2017. A fully organic retinal prosthesis restores vision in a rat model of degenerative blindness. *Nat Mater* 16: 681-89
McDaid J, Mustaly-Kalimi S, Stutzmann GE. 2020. Ca2+ Dyshomeostasis Disrupts Neuronal and Synaptic Function in Alzheimer's Disease. *Cells* 9
McNamara FN, Randall A, Gunthorpe MJ. 2005. Effects of piperine, the pungent component of black pepper, at the human vanilloid receptor (TRPV1). *Br J Pharmacol* 144: 781-90
Medagoda DI, Ghezzi D. 2021. Organic semiconductors for light-mediated neuromodulation. *Commun Mater* 2
Medina RJ, Barber CL, Sabatier F, Dignat-George F, Melero-Martin JM, et al. 2017. Endothelial Progenitors: A Consensus Statement on Nomenclature. *Stem Cells Transl Med* 6: 1316-20
Melero-Martin JM, Khan ZA, Picard A, Wu X, Paruchuri S, Bischoff J. 2007. In vivo vasculogenic potential of human blood-derived endothelial progenitor cells. *Blood* 109: 4761-8
Mena HA, Carestia A, Scotti L, Parborell F, Schattner M, Negrotto S. 2016. Extracellular histones reduce survival and angiogenic responses of late outgrowth progenitor and mature endothelial cells. *J Thromb Haemost* 14: 397-410
Mena HA, Lokajczyk A, Dizier B, Strier SE, Voto LS, et al. 2014. Acidic preconditioning improves the proangiogenic responses of endothelial colony forming cells. *Angiogenesis* 17: 867-79
Mena HA, Zubiry PR, Dizier B, Mignon V, Parborell F, et al. 2019. Ceramide 1-Phosphate Protects Endothelial Colony-Forming Cells From Apoptosis and Increases Vasculogenesis In Vitro and In Vivo. *Arterioscl Throm Vas* 39: E219-E32
Mena HA, Zubiry PR, Dizier B, Schattner M, Boisson-Vidal C, Negrotto S. 2018. Acidic preconditioning of endothelial colony-forming cells (ECFC) promote vasculogenesis under proinflammatory and high glucose conditions in vitro and in vivo. *Stem Cell Res Ther* 9
Mergler S, Valtink M, Coulson-Thomas VJ, Lindemann D, Reinach PS, et al. 2010. TRPV channels mediate temperature-sensing in human corneal endothelial cells. *Exp Eye Res* 90: 758-70
Mergler S, Valtink M, Taetz K, Sahlmuller M, Fels G, et al. 2011. Characterization of transient receptor potential vanilloid channel 4 (TRPV4) in human corneal endothelial cells. *Exp Eye Res* 93: 710-9
Merola J, Reschke M, Pierce RW, Qin L, Spindler S, et al. 2019. Progenitor-derived human endothelial cells evade alloimmunity by CRISPR/Cas9-mediated complete ablation of MHC expression. *JCI Insight* 4
Min JK, Han KY, Kim EC, Kim YM, Lee SW, et al. 2004. Capsaicin inhibits in vitro and in vivo angiogenesis. *Cancer Res* 64: 644-51
Minke B. 1977. Drosophila mutant with a transducer defect. *Biophys Struct Mech* 3: 59-64
Minke B, Wu C, Pak WL. 1975. Induction of photoreceptor voltage noise in the dark in Drosophila mutant. *Nature* 258: 84-7
Mittal M, Urao N, Hecquet CM, Zhang M, Sudhahar V, et al. 2015. Novel role of reactive oxygen species-activated Trp melastatin channel-2 in mediating angiogenesis and postischemic neovascularization. *Arterioscler Thromb Vasc Biol* 35: 877-87
Moccia F. 2018. Endothelial Ca(2+) Signaling and the Resistance to Anticancer Treatments: Partners in Crime. *Int J Mol Sci* 19: pii: E217
Moccia F. 2020. Calcium Signaling in Endothelial Colony Forming Cells in Health and Disease. *Adv Exp Med Biol* 1131: 1013-30
Moccia F, Antognazza MR, Lodola F. 2020. Towards Novel Geneless Approaches for Therapeutic Angiogenesis. *Front Physiol* 11: 616189
Moccia F, Berra-Romani R, Rosti V. 2018a. Manipulating Intracellular Ca2+ Signals to Stimulate Therapeutic Angiogenesis in Cardiovascular Disorders. *Curr Pharm Biotechnol* 19: 686-99
Moccia F, Berra-Romani R, Tanzi F. 2012a. Ca2+ signalling in damaged endothelium and arterial remodelling: Do connexin hemichannels provide a suitable target to prevent in-stent restenosis? *Curr Drug Ther* 7: 268-80
Moccia F, Berra-Romani R, Tanzi F. 2012b. Update on vascular endothelial Ca2+ signalling: A tale of ion channels, pumps and transporters. *World J Biol Chem* 3: 127-58

Moccia F, Dragoni S, Lodola F, Bonetti E, Bottino C, et al. 2012c. Store-dependent Ca(2+) entry in endothelial progenitor cells as a perspective tool to enhance cell-based therapy and adverse tumour vascularization. *Curr Med Chem* 19: 5802-18

Moccia F, Fotia V, Tancredi R, Della Porta MG, Rosti V, et al. 2017. Breast and renal cancer-Derived endothelial colony forming cells share a common gene signature. *Eur J Cancer* 77: 155-64

Moccia F, Guerra G. 2016. Ca(2+) Signalling in Endothelial Progenitor Cells: Friend or Foe? *J Cell Physiol* 231: 314-27

Moccia F, Lodola F, Dragoni S, Bonetti E, Bottino C, et al. 2014a. Ca2+ signalling in endothelial progenitor cells: a novel means to improve cell-based therapy and impair tumour vascularisation. *Curr Vasc Pharmacol* 12: 87-105

Moccia F, Lucariello A, Guerra G. 2018b. TRPC3-mediated Ca(2+) signals as a promising strategy to boost therapeutic angiogenesis in failing hearts: The role of autologous endothelial colony forming cells. *J Cell Physiol* 233: 3901-17

Moccia F, Negri S, Shekha M, Faris P, Guerra G. 2019. Endothelial Ca(2+) Signaling, Angiogenesis and Vasculogenesis: just What It Takes to Make a Blood Vessel. *Int J Mol Sci* 20

Moccia F, Poletto V. 2015. May the remodeling of the Ca(2)(+) toolkit in endothelial progenitor cells derived from cancer patients suggest alternative targets for anti-angiogenic treatment? *Biochim Biophys Acta* 1853: 1958-73

Moccia F, Ruffinatti FA, Zuccolo E. 2015a. Intracellular Ca(2)(+) Signals to Reconstruct A Broken Heart: Still A Theoretical Approach? *Curr Drug Targets* 16: 793-815

Moccia F, Tanzi F, Munaron L. 2014b. Endothelial remodelling and intracellular calcium machinery. *Curr Mol Med* 14: 457-80

Moccia F, Zuccolo E, Di Nezza F, Pellavio G, Faris PS, et al. 2021. Nicotinic acid adenine dinucleotide phosphate activates two-pore channel TPC1 to mediate lysosomal Ca(2+) release in endothelial colony-forming cells. *J Cell Physiol* 236: 688-705

Moccia F, Zuccolo E, Poletto V, Turin I, Guerra G, et al. 2016. Targeting Stim and Orai Proteins as an Alternative Approach in Anticancer Therapy. *Curr Med Chem* 23: 3450-80

Moccia F, Zuccolo E, Soda T, Tanzi F, Guerra G, et al. 2015b. Stim and Orai proteins in neuronal Ca(2+) signaling and excitability. *Front Cell Neurosci* 9: 153

Montell C, Jones K, Hafen E, Rubin G. 1985. Rescue of the Drosophila phototransduction mutation trp by germline transformation. *Science* 230: 1040-3

Montell C, Rubin GM. 1989. Molecular characterization of the Drosophila trp locus: a putative integral membrane protein required for phototransduction. *Neuron* 2: 1313-23

Montezano AC, Burger D, Paravicini TM, Chignalia AZ, Yusuf H, et al. 2010. Nicotinamide adenine dinucleotide phosphate reduced oxidase 5 (Nox5) regulation by angiotensin II and endothelin-1 is mediated via calcium/calmodulin-dependent, rac-1-independent pathways in human endothelial cells. *Circ Res* 106: 1363-73

Morciano G, Marchi S, Morganti C, Sbano L, Bittremieux M, et al. 2018. Role of Mitochondria-Associated ER Membranes in Calcium Regulation in Cancer-Specific Settings. *Neoplasia* 20: 510-23

Morgan AJ, Jacob R. 1996. Ca2+ influx does more than provide releasable Ca2+ to maintain repetitive spiking in human umbilical vein endothelial cells. *Biochem J* 320 (Pt 2): 505-17

Mosconi E, Salvatori P, Saba MI, Matton A, Bellani S, et al. 2016. Surface Polarization Drives Photoinduced Charge Separation at the P3HT/Water Interface. *Acs Energy Lett* 1: 454-63

Mountian I, Manolopoulos VG, De Smedt H, Parys JB, Missiaen L, Wuytack F. 1999. Expression patterns of sarco/endoplasmic reticulum Ca(2+)-ATPase and inositol 1,4,5-trisphosphate receptor isoforms in vascular endothelial cells. *Cell Calcium* 25: 371-80

Mu P, Liu Q, Zheng R. 2010. Biphasic regulation of H2O2 on angiogenesis implicated NADPH oxidase. *Cell Biol Int* 34: 1013-20

Munns CH, Chung MK, Sanchez YE, Amzel LM, Caterina MJ. 2015. Role of the outer pore domain in transient receptor potential vanilloid 1 dynamic permeability to large cations. *J Biol Chem* 290: 5707-24

Munoz M, Lopez-Oliva ME, Pinilla E, Martinez MP, Sanchez A, et al. 2017. CYP epoxygenase-derived H2O2 is involved in the endothelium-derived hyperpolarization (EDH) and relaxation of intrarenal arteries. *Free Radic Biol Med* 106: 168-83

Naito H, Iba T, Takakura N. 2020. Mechanisms of new blood vessel formation and proliferative heterogeneity of endothelial cells. *Int Immunol*

Negri S, Faris P, Berra-Romani R, Guerra G, Moccia F. 2019. Endothelial Transient Receptor Potential Channels and Vascular Remodeling: Extracellular Ca(2 +) Entry for Angiogenesis, Arteriogenesis and Vasculogenesis. *Front Physiol* 10: 1618

Negri S, Faris P, Moccia F. 2021. Reactive Oxygen Species and Endothelial Ca(2+) Signaling: Brothers in Arms or Partners in Crime? *Int J Mol Sci* 22

Negri S, Faris P, Rosti V, Antognazza MR, Lodola F, Moccia F. 2020. Endothelial TRPV1 as an Emerging Molecular Target to Promote Therapeutic Angiogenesis. *Cells* 9

Nelidova D, Morikawa RK, Cowan CS, Raics Z, Goldblum D, et al. 2020. Restoring light sensitivity using tunable near-infrared sensors. *Science* 368: 1108-13

Niemeyer BA. 2017. The STIM-Orai Pathway: Regulation of STIM and Orai by Thiol Modifications. *Adv Exp Med Biol* 993: 99-116

Noren DP, Chou WH, Lee SH, Qutub AA, Warmflash A, et al. 2016. Endothelial cells decode VEGF-mediated Ca2+ signaling patterns to produce distinct functional responses. *Sci Signal* 9: ra20

Nozawa T, Iibushi J, Toh H, Minowa-Nozawa A, Murase K, et al. 2021. Intracellular Group A Streptococcus Induces Golgi Fragmentation To Impair Host Defenses through Streptolysin O and NAD-Glycohydrolase. *mBio* 12

O'Leary C, McGahon MK, Ashraf S, McNaughten J, Friedel T, et al. 2019. Involvement of TRPV1 and TRPV4 Channels in Retinal Angiogenesis. *Invest Ophthalmol Vis Sci* 60: 3297-309

O'Neill CL, McLoughlin KJ, Chambers SEJ, Guduric-Fuchs J, Stitt AW, Medina RJ. 2018. The Vasoreparative Potential of Endothelial Colony Forming Cells: A Journey Through Pre-clinical Studies. *Front Med (Lausanne)* 5: 273

O'Neill KM, Campbell DC, Edgar KS, Gill EK, Moez A, et al. 2019. NOX4 is a major regulator of cord blood-derived endothelial colony-forming cells which promotes postischaemic revascularisation. *Cardiovasc Res*

Ogawa N, Kurokawa T, Fujiwara K, Polat OK, Badr H, et al. 2016. Functional and Structural Divergence in Human TRPV1 Channel Subunits by Oxidative Cysteine Modification. *J Biol Chem* 291: 4197-210

Otto M, Bucher C, Liu W, Muller M, Schmidt T, et al. 2020. 12(S)-HETE mediates diabetes-induced endothelial dysfunction by activating intracellular endothelial cell TRPV1. *J Clin Invest* 130: 4999-5010

Panieri E, Santoro MM. 2015. ROS signaling and redox biology in endothelial cells. *Cell Mol Life Sci* 72: 3281-303

Pantke S, Fricke TC, Eberhardt MJ, Herzog C, Leffler A. 2021. Gating of the capsaicin receptor TRPV1 by UVA-light and oxidants are mediated by distinct mechanisms. *Cell Calcium* 96: 102391

Parekh AB. 2007. Functional consequences of activating store-operated CRAC channels. *Cell Calcium* 42: 111-21

Parekh AB, Penner R. 1995. Activation of store-operated calcium influx at resting InsP3 levels by sensitization of the InsP3 receptor in rat basophilic leukaemia cells. *J Physiol* 489 (Pt 2): 377-82

Park KM, Park KD. 2018. In Situ Cross-Linkable Hydrogels as a Dynamic Matrix for Tissue Regenerative Medicine. *Tissue Eng Regen Med* 15: 547-57

Paschalaki KE, Randi AM. 2018. Recent Advances in Endothelial Colony Forming Cells Toward Their Use in Clinical Translation. *Front Med (Lausanne)* 5: 295

Patacchini R, Santicioli P, Giuliani S, Maggi CA. 2005. Pharmacological investigation of hydrogen sulfide (H2S) contractile activity in rat detrusor muscle. *Eur J Pharmacol* 509: 171-7

Patel S. 2015. Function and dysfunction of two-pore channels. *Sci Signal* 8: re7

Patton AM, Kassis J, Doong H, Kohn EC. 2003. Calcium as a molecular target in angiogenesis. *Curr Pharm Des* 9: 543-51

Pecze L, Blum W, Henzi T, Schwaller B. 2016a. Endogenous TRPV1 stimulation leads to the activation of the inositol phospholipid pathway necessary for sustained Ca(2+) oscillations. *Biochim Biophys Acta* 1863: 2905-15

Pecze L, Josvay K, Blum W, Petrovics G, Vizler C, et al. 2016b. Activation of endogenous TRPV1 fails to induce overstimulation-based cytotoxicity in breast and prostate cancer cells but not in pain-sensing neurons. *Biochim Biophys Acta* 1863: 2054-64

Peters EC, Gee MT, Pawlowski LN, Kath AM, Polk FD, et al. 2022. Amyloid-beta disrupts unitary calcium entry through endothelial NMDA receptors in mouse cerebral arteries. *J Cerebr Blood F Met* 42: 145-61

Petersen CC, Berridge MJ, Borgese MF, Bennett DL. 1995. Putative capacitative calcium entry channels: expression of Drosophila trp and evidence for the existence of vertebrate homologues. *Biochem J* 311 (Pt 1): 41-4

Pfeiffer T, Li Y, Attwell D. 2021. Diverse mechanisms regulating brain energy supply at the capillary level. *Curr Opin Neurobiol* 69: 41-50

Pires PW, Earley S. 2017. Redox regulation of transient receptor potential channels in the endothelium. *Microcirculation* 24

Pires PW, Earley S. 2018. Neuroprotective effects of TRPA1 channels in the cerebral endothelium following ischemic stroke. *Elife* 7

Poletto V, Dragoni S, Lim D, Biggiogera M, Aronica A, et al. 2016. Endoplasmic Reticulum Ca(2+) Handling and Apoptotic Resistance in Tumor-Derived Endothelial Colony Forming Cells. *J Cell Biochem* 117: 2260-71

Poletto V, Rosti V, Biggiogera M, Guerra G, Moccia F, Porta C. 2018. The role of endothelial colony forming cells in kidney cancer's pathogenesis, and in resistance to anti-VEGFR agents and mTOR inhibitors: A speculative review. *Crit Rev Oncol Hematol* 132: 89-99

Potente M, Gerhardt H, Carmeliet P. 2011. Basic and therapeutic aspects of angiogenesis. *Cell* 146: 873-87

Prakriya M, Lewis RS. 2015. Store-Operated Calcium Channels. *Physiol Rev* 95: 1383-436

Prins D, Groenendyk J, Touret N, Michalak M. 2011. Modulation of STIM1 and capacitative Ca2+ entry by the endoplasmic reticulum luminal oxidoreductase ERp57. *EMBO Rep* 12: 1182-8

Prole DL, Taylor CW. 2019. Structure and Function of IP3 Receptors. *Cold Spring Harb Perspect Biol* 11

Ramirez-Barrantes R, Cordova C, Gatica S, Rodriguez B, Lozano C, et al. 2018. Transient Receptor Potential Vanilloid 1 Expression Mediates Capsaicin-Induced Cell Death. *Front Physiol* 9: 682

Rand D, Jakesova M, Lubin G, Vebraite I, David-Pur M, et al. 2018. Direct Electrical Neurostimulation with Organic Pigment Photocapacitors. *Advanced Materials* 30

Ranzato E, Bonsignore G, Patrone M, Martinotti S. 2021. Endothelial and Vascular Health: A Tale of Honey, H2O2 and Calcium. *Cells* 10

Reid E, Guduric-Fuchs J, O'Neill CL, Allen LD, Chambers SEJ, et al. 2017. Preclinical Evaluation and Optimization of a Cell Therapy Using Human Cord Blood-Derived Endothelial Colony-Forming Cells for Ischemic Retinopathies. *Stem Cells Transl Med*

Risau W, Flamme I. 1995. Vasculogenesis. *Annu Rev Cell Dev Biol* 11: 73-91

Rohacs T. 2014. Phosphoinositide regulation of TRP channels. *Handb Exp Pharmacol* 223: 1143-76

Ronco V, Potenza DM, Denti F, Vullo S, Gagliano G, et al. 2015. A novel Ca(2)(+)-mediated cross-talk between endoplasmic reticulum and acidic organelles: implications for NAADP-dependent Ca(2)(+) signalling. *Cell Calcium* 57: 89-100

Rosenbaum T, Simon SA. 2007. TRPV1 Receptors and Signal Transduction In *TRP Ion Channel Function in Sensory Transduction and Cellular Signaling Cascades*, ed. WB Liedtke, S Heller. Boca Raton (FL)

Rossi E, Poirault-Chassac S, Bieche I, Chocron R, Schnitzler A, et al. 2019. Human Endothelial Colony Forming Cells Express Intracellular CD133 that Modulates their Vasculogenic Properties. *Stem Cell Rev*

Rozen EJ, Roewenstrunk J, Barallobre MJ, Di Vona C, Jung C, et al. 2018. DYRK1A Kinase Positively Regulates Angiogenic Responses in Endothelial Cells. *Cell Rep* 23: 1867-78

Sakurada R, Odagiri K, Hakamata A, Kamiya C, Wei J, Watanabe H. 2019. Calcium Release from Endoplasmic Reticulum Involves Calmodulin-Mediated NADPH Oxidase-Derived Reactive Oxygen Species Production in Endothelial Cells. *Int J Mol Sci* 20

Sanchez-Hernandez Y, Laforenza U, Bonetti E, Fontana J, Dragoni S, et al. 2010. Store-operated Ca(2+) entry is expressed in human endothelial progenitor cells. *Stem Cells Dev* 19: 1967-81

Santulli G, Lewis D, des Georges A, Marks AR, Frank J. 2018. Ryanodine Receptor Structure and Function in Health and Disease. *Subcell Biochem* 87: 329-52

Sarlon G, Zemani F, David L, Duong Van Huyen JP, Dizier B, et al. 2012. Therapeutic effect of fucoidan-stimulated endothelial colony-forming cells in peripheral ischemia. *J Thromb Haemost* 10: 38-48

Savage AM, Kurusamy S, Chen Y, Jiang Z, Chhabria K, et al. 2019. tmem33 is essential for VEGF-mediated endothelial calcium oscillations and angiogenesis. *Nat Commun* 10: 732

Schindl R, Fritsch R, Jardin I, Frischauf I, Kahr H, et al. 2012. Canonical transient receptor potential (TRPC) 1 acts as a negative regulator for vanilloid TRPV6-mediated Ca2+ influx. *J Biol Chem* 287: 35612-20

Schroder K, Zhang M, Benkhoff S, Mieth A, Pliquett R, et al. 2012. Nox4 is a protective reactive oxygen species generating vascular NADPH oxidase. *Circ Res* 110: 1217-25

Shelley WC, Leapley AC, Huang L, Critser PJ, Zeng P, et al. 2012. Changes in the frequency and in vivo vessel-forming ability of rhesus monkey circulating endothelial colony-forming cells across the lifespan (birth to aged). *Pediatr Res* 71: 156-61

Shirakawa H. 2001. The Discovery of Polyacetylene Film: The Dawning of an Era of Conducting Polymers (Nobel Lecture). *Angew Chem Int Ed Engl* 40: 2574-80

Siegel G, Fleck E, Elser S, Hermanutz-Klein U, Waidmann M, et al. 2018. Manufacture of endothelial colony-forming progenitor cells from steady-state peripheral blood leukapheresis using pooled human platelet lysate. *Transfusion* 58: 1132-42

Siemens J, Zhou S, Piskorowski R, Nikai T, Lumpkin EA, et al. 2006. Spider toxins activate the capsaicin receptor to produce inflammatory pain. *Nature* 444: 208-12

Silva-Rojas R, Laporte J, Bohm J. 2020. STIM1/ORAI1 Loss-of-Function and Gain-of-Function Mutations Inversely Impact on SOCE and Calcium Homeostasis and Cause Multi-Systemic Mirror Diseases. *Frontiers in Physiology* 11

Simons M, Gordon E, Claesson-Welsh L. 2016. Mechanisms and regulation of endothelial VEGF receptor signalling. *Nat Rev Mol Cell Biol* 17: 611-25

Smadja DM. 2019. Vasculogenic Stem and Progenitor Cells in Human: Future Cell Therapy Product or Liquid Biopsy for Vascular Disease. *Adv Exp Med Biol* 1201: 215-37

Smadja DM, Mauge L, Susen S, Bieche I, Gaussem P. 2009. Blood outgrowth endothelial cells from cord blood and peripheral blood: angiogenesis-related characteristics in vitro: a rebuttal. *J Thromb Haemost* 7: 504-6; author reply 06-8

Smadja DM, Mulliken JB, Bischoff J. 2012. E-selectin mediates stem cell adhesion and formation of blood vessels in a murine model of infantile hemangioma. *Am J Pathol* 181: 2239-47

Smani T, Gomez LJ, Regodon S, Woodard GE, Siegfried G, et al. 2018. TRP Channels in Angiogenesis and Other Endothelial Functions. *Front Physiol* 9: 1731

Sobajima M, Nozawa T, Shida T, Ohori T, Suzuki T, et al. 2011. Repeated sauna therapy attenuates ventricular remodeling after myocardial infarction in rats by increasing coronary vascularity of noninfarcted myocardium. *Am J Physiol Heart Circ Physiol* 301: H548-54

Song MY, Makino A, Yuan JX. 2011. Role of reactive oxygen species and redox in regulating the function of transient receptor potential channels. *Antioxid Redox Signal* 15: 1549-65

Stewart AP, Smith GD, Sandford RN, Edwardson JM. 2010. Atomic force microscopy reveals the alternating subunit arrangement of the TRPP2-TRPV4 heterotetramer. *Biophys J* 99: 790-7

Storch U, Forst AL, Philipp M, Gudermann T, Mederos y Schnitzler M. 2012. Transient receptor potential channel 1 (TRPC1) reduces calcium permeability in heteromeric channel complexes. *J Biol Chem* 287: 3530-40

Stueber T, Eberhardt MJ, Caspi Y, Lev S, Binshtok A, Leffler A. 2017. Differential cytotoxicity and intracellular calcium-signalling following activation of the calcium-permeable ion channels TRPV1 and TRPA1. *Cell Calcium* 68: 34-44

Su KH, Lee KI, Shyue SK, Chen HY, Wei J, Lee TS. 2014a. Implication of transient receptor potential vanilloid type 1 in 14,15-epoxyeicosatrienoic acid-induced angiogenesis. *Int J Biol Sci* 10: 990-6

Su KH, Lin SJ, Wei J, Lee KI, Zhao JF, et al. 2014b. The essential role of transient receptor potential vanilloid 1 in simvastatin-induced activation of endothelial nitric oxide synthase and angiogenesis. *Acta Physiol (Oxf)* 212: 191-204

Su SH, Wu CH, Chiu YL, Chang SJ, Lo HH, et al. 2017. Dysregulation of Vascular Endothelial Growth Factor Receptor-2 by Multiple miRNAs in Endothelial Colony-Forming Cells of Coronary Artery Disease. *J Vasc Res* 54: 22-32

Suarez Y, Shepherd BR, Rao DA, Pober JS. 2007. Alloimmunity to human endothelial cells derived from cord blood progenitors. *J Immunol* 179: 7488-96

Sullivan MN, Gonzales AL, Pires PW, Bruhl A, Leo MD, et al. 2015. Localized TRPA1 channel Ca2+ signals stimulated by reactive oxygen species promote cerebral artery dilation. *Sci Signal* 8: ra2

Sun L, Yau HY, Lau OC, Huang Y, Yao X. 2011. Effect of hydrogen peroxide and superoxide anions on cytosolic Ca2+: comparison of endothelial cells from large-sized and small-sized arteries. *PLoS One* 6: e25432

Sun MY, Geyer M, Komarova YA. 2017. IP3 receptor signaling and endothelial barrier function. *Cell Mol Life Sci* 74: 4189-207

Sung SH, Wu TC, Chen JS, Chen YH, Huang PH, et al. 2013. Reduced number and impaired function of circulating endothelial progenitor cells in patients with abdominal aortic aneurysm. *Int J Cardiol* 168: 1070-7

Susankova K, Tousova K, Vyklicky L, Teisinger J, Vlachova V. 2006. Reducing and oxidizing agents sensitize heat-activated vanilloid receptor (TRPV1) current. *Mol Pharmacol* 70: 383-94

Tamareille S, Mignen O, Capiod T, Rucker-Martin C, Feuvray D. 2006. High glucose-induced apoptosis through store-operated calcium entry and calcineurin in human umbilical vein endothelial cells. *Cell Calcium* 39: 47-55

Tapella L, Soda T, Mapelli L, Bortolotto V, Bondi H, et al. 2020. Deletion of calcineurin from GFAP-expressing astrocytes impairs excitability of cerebellar and hippocampal neurons through astroglial Na(+) /K(+) ATPase. *Glia* 68: 543-60

Tasev D, Dekker-Vroling L, van Wijhe M, Broxterman HJ, Koolwijk P, van Hinsbergh VWM. 2018. Hypoxia Impairs Initial Outgrowth of Endothelial Colony Forming Cells and Reduces Their Proliferative and Sprouting Potential. *Front Med-Lausanne* 5

Tasev D, Koolwijk P, van Hinsbergh VW. 2016. Therapeutic Potential of Human-Derived Endothelial Colony-Forming Cells in Animal Models. *Tissue Eng Part B Rev* 22: 371-82

Tasev D, van Wijhe MH, Weijers EM, van Hinsbergh VW, Koolwijk P. 2015. Long-Term Expansion in Platelet Lysate Increases Growth of Peripheral Blood-Derived Endothelial-Colony Forming Cells and Their Growth Factor-Induced Sprouting Capacity. *PLoS One* 10: e0129935

Thakore P, Alvarado MG, Ali S, Mughal A, Pires PW, et al. 2021. Brain endothelial cell TRPA1 channels initiate neurovascular coupling. *Elife* 10

Thakore P, Earley S. 2019. Transient Receptor Potential Channels and Endothelial Cell Calcium Signaling. *Compr Physiol* 9: 1249-77

Thebault S, Lemonnier L, Bidaux G, Flourakis M, Bavencoffe A, et al. 2005. Novel role of cold/menthol-sensitive transient receptor potential melastatine family member 8 (TRPM8) in the activation of store-operated channels in LNCaP human prostate cancer epithelial cells. *J Biol Chem* 280: 39423-35

Thomas AP, Bird GS, Hajnoczky G, Robb-Gaspers LD, Putney JW, Jr. 1996. Spatial and temporal aspects of cellular calcium signaling. *Faseb J* 10: 1505-17

Tominaga M, Caterina MJ, Malmberg AB, Rosen TA, Gilbert H, et al. 1998. The cloned capsaicin receptor integrates multiple pain-producing stimuli. *Neuron* 21: 531-43

Toshner M, Dunmore BJ, McKinney EF, Southwood M, Caruso P, et al. 2014. Transcript analysis reveals a specific HOX signature associated with positional identity of human endothelial cells. *PLoS One* 9: e91334

Traktuev DO, Prater DN, Merfeld-Clauss S, Sanjeevaiah AR, Saadatzadeh MR, et al. 2009. Robust functional vascular network formation in vivo by cooperation of adipose progenitor and endothelial cells. *Circ Res* 104: 1410-20

Tu TC, Nagano M, Yamashita T, Hamada H, Ohneda K, et al. 2016. A Chemokine Receptor, CXCR4, Which Is Regulated by Hypoxia-Inducible Factor 2alpha, Is Crucial for Functional Endothelial Progenitor Cells Migration to Ischemic Tissue and Wound Repair. *Stem Cells Dev* 25: 266-76

Udan RS, Culver JC, Dickinson ME. 2013. Understanding vascular development. *Wiley Interdiscip Rev Dev Biol* 2: 327-46

Vaca L, Sinkins WG, Hu Y, Kunze DL, Schilling WP. 1994. Activation of recombinant trp by thapsigargin in Sf9 insect cells. *Am J Physiol* 267: C1501-5

Vaeth M, Yang J, Yamashita M, Zee I, Eckstein M, et al. 2017. ORAI2 modulates store-operated calcium entry and T cell-mediated immunity. *Nat Commun* 8: 14714

Veal E, Day A. 2011. Hydrogen peroxide as a signaling molecule. *Antioxid Redox Signal* 15: 147-51

Veldhuis NA, Lew MJ, Abogadie FC, Poole DP, Jennings EA, et al. 2012. N-glycosylation determines ionic permeability and desensitization of the TRPV1 capsaicin receptor. *J Biol Chem* 287: 21765-72

Venkatachalam K, Montell C. 2007. TRP channels. *Annu Rev Biochem* 76: 387-417

Vennekens R, Owsianik G, Nilius B. 2008. Vanilloid transient receptor potential cation channels: an overview. *Curr Pharm Des* 14: 18-31

Voets T, Droogmans G, Wissenbach U, Janssens A, Flockerzi V, Nilius B. 2004. The principle of temperature-dependent gating in cold- and heat-sensitive TRP channels. *Nature* 430: 748-54

Volk T, Hensel M, Kox WJ. 1997. Transient Ca2+ changes in endothelial cells induced by low doses of reactive oxygen species: role of hydrogen peroxide. *Mol Cell Biochem* 171: 11-21

Vriens J, Appendino G, Nilius B. 2009. Pharmacology of vanilloid transient receptor potential cation channels. *Mol Pharmacol* 75: 1262-79

Wang B, Wu LJ, Chen J, Dong LL, Chen C, et al. 2021. Metabolism pathways of arachidonic acids: mechanisms and potential therapeutic targets. *Signal Transduct Tar* 6

Wang Z, Yang J, Qi J, Jin Y, Tong L. 2020. Activation of NADPH/ROS pathway contributes to angiogenesis through JNK signaling in brain endothelial cells. *Microvasc Res* 131: 104012

Watanabe H, Vriens J, Suh SH, Benham CD, Droogmans G, Nilius B. 2002. Heat-evoked activation of TRPV4 channels in a HEK293 cell expression system and in native mouse aorta endothelial cells. *J Biol Chem* 277: 47044-51

Wes PD, Chevesich J, Jeromin A, Rosenberg C, Stetten G, Montell C. 1995. TRPC1, a human homolog of a Drosophila store-operated channel. *Proc Natl Acad Sci U S A* 92: 9652-6

Wesson DE, Elliott SJ. 1995. The H2O2-generating enzyme, xanthine oxidase, decreases luminal Ca2+ content of the IP3-sensitive Ca2+ store in vascular endothelial cells. *Microcirculation* 2: 195-203

Wilson C, Zhang X, Lee MD, MacDonald M, Heathcote HR, et al. 2020. Disrupted endothelial cell heterogeneity and network organization impair vascular function in prediabetic obesity. *Metabolism-Clinical and Experimental* 111

Woll KA, Van Petegem F. 2022. Calcium-release channels: structure and function of IP3 receptors and ryanodine receptors. *Physiol Rev* 102: 209-68

Wong CO, Yao X. 2011. TRP channels in vascular endothelial cells. *Adv Exp Med Biol* 704: 759-80

Wu TT, Peters AA, Tan PT, Roberts-Thomson SJ, Monteith GR. 2014. Consequences of activating the calcium-permeable ion channel TRPV1 in breast cancer cells with regulated TRPV1 expression. *Cell Calcium* 56: 59-67

Wu Y, He MY, Ye JK, Ma SY, Huang W, et al. 2017. Activation of ATP-sensitive potassium channels facilitates the function of human endothelial colony-forming cells via Ca(2+) /Akt/eNOS pathway. *J Cell Mol Med* 21: 609-20

Xu H, Blair NT, Clapham DE. 2005. Camphor activates and strongly desensitizes the transient receptor potential vanilloid subtype 1 channel in a vanilloid-independent mechanism. *J Neurosci* 25: 8924-37

Yamamura H, Suzuki Y, Yamamura H, Asai K, Imaizumi Y. 2016. Hypoxic stress up-regulates Kir2.1 expression and facilitates cell proliferation in brain capillary endothelial cells. *Biochem Biophys Res Commun* 476: 386-92

Yang J, Zhao Z, Gu M, Feng X, Xu H. 2018. Release and uptake mechanisms of vesicular Ca(2+) stores. *Protein Cell*

Yeon SI, Kim JY, Yeon DS, Abramowitz J, Birnbaumer L, et al. 2014. Transient receptor potential canonical type 3 channels control the vascular contractility of mouse mesenteric arteries. *PLoS One* 9: e110413

Yoder MC. 2012. Human endothelial progenitor cells. *Cold Spring Harb Perspect Med* 2: a006692

Yoder MC. 2018. Endothelial stem and progenitor cells (stem cells): (2017 Grover Conference Series). *Pulm Circ* 8: 2045893217743950

Yoder MC, Mead LE, Prater D, Krier TR, Mroueh KN, et al. 2007. Redefining endothelial progenitor cells via clonal analysis and hematopoietic stem/progenitor cell principals. *Blood* 109: 1801-9

Yokota Y, Nakajima H, Wakayama Y, Muto A, Kawakami K, et al. 2015. Endothelial Ca 2+ oscillations reflect VEGFR signaling-regulated angiogenic capacity in vivo. *Elife* 4

Yoon MN, Kim DK, Kim SH, Park HS. 2017. Hydrogen peroxide attenuates refilling of intracellular calcium store in mouse pancreatic acinar cells. *Korean J Physiol Pharmacol* 21: 233-39

Yu M, Liu Q, Sun J, Yi K, Wu L, Tan X. 2011. Nicotine improves the functional activity of late endothelial progenitor cells via nicotinic acetylcholine receptors. *Biochem Cell Biol* 89: 405-10

Yu YB, Su KH, Kou YR, Guo BC, Lee KI, et al. 2017. Role of transient receptor potential vanilloid 1 in regulating erythropoietin-induced activation of endothelial nitric oxide synthase. *Acta Physiol (Oxf)* 219: 465-77

Yuan W, Guo J, Li X, Zou Z, Chen G, et al. 2009. Hydrogen peroxide induces the activation of the phospholipase C-gamma1 survival pathway in PC12 cells: protective role in apoptosis. *Acta Biochim Biophys Sin (Shanghai)* 41: 625-30

Zemani F, Silvestre JS, Fauvel-Lafeve F, Bruel A, Vilar J, et al. 2008. Ex vivo priming of endothelial progenitor cells with SDF-1 before transplantation could increase their proangiogenic potential. *Arterioscler Thromb Vasc Biol* 28: 644-50

Zhang M, Shah AM. 2014. ROS signalling between endothelial cells and cardiac cells. *Cardiovasc Res* 102: 249-57

Zhang X, Lee MD, Wilson C, McCarron JG. 2019. Hydrogen peroxide depolarizes mitochondria and inhibits IP3-evoked Ca2+ release in the endothelium of intact arteries. *Cell Calcium* 84

Zheng Y, Shen X. 2005. H2O2 directly activates inositol 1,4,5-trisphosphate receptors in endothelial cells. *Redox Rep* 10: 29-36

Zhou MH, Zheng H, Si H, Jin Y, Peng JM, et al. 2014. Stromal interaction molecule 1 (STIM1) and Orai1 mediate histamine-evoked calcium entry and nuclear factor of activated T-cells (NFAT) signaling in human umbilical vein endothelial cells. *J Biol Chem* 289: 29446-56

Zhu X, Chu PB, Peyton M, Birnbaumer L. 1995. Molecular cloning of a widely expressed human homologue for the Drosophila trp gene. *Febs Lett* 373: 193-8

Zinkevich NS, Gutterman DD. 2011. ROS-induced ROS release in vascular biology: redox-redox signaling. *Am J Physiol Heart Circ Physiol* 301: H647-53

Zucchetti E, Zangoli M, Bargigia I, Bossio C, Di Maria F, et al. 2017. Poly(3-hexylthiophene) nanoparticles for biophotonics: study of the mutual interaction with living cells. *J Mater Chem B* 5: 565-74

Zuccolo E, Di Buduo C, Lodola F, Orecchioni S, Scarpellino G, et al. 2018. Stromal Cell-Derived Factor-1alpha Promotes Endothelial Colony-Forming Cell Migration Through the Ca(2+)-Dependent Activation of the Extracellular Signal-Regulated Kinase 1/2 and Phosphoinositide 3-Kinase/AKT Pathways. *Stem Cells Dev* 27: 23-34

Zuccolo E, Dragoni S, Poletto V, Catarsi P, Guido D, et al. 2016. Arachidonic acid-evoked Ca2+ signals promote nitric oxide release and proliferation in human endothelial colony forming cells. *Vascul Pharmacol* 87: 159-71

Zuccolo E, Laforenza U, Negri S, Botta L, Berra-Romani R, et al. 2019. Muscarinic M5 receptors trigger acetylcholine-induced Ca(2+) signals and nitric oxide release in human brain microvascular endothelial cells. *J Cell Physiol* 234: 4540-62

Zuccolo E, Lim D, Poletto V, Guerra G, Tanzi F, et al. 2015. Acidic Ca2 + stores interact with the endoplasmic reticulum to shape intracellular Ca2 + signals in human endothelial progenitor cells. *Vascular Pharmacology* 75: 70-71